Direct Radiative Effect of Mineral Dust on the Middle East and North Africa Climate

Dissertation by

Hamza Kunhu Bangalath

In Partial Fulfillment of the Requirements

For the Degree of

Doctor of Philosophy

King Abdullah University of Science and Technology

Thuwal, Kingdom of Saudi Arabia

(November, 2016)

EXAMINATION COMMITTEE PAGE

The dissertation of Your Full Name is approved by the examination committee

Committee Chairperson: Prof. Georgiy Stenchikov
Committee Members: Prof. Burton Jones
Committee Members: Prof. Matthew McCabe
Committee Members: Prof. Johannes Lelieveld

ABSTRACT

Direct Radiative Effect of Mineral Dust on the Middle East and North Africa Climate

Hamza Kunhu Bangalath

Dust-climate interaction over the Middle East and North Africa (MENA) has long been studied, as it is the "dustiest" region on earth. However, the quantitative and qualitative understanding of the role of dust direct radiative effect on MENA climate is still rudimentary. The present dissertation investigates dust direct radiative effect on MENA climate during summer with a special emphasis on the sensitivity of climate response to dust shortwave absorption, which is one of the most uncertain components of dust direct radiative effect. Simulations are conducted with and without dust radiative effect, to differentiate the effect of dust on climate. To elucidate the sensitivity of climate response to dust shortwave absorption, simulations with dust assume three different cases of dust shortwave absorption, representing dust as a very efficient, standard and inefficient shortwave absorber. The non-uniformly distributed dust perturb circulations at various scales. Therefore, the present study takes advantage of the high spatial resolution capabilities of an Atmospheric General Circulation Model (AGCM), High Resolution Atmospheric Model (HiRAM), which incorporates global and regional circulations. AMIP-style global high-resolution simulations are conducted at a spatial resolution of 25 km.

A significant response in the strength and position of the local Hadley circulation is predicted in response to meridionally asymmetric distribution of dust and

the corresponding radiative effects. Significant responses are also found in regional circulation features such as African Easterly Jet and West African Monsoon circulation. Consistent with these dynamic responses at various scales, the tropical rainbelt across MENA strengthens and shifts northward. Similarly, the temperature under rainbelt cools and that over subtropical deserts warms. Inter-comparison of various dust shortwave absorption cases shows that the response of the MENA tropical rainbelt is extremely sensitive to the strength of shortwave absorption. Further analyses reveal that the sensitivity of the rainbelt stems from the sensitivity of the multi-scale circulations that define the rainbelt.

Importantly, the summer precipitation over the semi-arid strip south of Sahara, including Sahel, increases in response to dust radiative effect. The maximum response and sensitivity are predicted over this region. The sensitivity of the responses over Sahel, especially that of precipitation, is comparable to the mean state. Locally, the precipitation increase reaches up to 50% of the mean, while dust is assumed to be a very efficient absorber. As the region is characterized by the "Sahel drought", the predicted precipitation sensitivity to the dust loading over this region has a wide-range of socioeconomic implications. The present study, therefore, suggests the importance of reducing uncertainty in dust shortwave absorption for a better simulation and interpretation of the MENA climate in general, and of Sahel in particular.

ACKNOWLEDGEMENTS

First and foremost, I would like to offer my sincere gratitude to my advisor Prof. Georgiy Stenchikov for his continuous support, appropriate guidance, motivation, and patience throughout my Ph.D. period. I was very fortunate to have him as my advisor; without him, the dissertation would have never been accomplished. I am especially thankful to him for giving me the independence to pursue my research ideas with his overall guidance, which greatly helps me to move much ahead on my path to becoming an independent researcher.

I would like to extend my gratitude to the rest of my dissertation committee: Prof. Burton Jones, Prof. Matthew McCabe, and Prof. Johannes Lelieveld, for their valuable time, comments and encouragement. I am also deeply indebted to Dr. Paul A. Ginoux of GFDL for providing dust optical properties data sets and for the useful discussions and insightful comments. Without his valuable support, it would be very hard to complete the dissertation.

My sincere gratitude also goes to Prof. V. Ramaswamy, Dr. Ming Zhao, Dr. Bruce Wyman, and Dr. Christopher Kerr of GFDL for helping to acquire and use HiRAM model. I would also like to acknowledge the computational facilities provided by the Supercomputing Laboratory at KAUST, which enabled me to conduct highly expensive global high-resolution simulations.

Special thank goes to my friend Dr. Udaya Bhaskar Gunturu for all those scientific and non-scientific discussions over coffee, which broadened my thinking and outlook.

A very special thank goes to my late friend and comrade, Rajesh Kumar K. K, who encouraged and convinced me to take the path of a scientific career while I was confused about my plans. Special thanks to Com. Pinarayi Vijayan and Com. A. N

Shamseer, for their valuable and timely help.

I would also like to thank my friends and colleagues, Vu, Mubashar, Andrew, Jenny, Sergey, Jish, Vijaya Kumar, Manju Vijaya Kumar, Abhisri, Sajeesh, Sanal, Shaiju Mash, Naveen, Anees, Asif, Shibu, Naseeb, Nishad and all others I cannot list one by one, for their support and help.

Last, but certainly not least, I want to thank my wife, Jerry Raj. Without her moral and emotional support and love, I would have never been able to pursue my scientific career dreams. Similarly, I would like to thank my parents and siblings for their support and guidance, especially during my school days, which helped me to dream of a scientific career.

TABLE OF CONTENTS

LIST OF ABBREVIATIONS

AEJ	African Easterly Jet
AEW	African Easterly Wave
AGCM	Atmospheric General Circulation Model
AHL	Arabian Heat Low
AOD	Aerosol Optical Depth
DDRF	Dust Direct Radiative Forcing
EHP	Elevated Heat Pump
GCM	General Circulation Model
GFDL	Geophysical Fluid Dynamics Laboratory
GOCART	Goddard Chemistry Aerosol Radiation and Transport
GPCP	Global Precipitation Climatology Project
HiRAM	High Resolution Atmospheric Model
IPCC	Intergovernmental Panel on Climate Change
ISM	Indian Summer Monsoon
ITCZ	Inter Tropical Convergence Zone
JJA	June-July-August
MENA	Middle East and North Africa
MOZART	Model for OZone and Related chemical Tracers
RCM	Regional Climate Model

SAL	Saharan Air Layer
SHL	Saharan Heat Low
SLLJ	Somali Low Level Jet
SSA	Single Scattering Albedo
SST	Sea Surface Temperature
SuHL	Sudan Heat Low
TEJ	Tropical Easterly Jet
TOA	Top Of the Atmosphere
TRMM	Tropical Rainfall Measurement Mission Project
WAM	West African Monsoon
WAWJ	West African Westerly Jet

LIST OF FIGURES

LIST OF TABLES

Chapter 1

Introduction

1.1 Overview

As an omnipresent and the most mass abundant aerosol species in the atmosphere, mineral dust aerosol and its interaction with climate system has long been recognized as an important process (e.g., *Carlson and Benjamin*, 1980; *Cess et al.*, 1985; *Ramaswamy and Kiehl*, 1985; *Tegen et al.*, 1996). Dust-climate interactions span all the five elements of the climate system: atmosphere, hydrosphere, cryosphere, geosphere, and biosphere; and these interactions are complex, multifaceted and bidirectional. One such interaction primarily happens in the atmosphere, is the *direct radiative effect* by which dust alter earth's radiation budget by scattering and absorbing solar and planetary radiations and by emitting the latter. The present dissertation focuses on the dust induced direct radiative effect on the Middle East and North Africa (MENA) climate and its sensitivity to dust shortwave absorption, using a high-resolution Atmospheric General Circulation Model (AGCM).

MENA is arguably the most dust-laden region around the globe, owing to the presence of world's major dust source regions including Sahara and Arabian deserts and the semi-arid Sahel. The region has a typical hot arid or semi-arid climate characterized by inadequate and highly variable rainfall, scarce vegetation and hot and dry weather. Sahel–the semi-arid strip across Northern Africa sandwiched between humid savanna to the south and dry Sahara desert to the north–underwent perpetual drought from the 1960s to the 1980s ("Sahel-drought") and a recovery in the follow-

ing decades. The Sahel-drought has been widely considered as one of the most severe climate variation of any region in the era of instrumental records (e.g., *Dai et al.*, 2004; *Hulme*, 1996). However, the exact reasons that lead to a prolonged drought condition are not very well known yet and is an ongoing debate among climate scientists (e.g., *Nicholson*, 1980; *Folland et al.*, 1986; *Held et al.*, 2005). Interestingly, and importantly, dust variability has been discussed as one of the plausible causative mechanism (e.g., *Brooks and Legrand*, 2000; *Biasutti and Giannini*, 2006; *Nicholson*, 2000; *Yoshioka et al.*, 2007). In view of the meteorological and socio-political importance of the Sahel drought, the current study gives a particular emphasis to the response and sensitivity of the tropical rainbelt, whose strength and the latitudinal extent largely determine the drought conditions over Sahel. It should be noted that the current research focuses only on the boreal summer (June-July-August (JJA)) season, as it is the season of maximum precipitation and dust loading in the domain.

Another aspect of the current dissertation is to elucidate the sensitivity of climate response to dust shortwave absorption, which is considered to be one of the most decisive but a highly uncertain component in the estimation of dust direct radiative effect. There is no consensus on the strength of dust shortwave absorption among researchers. The estimate of the imaginary part of the shortwave refractive index, which determines the efficiency of shortwave absorption by dust particles, vary by an order of magnitude among different observational and modeling studies (*Balkanski et al.*, 2007). Such uncertainty could potentially induce significant uncertainties in the estimation of the direct radiative effect of dust and the corresponding climate responses. Therefore, the current study also examines the sensitivity of climate response to a plausible range of dust shortwave absorption.

A further highlight of the present dissertation is the use of a high-resolution global model instead of a Regional Climate Model (RCM), to investigate regional climate responses. Global simulations at a typical RCM resolution, in the present case 25 Km,

enables to incorporate multi-scale circulation and climate processes in the simulations that are decisive in defining the regional climate. Such simulations are capable of resolving circulations ranging from planetary scale overturning to regional scale jets and waves. High-resolution global simulations are particularly relevant in the present case, where the dust induced radiative effect perturb circulations at various scales, which defines the net climate response at regional scales to a large extent. Accordingly, global high-resolution simulations with and without dust are conducted to elucidate the climate responses to dust radiative effect. The current dissertation, therefore, analyses the responses and sensitivity of a range of multi-scale circulations by utilizing the high-resolution global simulations.

The dissertation is organized in six chapters. The rest of this introductory chapter provides an overview and background of dust direct radiative effect and climate response, which contextualize the research questions addressed in the dissertation. The introductory chapter is partly composed of the materials from two published papers, *Bangalath and Stenchikov* (2015, 2016). Similarly, Chapters 2, 3 and 4 are mostly composed of the same two papers but have been formatted to be compatible with dissertation guidelines. Chapter 2 describes the model and the experiment design. Dust direct radiative forcing and the radiative heating are discussed in chapter 3. Chapter 4, in general, portrays the climate response over MENA to dust direct radiative effect. The chapter specifically investigates the response in the local and regional overturning circulations and the consequent response in the strength and position of tropical rainbelt across MENA . Chapter 5 then primarily centers on the responses in regional or synoptic scale circulation features, which are crucial for the net rainfall and temperature responses over the region. The main circulation features analyzed are West African Monsoon (WAM), African Easterly Jet (AEJ), Tropical Easterly Jet (TEJ), African Easterly Wave (AEW) and Saharan Heat Low (SHL). Finally, in Chapter 6, main findings are summarized with conclusions.

1.2 Background and Motivation

1.2.1 Mineral Dust Aerosol

Spatiotemporal characteristics

Mineral dust is a unique aerosol species in its loading, optical characteristics, source, and transport. Dust is arguably the most dominant particulate matter in the atmosphere. It constitutes the major fraction of the atmospheric aerosol loading and hence a significant share of the global aerosol forcing (*Kaufman et al.*, 2002; *Tegen et al.*, 1997; *Christopher and Zhang*, 2002). By comparing results from 16 models, Aerosol Comparison between Observations and Models (AeroCom) project showed there are about 700 to 4000 trillion grams (Tg) of dust influx into the atmosphere, annually. However, the dust released into the atmosphere is not uniformly distributed; rather it has a highly non-uniform distribution in space as well as in time. Spatially, the dust loading is concentrated in the subtropics associated with the major dust source regions such as subtropical deserts and semi-arid regions. And, there is a hemispheric contrast in the dust distributions with a higher concentration in the Northern hemisphere associated with the fact that major portion of the global arid semi-arid land masses resides in the Northern hemisphere. Dust loading is also characterized by strong seasonal cycle. Over MENA dust loading is maximum during the summer season.

Apart from the seasonal cycle, there are interannual and interdecadal variabilities. There is a growing body of evidence that the dust burden changes in response to natural modes of climate variability. *Prospero and Nees* (1986) showed a positive correlation between Saharan dust transport and El Nio. Similarly, dust loading in the Mediterranean and the North Atlantic is correlated with the North Atlantic Oscillation (e.g., *Moulin et al.*, 1997; *Chiapello and Moulin*, 2002). A regional differential trend in the dust storm frequency is also observed in the past several decades

(*Goudie and Middleton*, 1992). And most importantly, dust loading is sensitive to climate change. *Mahowald et al.* (1999) showed that dust loading varied 2-4 fold between current and last glacial maximum, using linked terrestrial biosphere, dust source, and transport model. Likewise, it was also found that the dust production was acutely sensitive to Sahel drought, with a substantial increase in production during drought period (*Prospero and Nees*, 1986; *Middleton*, 1985). By considering 6 different scenarios of changes in sources, a study by *Mahowald and Luo* (2003) projected a 20 to 60% reduction in dust loading by the end of the 21^{st} century, compared to present climate. In contrast, *Woodward et al.* (2005) predict a tripling of dust burden by the end of 21^{st} century. Other studies also projected an increase or decrease of dust loading, but with lesser a magnitude (e.g., *Jacobson and Streets*, 2009; *Liao et al.*, 2009; *Tegen et al.*, 2004). In short, dust emission and loading is very sensitive to changes and variabilities in climate and their future projection is extremely uncertain.

Though the state of the art research recognizes all aspects of dust-climate interactions, the uncertainty in the estimation of dust loading is still challenging. The modeled estimates of the global dust emission range over more than a factor of two, which could translate into a corresponding uncertainty in the radiative effect of the dust (*Zender et al.*, 2004). Inter-comparison studies among satellite retrievals of Aerosol Optical Depth (AOD) also showed a difference of at least a factor of 2 (*Myhre et al.*, 2004, 2005), which indicates the uncertainty in estimating the aerosols in the atmosphere from space. Besides the natural fraction of the dust emission, human activities also cause dust entrainment to the atmosphere through desertification (anthropogenic fraction of the total dust loading). Different modeling estimates show that the anthropogenic part of the total burden is highly uncertain, which varies from insignificant values (*Ginoux et al.*, 2001; *Prospero et al.*, 2002; *Tegen et al.*, 2004) to 50% of the total burden (*Mahowald et al.*, 2005; *Tegen et al.*, 1996).

Dust-climate Interaction

Although the dust in the atmosphere has been documented as far back as the nineteenth century (e.g., *Darwin*, 1846), the physical, chemical and biological interaction of dust with climate has got considerable attention in the last few decades. Dust-climate interactions, ranging from radiative perturbations in the atmosphere to influences in the global biogeochemical cycles, have been recognized in the last few decades. However, these interactions are poorly understood and quantified compared to CO_2 induced changes in the climate.

Once airborne, dust exerts direct radiative effect by scattering and absorbing both solar and planetary radiation along with the emission of thermal Infrared radiation (e.g., *Carlson and Benjamin*, 1980; *Cess et al.*, 1985; *Ramaswamy and Kiehl*, 1985; *Tegen et al.*, 1996; *Kaufman et al.*, 2001; *Miller and Tegen*, 1998; *Sokolik and Toon*, 1996). As a rapid atmospheric adjustment to the radiative perturbations, dust also causes a semi-direct radiative effect *Hansen et al.* (1997). In this process, the absorption of solar radiation and the consequent warming of the atmosphere leads to changes in cloud cover and liquid water path. In addition, dust causes indirect radiative effect on climate by modifying the microphysical and radiative properties of clouds by serving as cloud condensation nuclei (e.g., *Gunn and Phillips*, 1957; *Liou and Ou*, 1989; *Forster et al.*, 2007; *Levin et al.*, 1996; *Rotstayn and Lohmann*, 2002). Furthermore, dust in the atmosphere modifies the atmospheric circulation (*Miller and Tegen*, 1998; *Perlwitz et al.*, 2001) as a response to spatially inhomogeneous heating/cooling induced by dust. Another aspect of dust-climate interaction is the role of dust in the global biogeochemical cycles. The deposition of dust, especially that of transported dust far away from the source region, has significant impact on both oceanic and terrestrial ecosystems(*Prospero*, 1998; *Mahowald et al.*, 2005, 2009; *Jickells and Spokes*, 2001). By functioning as the fertilizer for ecosystems, it plays a significant role in the global carbon cycle. Another influence of dust on climate is reducing visibility and

causing poor air-quality.

Dust-climate interaction is bidirectional, so that dust acts upon the climate system and the climate system, in turn, influences the dust entrainment and transport. Any changes in climate, especially that of the wind, aridity and soil properties, could potentially influence the dust entrainment from the surface. Therefore, changes in climate either induced by dust itself or any other forcing such as CO2 warming, alter the dust production and hence the loading in the atmosphere.

Due to the manifold and bidirectional interactions of dust with climate, the dust effect on climate cannot be overlooked and should be accurately accounted in the modeling of present climate as well as in the prediction and assessment of the global climate change. However, by comparing the past and latest Intergovernmental Panel on Climate Change (IPCC) reports (*Solomon*, 2007; *Houghton et al.*, 2001), it is also evident that the level of scientific understanding of the role of aerosol in general and dust in particular on the projected climate is low compared to the role of greenhouse warming. All the aforementioned facts demand comprehensive and far-reaching research on dust-climate interaction. The present study, however, particularly focuses on the direct radiative effect of dust on regional climate, using a high-resolution AGCM. Unless otherwise mentioned, any radiative effect that is being discussed in the current dissertation is the direct radiative effect of dust.

Dust Optical Properties

An accurate quantification of the direct radiative effect of any aerosol requires information of its concentration, composition, particle size distribution and optical properties. Amongst those, optical properties are the most uncertain and difficult to quantify properties. Primarily there are three optical parameters which are required to estimate the aerosol direct radiative effect or forcing, which are the AOD, Single Scattering Albedo (SSA), and the asymmetry factor (g) (e.g., *Penner et al.*, 1994;

Charlson et al., 1992). However, complex radiative transfer codes require more information such as phase function. All of these quantities are wavelength dependent and relative humidity dependent in case of a hygroscopic aerosol such as dust.

AOD is the measure of the total radiative attenuation and is a unit-less quantity. It can be estimated as the product of the aerosol mass loading in g/m^2 unit and the mass extinction coefficient (MEC) in m^2/g unit. The mass extinction coefficient is a function of both the particle size distribution, wavelength, and the refractive index. SSA is the ratio of scattering of the radiation by a particle to the total attenuation (sum of absorption and scattering), which ranges from zero to unity. However, estimation of the SSA requires the particle size and refractive index information (*Jacobson and Streets*, 2009; *Sokolik and Toon*, 1999; *Tegen et al.*, 1996). Another important quantity g, is the measure of the preferred scattering direction for the radiation encountering an aerosol particle. The value of g ranges from -1 (complete backward scattering) to 1 (complete forward scattering). Since g is a function of the particle size, the estimation requires the particle size information, which is partially provided by Angstrom exponent (A). A is an exponent expressing the spectral dependence of AOD with the wavelength of the radiation. A is inversely proportional to the particle size; that is, A is small for big particle and vice versa. Hence A can be used as a measure of the particle size. Along with the wavelength and humidity dependence, the above-mentioned optical properties depend on the aerosol loading and the spatial and temporal distribution of the aerosols (*Haywood and Boucher*, 2000; *Ramaswamy et al.*, 2001; *Penner et al.*, 2001).

1.2.2 Dust Direct Radiative Effect

Direct radiative effect of dust comprises of various processes; the scattering of incoming shortwave radiation ("global dimming"), absorption of both solar and planetary radiation, and the backscattering of thermal infrared radiation emits from the earth's

surface (planetary radiation) (*Forster et al.*, 2007). The concept of direct radiative effect and direct radiative forcing has been used interchangeably in many aerosol related literature especially that of dust aerosol (e.g., *Miller and Tegen*, 1998, 1999; *Yoshioka et al.*, 2007; *Perlwitz et al.*, 2001). Nevertheless, recent IPCC reports demarcate both, by constraining the concept of radiative forcing only to the radiative perturbation caused by anthropogenic aerosols/gases, while the concept of radiative effect includes perturbations from both natural and the anthropogenic part (*Forster et al.*, 2007). However, to comply with the terminologies of previous literature in dust radiative effect and since no separation of anthropogenic and natural part of dust is considered in the present experiments, the study uses the term Dust Direct Radiative Forcing (DDRF) to measure the radiative perturbation caused by both natural and anthropogenic component of dust. The concept of radiative forcing is widely used in assessing the corresponding changes in the climate to a change in the composition of the atmosphere.

The concept has its roots in the one-dimensional radiative-convective model experiments which investigated annual mean surface temperature responses to the radiative perturbations arise from the changes in the atmospheric compositions (*Manabe and Wetherald*, 1967; *Ramanathan and Coakley*, 1978). The radiative forcing and climate response relationship can be thought as a linear relationship, $\Delta Ts = \lambda RF$, where ΔTs is the equilibrium surface temperature change and λ is the climate sensitivity parameter (*Ramaswamy et al.*, 2001). Though this simple linear view of 'forcing-response' relationship does not represent a comprehensive analysis of the climate responses, it is very useful in assessing the wide-ranging changes in the climate. In general, aerosol radiative forcing must be defined as a radiative perturbation from an initial state; whether that state is the complete absence of aerosols, the estimate of aerosol loading from pre-industrial times, or an estimate of aerosol loading for today's natural aerosols (*Remer et al.*, 2009). A detailed discussion and precise definitions in

this regard are provided in Section 2.3.

For absorbing aerosols, the climate response depends, not only upon the forcing estimated at the Top Of the Atmosphere (TOA) or at surface, but also upon the forcing within the atmosphere due to radiative heating from dust shortwave absorption (e.g., *Miller and Tegen*, 1998, 1999; *Ramanathan et al.*, 2001). It should be noted that absorbing aerosol forcing and response are quite different from that of reflective aerosol forcing (e.g., *Hansen et al.*, 2005). The aerosol absorption of the radiation warms the aerosol layer and redistributes the energy throughout the troposphere and the stratosphere, while reflective aerosols distinctively cool the troposphere and warm the stratosphere. Since dust is both an absorbing and scattering aerosol, the net radiative forcing at TOA is very sensitive to the SSA, which is the measure of the relative efficiency of an aerosol for scattering and absorption.

Globally averaged net forcing due to dust is small compared to other aerosol species. This smallness in the net forcing arises mainly from two facts: the partial cancellation of the scattering and absorption radiative forcing with opposite signs and cancellation between the positive net forcing over bright deserts and the net negative forcing over oceans (*Tegen et al.*, 1996). However, regionally and seasonally the dust radiative forcing is huge, in and downwind of the source regions. The local abundance of dust makes it a major fraction of the atmospheric radiation budget over subtropical deserts and downwind of these dust source region (e.g., *Carlson and Benjamin*, 1980; *Li et al.*, 1996; *d'Almeida*, 1989; *Jish Prakash et al.*, 2014). Over deserts, the dust forcing can go up to 260 W/m2 (*Miller and Tegen*, 1998)

1.2.3 Climate Response to Dust Direct Radiative Effect

The climate response to direct radiative forcing is possible in multiple ways. The first and immediate interactions are through the changes in the radiative balance of the local atmospheric column due to aerosol extinction, which alters the temperature

profile and stability of the corresponding column. Secondarily, the aerosol-induced differential heating/cooling of the local atmosphere and the associated pressure gradients cause changes in the atmospheric circulation, which further changes the cloud formation and precipitation. The anomalous diabatic heating from cloud formation and rainfall further alter the regional or global circulations.

Over the past few decades, considerable attention has been devoted to the role of dust-induced direct radiative effect on climate (e.g., *Miller and Tegen*, 1998, 1999; *Ackerman and Chung*, 1992; *Sokolik and Toon*, 1996). Several modeling studies have already been conducted to explore the influence of direct radiative effect of dust on the climate, using models with various complexities ranging from simplified conceptual models to comprehensive earth system models (e.g., *Miller and Tegen*, 1998, 1999; *Yoshioka et al.*, 2007; *Perlwitz et al.*, 2001; *Lau et al.*, 2009; *Milton et al.*, 2008), including both global (e.g., *Lau et al.*, 2006, 2009; *Mahowald et al.*, 2006; *Miller and Tegen*, 1998; *Yoshioka et al.*, 2007; *Miller and Tegen*, 1999; *Perlwitz and Miller*, 2010; *Yue et al.*, 2010) and regional (e.g., *Ahn et al.*, 2007; *Konare et al.*, 2008; *Solmon et al.*, 2008, 2012; *Zhang et al.*, 2009) models. However, irrespective of the general agreement on spatially (generally global) and temporally averaged values, significant regional disparities are evident in both magnitude and sign of the climate responses among these studies. A typical example of the regional disparity is the contrasting response of the tropical rainbelt of Africa, especially over Sahel region, predicted from various modeling studies. Many of them predicted an increase in precipitation over Sahel (e.g., *Lau et al.*, 2009; *Yue et al.*, 2011a; *Miller et al.*, 2004a) in response to dust radiative effect, while others predicted a decrease in precipitation (e.g., *Yoshioka et al.*, 2007; *Yue et al.*, 2011b). The disagreement may arise from various sources of uncertainties spanning from those associated with the difference in dust optical properties to the ability of models to resolve regional circulation features.

Conventionally, aerosol climate interaction is explained based on either "solar

dimming" hypothesis or semi-direct effect including Elevated Heat Pump (EHP) hypotheses. "Solar dimming" refers to the partial shutdown of solar radiation at surface, due to scattering and absorption by aerosols, which eventually leads to a reduced latent heat flux and weakened water-cycle. However, *Miller* (2012) emphasized the primacy of the TOA forcing over surface forcing in controlling the atmospheric and oceanic temperature anomalies using a simple coupled ocean-atmosphere model. The atmospheric temperature is primarily determined by the TOA forcing not only at the equilibrium stage (*Miller*, 2012; *Cess et al.*, 1985), but during nearly the entire approach to equilibrium. In case of absorbing aerosol, the anomalous diabatic heating from shortwave absorption by dust layer induce local or global circulation changes, leads to further changes in aerosol forcing. EHP hypothesis is a manifestation of this effect based on specific assumptions on the horizontal distribution, elevation of the dust layer and season, which is explained in (*Lau et al.*, 2006) as follows. Black carbon mixed dust accumulated along the foothills of Himalayas in April and May months provides an elevated heat source from the shortwave heating, causing the air warm and rise above the southern escarpment of the Tibetan Plateau. This enhanced rising motion draws warmer and moist low-level air from the Indian Ocean as the Indian summer monsoon approaches and enhances the rainfall, which positively feedbacks to the strength of monsoon due to diabatic heating from precipitation. *Lau et al.* (2009) found a similar mechanism over WAM region, which emphasize the responses of the atmospheric water cycle to dust forcing.

1.2.4 Dust Direct Radiative Effect and MENA climate

The direct radiative effect of dust on MENA climate is of great interest due primarily to the fact that global dust loading is mainly confined in this region, specifically to the north of the tropical rainbelt. The radiative balance, and hence the temperature, of the region is immediately influenced by the radiative perturbations induced by

dust. Furthermore, the region includes Sahel, which is one of the most vulnerable regions to climate variability and changes. The Sahel climate greatly depends on the strength and seasonal march of the tropical rainbelt (e.g., *Lamb*, 1978; *Janicot*, 1992a; *Sultan and Janicot*, 2000). The succession of dry and wet years is a characteristic feature of the Sahelian climate, where a prolonged drought commenced in the late 1960s and continued until the 1990s. This prolonged drought is considered to be one of the largest climate variations recorded in the twentieth century (*Dai et al.*, 2004; *Hulme*, 1996). Dust radiative forcing and feedback was proposed as one of the possible mechanisms for these variabilities in the Sahel climate (e.g., *Brooks and Legrand*, 2000; *Nicholson*, 2000; *Prospero and Lamb*, 2003; *Yoshioka et al.*, 2007), which emphasizes the significant role of dust radiative effects in the region's climate. Similarly, eastern equatorial Africa is noted for extreme climate variability, with severe droughts and massive floods in alternate years (*Nicholson*, 2014a,b). Therefore, dust-induced changes in the strength and position of the tropical rainbelt are of great importance in this region.

Conventionally, the mean climate and its variability in equatorial Africa is explained based on the strength and the seasonal march of the rainbelt or the Inter Tropical Convergence Zone (ITCZ). Many of the previous studies linked the Sahel drought to an anomalous southward shift of ITCZ (*Janicot*, 1992a,b; *Lamb*, 1978; *Lamb and Peppler*, 1992) from its climatological mean summer position. By comparing simulations from 22 coupled General Circulation Model (GCM)s, conducted for the IPCC Fourth Assessment Report (AR4), *Suzuki* (2011) showed that the seasonal march of the ITCZ over Africa is a robust phenomenon unlike that over other regions and has the least intermodel difference in ITCZ. Nonetheless, the terms "ITCZ" and "tropical rainbelt" have been treated synonymously in many of these previous studies. Recent studies (e.g., *Nicholson*, 2009) showed that the ITCZ, which is classically defined as a zone of surface wind convergence, is effectively detached from the systems

that produce much of the tropical rainfall over West Africa. *Žagar et al.* (2011) also showed that the ITCZ defined by precipitation maxima and that defined by wind convergence are not collocated over land. The bulk of the rainfall over tropical Africa is associated with a deep core of ascent lying between the AEJ and TEJ, which is far south of the location of the ITCZ defined by wind convergence (*Nicholson*, 2009). Following these studies, the current study distinguishes between "ITCZ" and "rainbelt," where the former represents the loci of meridional wind convergence and the latter represents the belt of maximum precipitation representing the ascending limb of the Hadley circulation.

As in the upper-middle troposphere, there are synoptic-scale circulation features in the lower troposhere with a strong zonal component, which are considered to be key features of the MENA climate. The world's two major monsoons, Indian Summer Monsoon (ISM) and WAM, are the major circulations among them. These circulations reside in the proximity of the MENA dust belt, at the eastern and western boundaries, respectively; which is not by coincidence but due to the strong coupling between monsoon and deserts (e.g., *Rodwell and Hoskins*, 1996). Though these two synoptic systems have their origin partly outside of the MENA domain, especially ISM, they are considered to be some of the major drivers of climate in the region. Therefore the dust impact on these synoptic circulations could effectively feedback the responses inside MENA. Again, this is another good example, showing the advantage of a GCM over RCM for the regional climate sensitivity to some forcings, since GCMs account for the forcing induced changes outside the domain of interest and its influence back in the domain. WAM is particularly decisive in defining the regional climate over equatorial Africa, as they are the major moisture supplying circulation for the interior tropical Africa. Hence, changes in the strength and latitudinal extent of WAM are particularly important for equatorial Africa, especially for Sahel which marks the boundary of the ascending limb of regional Hadley circulation.

Similarly, the heat lows over interior deserts such as SHL, Sudan Heat Low (SuHL) and Arabian Heat Low (AHL) are also vital in configuring the circulation pattern over MENA region. Any changes in the strength and position of these quasi-static lows due to dust direct radiative effect could also mediate the net climate response over this region.

1.2.5 Dust Shortwave Absorption: An important Uncertainty in the Estimation of Direct Radiative Effect

Although prior studies demonstrated various plausible mechanisms involved in the dust-rainbelt interaction, significant uncertainty still remains in both quantitative and qualitative conclusions among these studies. Uncertainty in the response of tropical rainbelt across MENA to dust radiative effect is a good example. Many of the prior modeling studies showed strengthening of the summer rainbelt across MENA, in response to dust direct radiative effect (e.g., *Lau et al.*, 2009; *Yue et al.*, 2011b; *Bangalath and Stenchikov*, 2015), while others predict its weakening (e.g., *Yoshioka et al.*, 2007; *Yue et al.*, 2011a). The uncertainty in the dust refractive index estimates and the consequent uncertainty in the dust shortwave absorption are proposed to be a major cause of the disparity (e.g., *Solmon et al.*, 2008; *Miller et al.*, 2004b).

The imaginary part of complex refractive index represents the strength of dust absorption, which is a function of the iron oxide content in the particle such as hematite and geothite (e.g., *Patterson et al.*, 1977; *Claquin et al.*, 1998; *Sokolik and Toon*, 1999). It has been shown that the values of the imaginary part of the shortwave refractive index, vary by an order of magnitude among various studies (*Balkanski et al.*, 2007). As a result, the SSA, an optical measure that characterizes the ratio between scattering and absorption in the total extinction, also varies significantly. Among various estimates, the value of bulk SSA (at 500 nm) ranges from highly absorbing values (0.7 - 0.9) (e.g., *Otto et al.*, 2009; *Slingo et al.*, 2006; *Raut and Chazette*,

2008; *Haywood et al.*, 2001) to almost non-absorbing values that go higher up to 0.99 (e.g., *Tanré et al.*, 2001; *Osborne et al.*, 2008; *Dubovik et al.*, 2002). Furthermore, measurements from in situ dust samples generally infer higher shortwave absorption than that from remote sensing techniques (e.g., *Haywood et al.*, 2003; *Kaufman et al.*, 2001). It should also be noted that dust chemical properties and refractive indices vary depending on the source region. That is, each dust particle is different in terms of SSA. In short, there is no general agreement on the strength of dust shortwave absorption and the value of SSA. This disagreement among various estimates continues to be an area of active debate among climate scientists.

The large uncertainty in the dust SSA estimates among various observational and modeling studies could induce similar uncertainties in the sign and magnitude of radiative forcing and corresponding climate responses. Many previous studies attempted to quantify the uncertainty in radiative forcing related to shortwave absorption (e.g., *Balkanski et al.*, 2007), however, very few attempted to estimate the sensitivity of the resulting climate responses, especially on a regional scale. That said, a broad scrutiny of the previous modeling studies shows that the simulations that predicted weakening of the MENA rainbelt in response to dust radiative effect used less absorbing dust (large SSA) (e.g., *Yoshioka et al.*, 2007; *Yue et al.*, 2011a), whereas those that predicted a strengthening of the rainbelt used highly absorbing dust (e.g., *Lau et al.*, 2009; *Yue et al.*, 2011b; *Bangalath and Stenchikov*, 2015). However, models used in these previous studies differ from each other not only in the strength of dust shortwave absorption but also in other aspects such as total dust loading and its spatio-temporal variability, various optical properties of dust, model resolution, model components and models' internal variability. Therefore, an inter-comparison of these previous studies cannot faithfully draw conclusions on the sensitivity of climate response to dust shortwave absorption. It all boils down to the need for simulations from a single model with varying amounts of dust shortwave absorption, for a better

assessment of the sensitivity. There were some specific efforts along this line, which were conducted using either coarse resolution global models or regional climate models. The global experiments with GCMs generally focus on global scale responses and they refrain from detailed regional analysis mainly due to their conventional coarser spatial resolution (e.g., *Colarco et al.*, 2014). On the contrary, the experiments using RCMs (e.g., *Solmon et al.*, 2008) fail to incorporate the global-scale circulation response to dust radiative forcing that span outside the domain of RCM, although they represent regional-scale responses in detail. An original and forthright solution to overcoming these issues is to use high-resolution global simulation.

1.2.6 High-resolution global simulations for regional climate studies

Dust in the atmosphere is not uniformly distributed in space as well as in time. Spatially, the dust loading is mainly confined to the dry subtropics associated with major deserts, among which North African and Arabian deserts are the most prominent dust source regions, accounting for more than half of the global dust emissions (*Prospero et al.*, 2002). It has already been demonstrated that the climate response to such spatially inhomogeneous forcing is not necessarily collocated with the forcing (e.g., *Mitchell et al.*, 1995; *Shindell and Faluvegi*, 2009; *Shindell et al.*, 2010). Rather, the response could extend well beyond the forcing location. Tropical atmosphere is especially efficient in adjusting and redistributing localized forcings throughout the tropics, because of its large Rossby Radius of deformation, compared to mid-latitude (*Yu and Neelin*, 1997). Unlike the mid-latitudes, where the poleward heat transport is achieved by transient baroclinic eddies and stationary waves, large-scale overturning circulations function as heat transporting mechanism in the tropics (e.g., *Trenberth and Solomon*, 1994). The regional climate in the tropics thus greatly depends on the strength and spatio-temporal extent of the global scale overturning circulations

such as Hadley and Walker circulations along with synoptic scale circulations such as Jet streams and monsoons. As these circulations determine the sequence of weather events, they ultimately define the climatic regimes of a given region (*Giorgi and Mearns*, 1991). Therefore it is essential to incorporate not only the regional circulation features but also global circulation responses to study the regional climate response to dust forcing. However, the coarser spatial resolution of conventional GCMs and the forced boundary conditions in the RCMs were the main hurdles in modelling and analyzing these aspects (*Sud et al.*, 2009). The Majority of modeling studies, which explored the influence of mineral dust radiative forcing on the climate, used coarse resolution GCMs (e.g., *Miller and Tegen*, 1998; *Yoshioka et al.*, 2007; *Perlwitz et al.*, 2001; *Lau et al.*, 2009; *Yue et al.*, 2011a), though there are a few studies using RCMs (e.g., *Ahn et al.*, 2007; *Konare et al.*, 2008; *Solmon et al.*, 2008). On the one hand, RCMs offer the advantages of a sufficient resolution for regional climate sensitivity studies, but with the caveat of lacking the two-way interaction between regional and global scale responses to dust. On the other hand GCM experiments were constrained by their coarse resolution to analyze the regional climate responses, though they incorporate the expansive representation of dust-climate interaction.

In this context, the current research exploits the high spatial resolution capabilities of an AGCM, High Resolution Atmospheric Model (HiRAM), to investigate the dust direct radiative effect on the regional climate of MENA. Global simulations have been conducted at a spatial resolution of 25 km, which ensure an ample resolution for regional climate sensitivity analysis in conjunction with the ability to account for global and regional responses to dust direct radiative effect. More specifically, our high-resolution simulations provide a unique opportunity to examine, how the dust induced circulation anomalies at various scales, influence regional climate. To the best of the authors' knowledge, there are few published results on dust-climate interaction using a GCM at a spatial resolution of about 25 km or better and, in this

sense, this study is a forerunner.

1.3 Research Questions

The dissertation aims to explore the direct radiative effect of mineral dust on MENA climate. In view of the fact that regional climates are determined by both the local radiative balance and the global to regional scale circulation patterns, the study utilizes the high-resolution capabilities of a global model (HiRAM), which account for multi-scale circulations and their mutual interactions. HiRAM simulations at a spatial resolution of 25 km, with and without dust radiative effects, are conducted to demonstrate the climate response to direct radiative effect. Specific research questions addressed by the dissertation are listed below.

1. **Estimation of DDRF and radiative heating rates, as measures of dust direct radiative effect.**

   To assess and attribute the mineral dust radiative effect on the climate, estimation of the DDRF is indispensable. The spatiotemporal characteristics of the DDRF, at surface, within the atmosphere and at the TOA is estimated. Since the instantaneous response to the dust radiative effect in the atmosphere is to change the atmospheric energy balance, the corresponding changes in the radiative heating rate will also be analyzed in detail.

2. **How does MENA climate respond to dust direct radiative effect? And, how do multi-scale circulation responses mediate the net climate response?**

   MENA is the most dust laden region on the globe and supposedly a region that is hugely impacted by dust radiative effect. The region is characterized by extremely high temperature and scarce rainfall. The climate of this region is greatly controlled by both the large-scale overturning circulations, and regional

scale circulations such as monsoon, jets and waves. Therefore, responses in circulations to dust radiative effect at different scales could greatly mediate the net response in the rainfall and temperature of the region. The study thus analyses the responses in the main circulation features at various scales and their mutual interactions, to understand the climate response of MENA to dust radiative effect.

3. **What is the role of dust direct radiative effect on Sahel rainfall?**

   A major focus of the study will be the much debated scientific question on the role of dust forcing on Sahel rainfall: Whether dust radiative effect will green Sahel or not? To answer this question, the response of regional Hadley circulation over Africa, whose strength and spatial extent are crucial in defining the climate of Sahel, is analyzed extensively. The study give a special emphasize to this question through out the dissertation.

4. **How sensitive are the climate responses to varying dust shortwave absorption?**

   Shortwave absorption is one of the most important, but the most uncertain, components of direct radiative effect by mineral dust. It has a broad range of estimates from different observational and modeling studies and there is no consensus on the strength of absorption. The study aims to elucidate the sensitivity of the MENA climate to a plausible range of uncertainty in dust shortwave absorption. By conducting simulations with various dust shortwave absorption, the study explores the sensitivity of the climate and circulation responses at different scales.

Chapter 2

Model and Experiment Design

The global simulations at horizontal resolution of 25 km and even higher are becoming possible nowadays due to improved super-computing infrastructure and highly scalable dynamical cores (e.g., *Zhao et al.*, 2009; *Shaffrey et al.*, 2009; *Lin*, 2004; *Putman et al.*, 2005; *Hack et al.*, 2006). At this range of spatial resolution, models explicitly resolve important mesoscale features, weather events (e.g., *Zhao et al.*, 2009; *Jung et al.*, 2012) and better simulate the orographically induced circulations and associated precipitation modulations (e.g., *Boyle and Klein*, 2010; *Lau and Ploshay*, 2009). In the present study experiments are conducted using such a high resolution AGCM, HiRAM, developed at Geophysical Fluid Dynamics Laboratory (GFDL) (*Zhao et al.*, 2009).

The general idea of the experiment is to conduct HiRAM simulations with and without dust radiative effects, to descry the dust effect on climate. In order to delineate the sensitivity the sensitivity of climate response to dust shortwave absorption, simulations with varying shortwave absorption have been conducted.

2.1 High Resolution Atmospheric Model (HiRAM)

HiRAM was designed to provide an improved representation of weather events in a GCM and to use for applications ranging from weekly forecast to climate projections. The model is developed based on the GFDL Atmospheric Model version 2 (AM2) with certain modifications, as explained in *Zhao et al.* (2009). It has horizontal resolution

flexibility up to a few kilometers and has an improved vertical resolution (32 levels) compared to AM2. HiRAM employs a finite-volume cubed-sphere dynamical core (*Lin*, 2004; *Putman and Lin*, 2007). The present study uses the C360 version of HiRAM which has 25-km horizontal grid spacing with 360 by 360 finite-volume cells on each face of the cube. A non-intrusive shallow convective scheme (*Bretherton et al.*, 2004) replaces the customary deep convective scheme by extending the former to simulate deep convection (*Zhao et al.*, 2009). The model preserves most of the parameterizations of its parent model AM2, including radiative transfer, surface flux, boundary layer, orographic gravity wave drag parameterizations and large-scale cloud microphysics, with necessary modifications as resolution increases. The shortwave and longwave radiative parameterizations are the modified *Anderson et al.* (2004) schemes of *Freidenreich and Ramaswamy* (1999) and *Schwarzkopf and Ramaswamy* (1999), respectively. The present study conducts AMIP-style simulations forced with the observed monthly Sea Surface Temperature (SST) from the Hadley Centre Sea Ice and Sea Surface Temperature (HadISST) data set (*Rayner et al.*, 2003). The model is coupled to the new GFDL land model version 3 (LM3), as the land component.

The aerosol concentrations, including dust, are prescribed from the offline calculations of a global chemistry transport model, the Model for OZone and Related chemical Tracers (MOZART) (*Horowitz et al.*, 2003). The estimates of the concentrations of aerosol are found to be within a factor of 2 of the observed values (*Ginoux et al.*, 2006). Dust sources are from the Goddard Chemistry Aerosol Radiation and Transport (GOCART) model (*Ginoux et al.*, 2001). Dust size distribution is discretized into eight bins from 0.1 to 10 μm. Dust optical properties are estimated by assuming all dust particles originates from Sahara. The study also assumes the dust particles are hydrophobic, which makes the dust optical properties independent of ambient humidity. A detailed validation of the concentration and distribution of dust loading data used in the present study has been done in *Ginoux et al.* (2006). The

seasonal cycle and spatial distribution of dust loading have been well represented. And it has also been shown that the comparison of AOD (in the present data set) with satellite and ground-based measurements is most accurate over regions where and when dust dominates the total extinction (*Ginoux et al.*, 2006). The specific extinction coefficients of dust are calculated from Mie theory using refractive indices from the recent estimates of *Balkanski et al.* (2007), for shortwave bands, and from *Volz* (1973) for longwave bands. Calculations assume three different cases of hematite content in dust by volume, 2.7%, 1.5% and 0.9%, which represent dust as a very efficient, standard and inefficient shortwave absorber, respectively (*Balkanski et al.*, 2007).

2.2 Experiment Design

Four HiRAM experiments (Table 2.1) are conducted for a 11 year period (1999−2009). Each of these experiments comprises three ensemble members simulated from slightly different initial conditions. One seasonal cycles (one year) is omitted from further analysis to avoid a spin-up period. The "NoDUST" experiment omits dust radiative forcing in the simulations. The three other simulations, "DUST0.9", "DUST1.5" and "DUST2.7" accounts for the radiative effect of dust with a hematite content of 0.9%, 1.5% and 2.7% respectively. Atmospheric response to dust direct radiative effect can then be estimated as the difference in climate variables between with and without dust experiments. Similarly, the sensitivity of atmospheric response to varying dust shortwave absorption can be estimated by an inter-comparison of the anomalies of climate variables in these three different simulations, compared to the NoDUST simulation.

2.3 Calculations of Direct Radiative Effect

In general, radiative forcing and heating rate anomalies are used as a general metric to characterize the radiative impact of aerosol on climate. Fundamentally, both the measures represent the change in radiation or heating rate due to the presence of aerosol in the atmosphere. However the estimation of these metrics require the calculation of instantaneous changes in radiative fluxes due to aerosol. In the present study, to estimate the instantaneous radiative flux changes due to dust loading, the model calls the radiation calculation twice at each radiation time step: one with dust influence and the other without dust influence. But, only the radiation fluxes calculated with dust radiative effect feedback to the model evolution. Thus, the instantaneous radiative forcing and heating rate anomalies can be estimated as the differences in instantaneous fluxes and heating rates calculated with and without the dust effect, respectively.

Table 2.1: Experiment design

Experiment	Description
NoDUST	Omit dust radiative effect in the simulation
DUST0.9	Include dust radiative effect with optical properties assuming 0.9% of hematite content by volume.
DUST1.5	Include dust radiative effect with optical properties assuming 1.5% of hematite content by volume.
DUST2.7	Include dust radiative effect with optical properties assuming 2.7% of hematite content by volume.

2.4 AMIP type simulations and SST feedback

It is important to note that in our Atmospheric Model Intercomparison Project (AMIP)-style simulations SST is prescribed with observed values. Such simulations fail to account for the the potentially important SST feedback on the hydrologic cycle. However, since prescribed SST assumes an ocean with infinite heat capacity,

climate response from these simulations could be more representative of the response over a time period of ocean response delay due to thermal inertia (*Allen and Sherwood*, 2011; *Lau et al.*, 2006; *Randles et al.*, 2013). In other words, the analyses and interpretations in the present study should be understood as those based on the atmosphere-only processes. Nevertheless, since the observed SST comprises the anomaly caused by the physical-world forcings, simulations will be able to capture the features which usually fail in coupled GCM experiments (*Ott et al.*, 2010; *Randles et al.*, 2013). In other words, AMIP-style approach provides an ideal mean ocean forcing, which helps to avoid the cold SST bias in equatorial ocean common to most of the coupled GCMs, and hence helps to improve the representation of the strength and position of the climatological mean rainbelt. It is well known that the Atlantic SST in general, and specifically the near-equatorial SST gradient, plays an important role in defining the strength and position of the rainbelt over MENA region (e.g., *Folland et al.*, 1986; *Nicholson and Dezfuli*, 2013; *Davey et al.*, 2002; *Cook*, 2008).

Chapter 3

Dust Direct Radiative Effect

Radiative forcing and heating rate are the two most often used measures to characterize aerosol radiative effect on climate (e.g., *Miller and Tegen*, 1998; *Yoshioka et al.*, 2007; *Perlwitz et al.*, 2001; *Lau et al.*, 2009; *Yue et al.*, 2010). Both the measures help to quantify the perturbations in the radiative energy balance of the system, due to the presence of aerosols. Direct radiative forcing and heating rate anomalies are calculated and presented in the present chapter, to characterize the direct radiative effect of dust aerosols on the climate. This chapter is largely composed of the content from the two papers (*Bangalath and Stenchikov*, 2015, 2016) published as part of the dissertation research.

3.1 Dust Direct Radiative Forcing

A generic definition of radiative forcing of aerosols would be the radiative flux perturbation induced by aerosols prior to any climate response (*Hansen et al.*, 2005). Complying with this, DDRF is defined and estimated as the "*net (longwave + shortwave) radiative flux difference between a state with dust loading and that without dust loading (downwelling minus upwelling), calculated under the same meteorological conditions*," in the current research. Hence, positive values represent warming of the system, due to the presence of dust, while negative values indicate a cooling of the system. Since mineral dust aerosol is an effective absorber at short wavelength, the change in radiative fluxes within the atmosphere and at surface are equally as

important as of that at the top of the atmosphere (e.g., *Miller et al.*, 2004a). Therefore the DDRF is estimated at both the surface and TOA. The difference between the DDRF at TOA and that at surface can be deduced as the dust induced heating or cooling in the atmosphere, which has the potential to alter the vertical stability of the atmospheric column and temperature gradients, resulting in further circulation changes.

Typically, aerosol radiative forcing estimations using information derived from satellite or AERONET observations, are done only under clear-sky conditions, as it is not straightforward to screen out the cloud effect on radiation from that of the aerosols when they are collocated. Modeling studies generally prefer to estimate forcing under all-sky conditions, mainly due to the uncertainties in cloud-free scenes in the models (*Chin*, 2009). However, keeping in mind the disagreement between satellite and modeling based estimates on dust absorption and DDRF (e.g., *Haywood et al.*, 2003; *Kaufman et al.*, 2001; *Moulin et al.*, 2001), the present study estimates both clear-sky and all-sky forcing. Since clouds can mask the light scattered from aerosols, aerosol direct radiative forcing is generally less at all-sky conditions than that at clear-sky conditions (e.g., *Schulz et al.*, 2006).

3.1.1 Global and Regional Averages

Annually averaged estimates of DDRF, for the three experiments assuming different shortwave absorption, are shown in Table 3.3 and 3.4. DDRF is averaged separately for Global and MENA domain, to show the heightened regional impact over MENA. Averaged values of dust SSA corresponding to each experiment and domain are shown in Table 3.1. The globally averaged dust SSA estimates range from 0.94 (in DUST0.9) to 0.86 (in DUST2.7). As dust shortwave absorption increases, the SSA value naturally decreases as it is the ratio of scattering to total extinction.

The globally averaged DDRF at TOA is negative (cooling) in experiments as-

Table 3.1: Averge SSA

Experiment	*Domain*	*Average SSA* (at 550 nm)
DUST0.9	Global	**0.94**
	MENA	**0.93**
DUST1.5	Global	**0.90**
	MENA	**0.89**
DUST2.7	Global	**0.86**
	MENA	**0.84**

suming dust as an inefficient (DUST0.9) and standard (DUST1.5) absorber, in both all-sky (Table 3.2) and clear-sky (Table 3.3) conditions. However, the magnitude of forcing reduces as absorption increases and ultimately changes the sign (except for global clear-sky) into positive (warming) in efficient absorber experiment (DUST2.7). The globally averaged estimates range from -0.18 W/m^2 (DUST0.9) to +0.04 W/m^2 (DUST2.7) in all-sky condition and from -0.34 W/m^2 (DUST0.9) to -0.14 W/m^2 (DUST2.7) in clear-sky condition, as shortwave absorption increases. These values compare well with the previous estimates (see Table 1 in *Yue et al.* (2010) and Table 6 in *Balkanski et al.* (2007)). Consistent with the previous studies, the all-sky forcing is in general significantly less than the clear sky forcing. Regionally, over MENA the forcing is almost one order higher than the global average.

Table 3.2: Annual All-sky DDRF

Experiment	*Domain*	*DDRF TOA*			*DDRF Surface*			*DDRF ATM*
		SW	LW	NET	SW	LW	NET	NET
DUST0.9	Global	-0.29	+0.11	-0.18	-0.83	+0.37	-0.46	**+0.27**
	MENA	-2.11	+1.08	-1.03	-7.47	+4.35	-3.12	**+2.09**
DUST1.5	Global	-0.20	+0.11	-0.09	-0.95	+0.36	-0.59	**+0.49**
	MENA	-1.28	+1.05	-0.23	-8.60	+4.22	-4.38	**+4.15**
DUST2.7	Global	-0.07	+0.11	+0.04	-1.15	+0.36	-0.79	**+0.83**
	MENA	-0.08	+1.04	+0.96	-10.49	+4.19	-6.30	**+7.27**

At surface the net forcing is the sum of the radiative perturbations due to absorption and scattering in the atmosphere and hence is always negative (cooling). Since dust is a good absorber at short-wavelength, the magnitude of surface DDRF is always much higher than the TOA forcing. Surface forcing significantly increases

Table 3.3: Annual Clear-sky DDRF

Experiment	*Domain*	*DDRF TOA*			*DDRF Surface*			*DDRF ATM*
		SW	LW	NET	SW	LW	NET	NET
DUST0.9	Global	-0.48	+0.15	-0.34	-1.07	+0.45	-0.63	**+0.29**
	MENA	-2.68	+1.36	-1.32	-8.68	+5.01	-3.67	**+2.35**
DUST1.5	Global	-0.41	+0.15	-0.26	-1.23	+0.45	-0.78	**+0.52**
	MENA	-1.87	+1.33	-0.54	-10.05	+4.89	-5.16	**+4.63**
DUST2.7	Global	-0.28	+0.14	-0.14	-1.46	+0.44	-1.02	**+0.88**
	MENA	-0.63	+1.31	+0.68	-12.20	+4.86	-7.33	**+8.02**

as shortwave absorption increases (Table 3.2 & 3.3). The globally averaged values lie between -0.46 W/m^2 (DUST0.9) to -0.79 W/m^2 (DUST2.7) in all-sky condition and between -0.63 W/m^2 (DUST0.9) to -1.02 W/m^2 (DUST2.7) in clear-sky condition. Again, these forcings are much higher over MENA.

The DDRF within the atmosphere (difference between DDRF at TOA and at surface) can be deduced as the net dust induced heating within the atmosphere, which ultimately perturbs the stability, cloud formation (semi-direct effect)(e.g., *Hansen et al.*, 1997) and consequently multi-scale circulations and precipitation. The DDRF within the atmosphere is always warming (positive), which indicates that the shortwave heating dominates the longwave cooling (Table 3.2 & 3.3). Atmospheric warming increases as shortwave absorption increases. The globally averaged forcing ranges from +0.27 W/m^2 to +0.83 W/m^2 in all-sky conditions and from +0.29 W/m^2 to +0.88 W/m^2 in clear-sky conditions.

In general, the MENA region experiences contrastingly high forcing at all levels compared to the global average and the difference is almost one order of magnitude. This is because the region has high dust loading associated with major source regions and a relatively higher ratio of coarse to fine mode dust particles (not shown) near these source regions. Higher coarse mode dust fraction leads to reduced SSA and increased absorption (e.g., *Otto et al.*, 2009; *Ryder et al.*, 2013). This is why the MENA region experiences reduced SSA compared to the global average (Table 3.1).

3.1.2 Spatial Characteristics

As the present study specifically focuses on climate responses during the boreal summer season, the spatial pattern of summer DDRF are depicted for different experiments separately at TOA, surface and within the atmosphere. Figure 3.1. shows global patterns of all-sky DDRF at TOA during summer, for all the three experiments, assuming varying dust shortwave absorption.

The most noticeable feature of the TOA forcing, in general, is the change in the sign of the forcing regionally. Over bright deserts the forcing is positive (warming) and over darker ocean, it is negative (cooling). This is due to the fact that the TOA aerosol forcing is highly dependent on the effective albedo of the underlying surface ("albedo effect") in addition to its dependency on the physical, chemical and optical properties of the particles (e.g., *Liao and Seinfeld*, 1998; *Claquin et al.*, 1998; *Stier et al.*, 2007; *Chỳlek and Coakley*, 1974; *Kaufman*, 1987). In other words, if the combined aerosol-surface system reflects less solar radiation than does the surface alone, the TOA forcing becomes positive (warming the system). Over bright deserts, where surface albedo generally exceeds 0.3, the low SSA values of dust can lead to a combined dust-surface system darker than the underlying surface. Therefore, the value of dust SSA becomes a decisive factor in determining the sign of the TOA forcing over deserts. However, over dark surfaces like the ocean, where surface albedo is generally less than 0.1, it is less probable to have positive forcing with the range of SSA that dust generally has. Moreover, absorbing aerosols such as dust, situated above a cloud layer, can induce positive TOA forcing in all-sky conditions, as the cloud layer can effectively act as a brighter underlying surface in this case (e.g., *Schulz et al.*, 2006; *Haywood and Ramaswamy*, 1998).

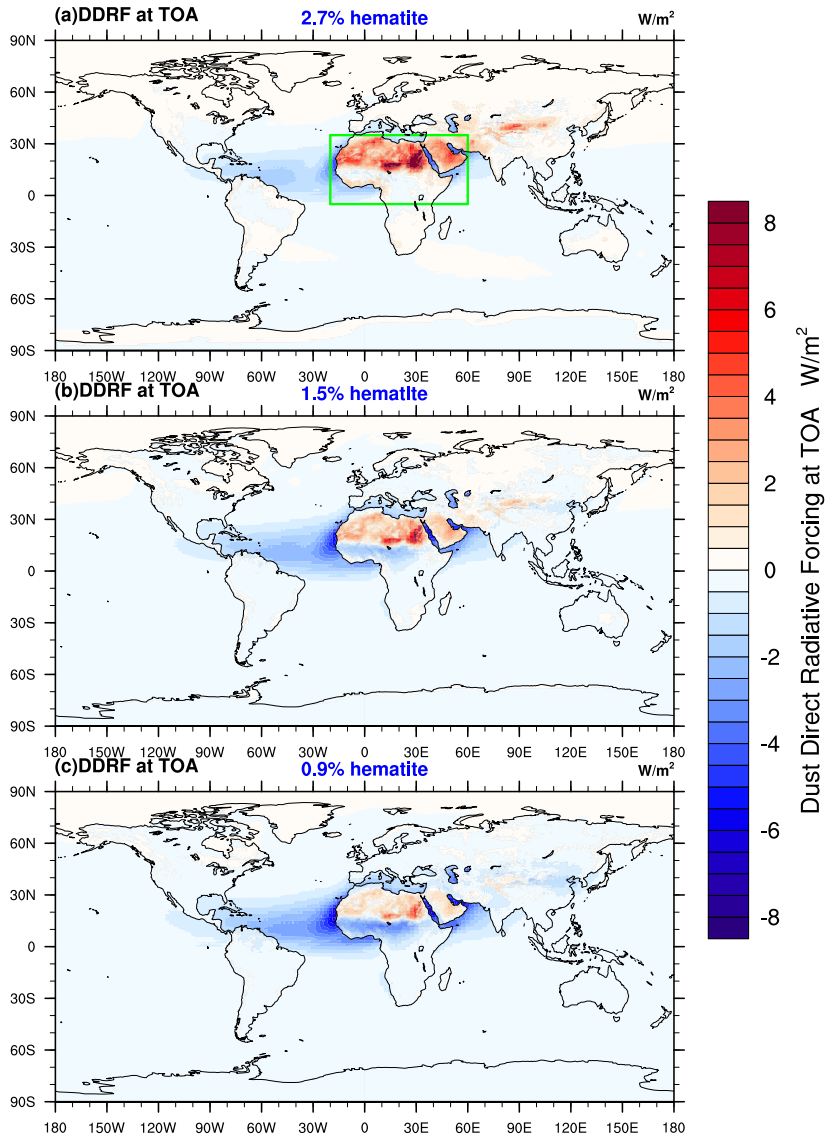

Figure 3.1: Mean summer (JJA) all-sky DDRF (W/m^2) at TOA while dust is assumed to be a (a) very efficient (DUST2.7 case), (b) standard (DUST1.5 case) and (c) inefficient (DUST0.9 case) absorber at shortwave. Positive values represent warming of the system and negative values denote cooling of the system, by definition. The green rectangle in Figure 1a outlines the borders of MENA region.

In terms of the sensitivity of the TOA forcing to varying dust shortwave absorption, the positive forcing (warming) over MENA diminishes and even changes the sign as SSA increases (going from DUST2.7 to DUST0.9), especially at regions like Sahel. Similarly, the cooling over the oceanic region (negative TOA forcing) enhances as the shortwave absorption reduces. In effect there is a contrast even in the magnitude

of the TOA forcing between adjacent land and ocean. As the shortwave absorption increases (from DUST0.9 to DUST2.7), positive TOA forcing over land intensifies and negative TOA forcing over ocean reduces significantly. It implies that if the dust assumes high SSA value, the major impact will be over land (deserts) rather than the downwind oceanic region, in terms of TOA forcing. This differential TOA forcing over adjacent land and ocean could potentially influence local circulations originating from the land-sea thermal contrast, such as WAM and land-sea breezes.

Figure 3.2 depicts all-sky DDRF at surface. At surface, the DDRF is always cooling (negative) as it is the combined effect of absorption and scattering in the atmosphere. Surface forcing is extremely sensitive to the SSA or hematite content, as it is a strong function of the shortwave absorption within the atmosphere. Therefore, as the absorption reduces (Figure 3.2), DDRF at surface also reduces. This indicates the significant role of atmospheric shortwave absorption to the surface DDRF.

Forcing within the atmosphere can be seen as the difference between TOA and surface forcing, which can induce a variety of climate effects by influencing the vertical stability, cloud formation (semi-direct effect or "cloud burning off") and circulation patterns. EHP hypotheses (*Lau et al.*, 2009, 2006) (a regional manifestation of semi-direct effect), is a typical example of how the heating within the atmosphere induced by dust will influence circulation. DDRF (all-sky) within the atmosphere is estimated by subtracting forcing at TOA from that at surface (Fig. 3.3). The forcing is always warming (positive) within the atmosphere, to which the atmosphere primarily respond dynamically. And the magnitude of the forcing is sensitive to shortwave absorption. As expected, warming reduces as shortwave absorption reduces. The heat trapped in the atmosphere (warming) in DUST1.5 experiment is almost twice larger than that of DUST0.9 and it becomes thrice larger in DUST2.7 case.

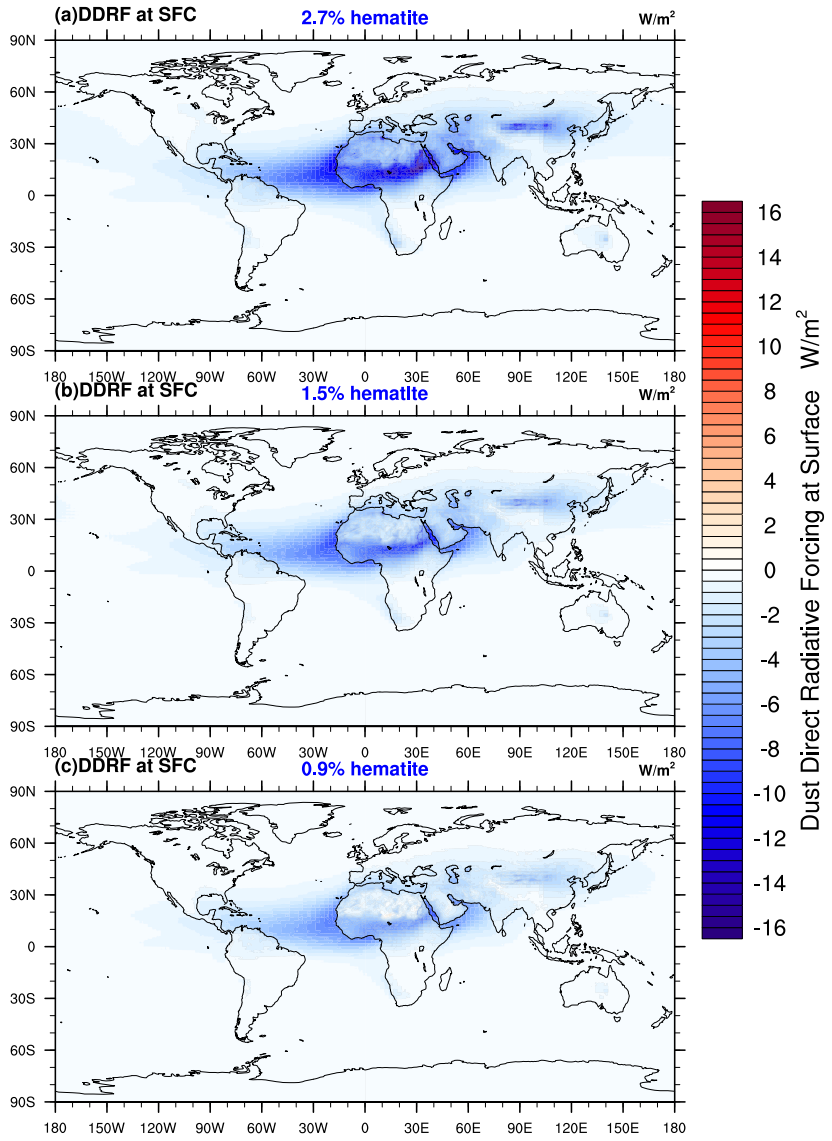

Figure 3.2: Mean summer (JJA) all-sky DDRF (W/m^2) at surface while dust is assumed to be a (a) very efficient (DUST2.7 case), (b) standard (DUST1.5 case) and (c) inefficient (DUST0.9 case) absorber at shortwave. Positive values represent warming of the system and negative values denote cooling of the system, by definition.

The role of surface radiative forcing (reduced radiation in the present case) in the climate response is through changes in surface heat fluxes, dominantly in latent heat flux over the oceanic region. However, negative forcing at the ocean surface does not feedback as reduced latent heat flux in the present simulations, as the bottom boundary condition is prescribed by observed SST. Therefore, as we omit the main feedback from surface forcing, climate response is primarily to the forcing within the

atmosphere (atmosphere-only response).

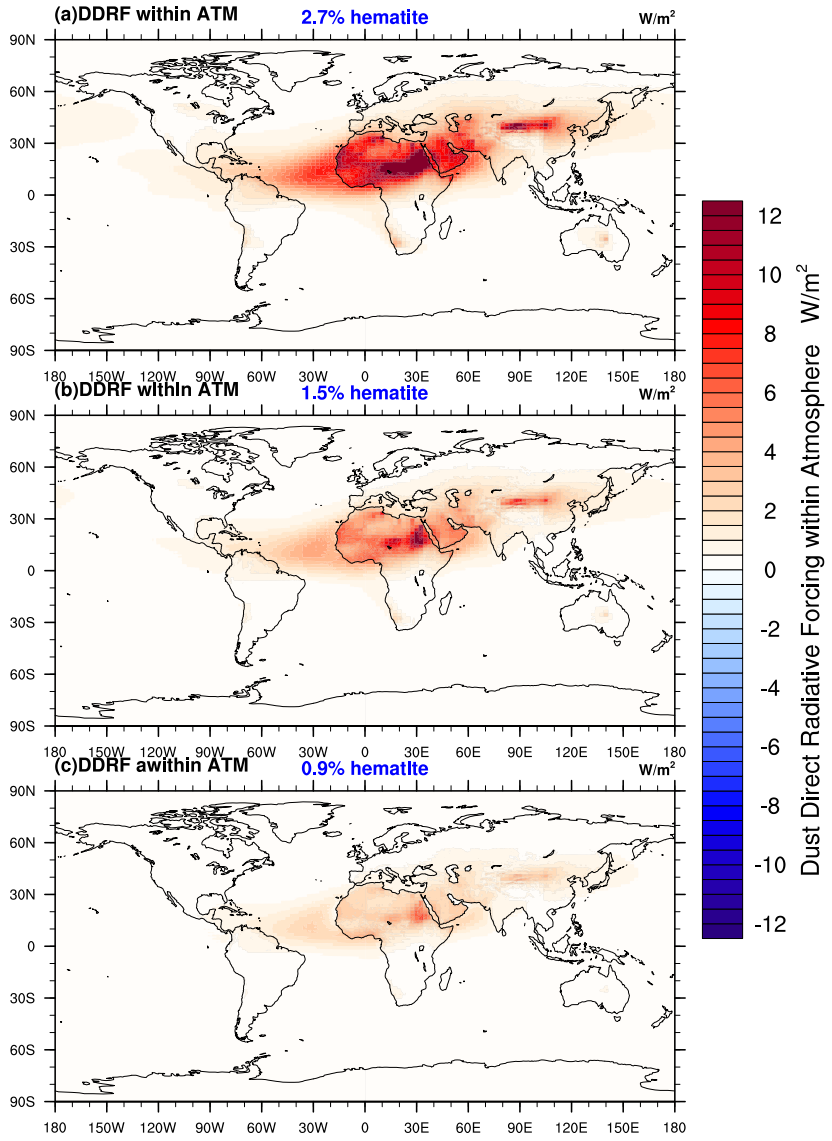

Figure 3.3: Mean summer (JJA) all-sky DDRF (W/m^2) within the atmosphere while dust is assumed to be a (a) very efficient (DUST2.7 case), (b) standard (DUST1.5 case) and (c) inefficient (DUST0.9 case) absorber at shortwave. Positive values represent warming of the system and negative values denote cooling of the system, by definition.

DDRF has a strong hemispheric contrast associated with the fact that the geographical location of the major dust source regions, including major deserts, lies in the northern hemisphere (NH). This contrast in DDRF distribution is most evident over MENA region. To the north of the tropical rainbelt, there is an immense dust

loading and corresponding radiative effect, while dust radiative effect is negligible to the south of the rainbelt. This could induce inter-hemispheric differential heating, which presumably influences the north-south temperature gradient and the local Hadley circulation.

3.2 Dust Induced Radiative Heating Rate

To explicitly portray the radiative perturbation within the atmosphere, its distribution aloft and the north-south gradient in the perturbations, a latitude-height cross section of zonally averaged (20^0W-60^0E) dust induced anomaly (shaded contours) in radiative heating rate (shortwave+longwave) is plotted (Figure 3.4).

To compare the relative importance of the dust induced heating anomaly in the net radiation budget of the region, net radiative heating rate is overlaid as contour lines. Dust induced radiative heating is concentrated over the northern hemispheric subtropics, associated with Sahara and Arabian deserts. The magnitude of the dust induced heating is comparable to the values of the climatological net radiative heating rate and the core of this heating goes up to the middle troposphere (up to 500 hPa). In effect, dust causes a strong hemispheric gradient in the net heating rate throughout the lower-mid troposphere. Most importantly, the net radiative cooling over the northern subtropics is visibly half of that of the remaining tropics, indicating the importance of dust induced heating in the radiative profile of this region. That is to say, the dust induced positive heating rate can effectively reduce the net radiative cooling from the region and it can potentially act as an off-equator heating source. *Lindzen and Hou* (1988) proved that heating off the equator induces profound asymmetries in the Hadley circulation. Their simplified calculations showed that, as the heating moves off the equator, the latitude separating the two cells moves further into the summer hemisphere. In this context, dust induced radiative heating, asymmetrically placed over the northern hemispheric subtropics, is thought to alter the local Hadley

circulation strength and position.

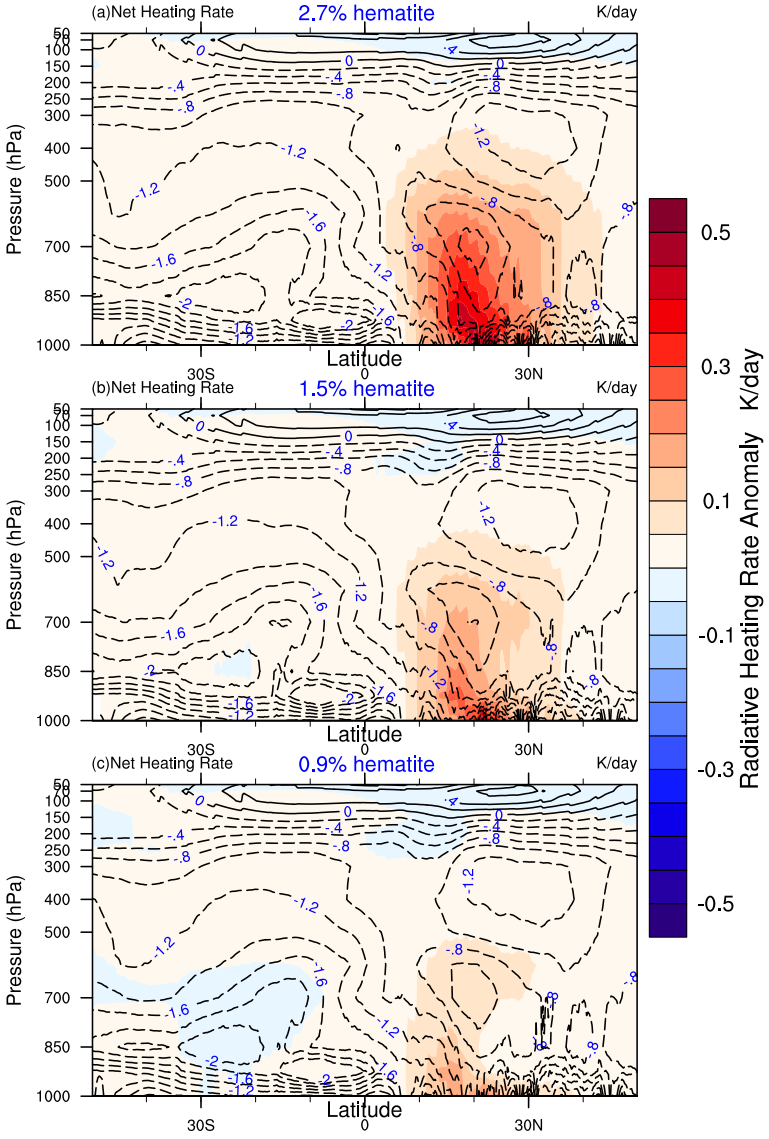

Figure 3.4: Vertical cross-section of zonally averaged ($20^0W - 60^0E$) mean summer (JJA) radiative heating rate (shortwave + longwave) anomaly induced by dust (shaded contours) overlaid on net radiative heating rate as contour lines, while dust is assumed to be a (a) very efficient (DUST2.7 case), (b) standard (DUST1.5 case) and (c) inefficient (DUST0.9 case) absorber at shortwave.

Sensitivity of this asymmetric heating pattern to shortwave absorption, are delineated by portraying the dust induced heating rate anomalies for all three experiments (Figure 3.4). As absorption increases (from DUST0.9 to DUST2.7), the heating rate increases and hence the inter-hemispheric heating gradient also strengthens. This

strengthening of inter-hemispheric heating gradient could potentially make the circulation responses, especially that of those circulations driven by the meridional heating or temperature gradient, sensitive to dust shortwave absorption.

Chapter 4

Climate Responses over MENA and the Role of Overturning Circulations

As seen from the previous chapter (3), scattering and absorption of solar and planetary radiation by dust particles, perturb the radiative energy balance of the atmospheric column. However, the perturbation in the energy balance is not uniform in space as well as in time; rather it varies as a function of dust loading, dust optical properties and the properties of the underlying surface and the atmospheric column. The climate responds to the radiative perturbations, primarily, by adjusting the local temperature profiles which in turn creates pressure gradients in the atmosphere. As a consequence, circulations at various scales changes since they are essentially driven by the pressure gradients in the atmosphere. This chapter provides a detailed investigation on how precipitation and temperature, the two fundamental variables for describing a region's climate, over MENA are influenced by the dust radiative effect and how do the overturning circulation and rainbelt responses mediate the net responses in precipitation and temperature over MENA.

Climate response forced by the direct radiative effect of dust has been characterized and estimated by the difference in the seasonal ensemble mean of meteorological fields between various simulations with dust and that without dust. A statistical significance of the response is estimated at 95% confidence for all these variables, using the two-tailed Student's t-test. The statistically significant areas are marked by hatching in the figures. The model performance has been evaluated by comparing simulated state against observation and re-analyses datasets, in respective sections.

The standard shortwave absorbing case, DUST1.5, is considered for validating the model performance.

4.1 Tropical Rainbelt and Sahel Rainfall

In terms of precipitation, the dominant meteorological feature in the MENA domain is the tropical rainbelt, during summer. The strength, position and the seasonal march of the rainbelt greatly define the region's climate in general, and of Sahel in particular. Tropical rainbelt can be viewed in the first place as the ascending limb of Hadley circulation. However, the regional and local circulations embedded within this large-scale overturning, modify the mean picture of the rainbelt. It is discussed in chapter (5), in detail. The responses in precipitation and cloudiness have been analyzed as a proxy for the response of rainbelt.

Firstly, to evaluate the model performance in reproducing precipitation climatology over MENA, the mean summer (JJA) precipitation has been validated (Figure 4.1) against the GPCP (*Adler et al.*, 2003) data set. Model averaged precipitation captures the key features of the observed precipitation climatology (Figure 4.1) quite realistically, especially the strength and shape of the tropical rainbelt across this region. Additionally, the local precipitation maxima associated with the orographic features are better represented in HiRAM simulations, due to its high spatial resolution. To demonstrate the location of ITCZ defined by wind convergence, zero meridional wind contour between 5^0S to 20^0N is overlaid on the mean precipitation (Figure 4.1b). As previously noted by *Nicholson* (2009), the ITCZ and the tropical rain belts are completely detached and the separation even goes up to about 1000 km in West Africa.

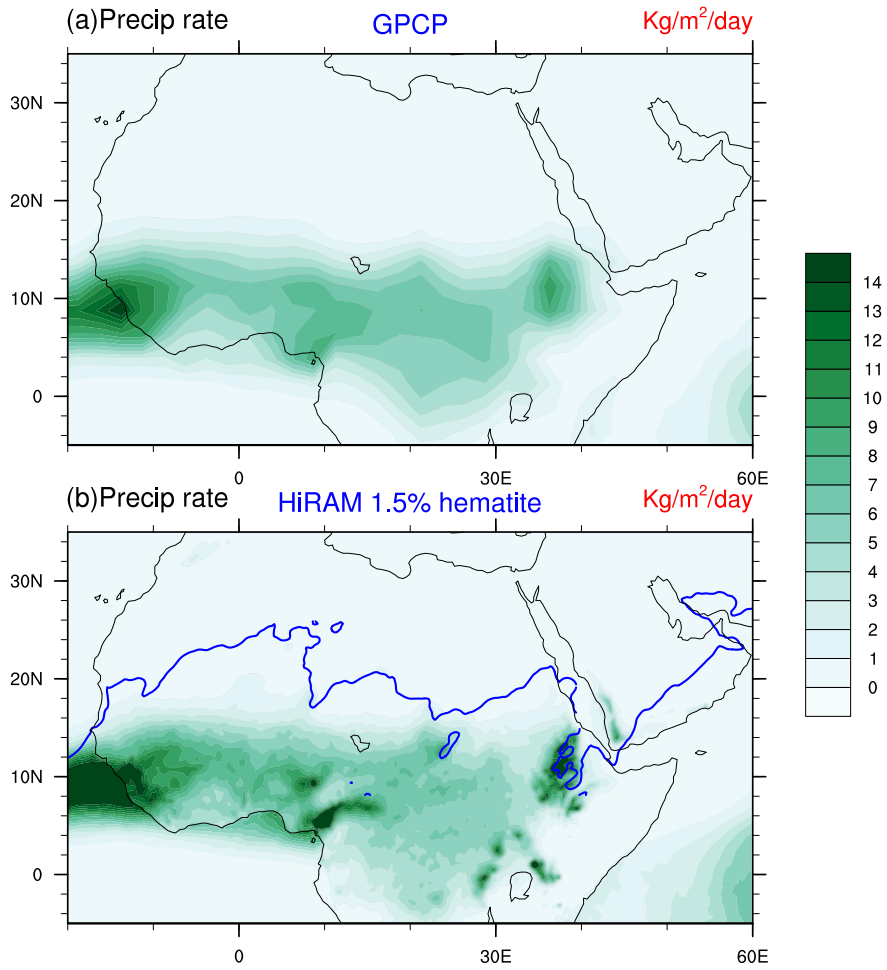

Figure 4.1: Mean Summer (JJA) precipitation rate ($kg/m^2/day$) in (a) Global Precipitation Climatology Project (GPCP) and in (b) HiRAM (DUST1.5 case) simulations.

The response of precipitation to dust radiative effect in all the three cases are shown in Figure 4.2. The thick red contour bounds the area where rainfall is above 3 $kg/m^2/day$ to depict the position of the rainbelt. The shaded contours are the precipitation response in each experiment calculated by subtracting the mean summer precipitation of each experiment with dust from that of the NoDUST experiment. Therefore, the values can be inferred as the changes due to dust radiative effect. In general, a statistically significant precipitation enhancement is predicted in the northern half of the tropical rain belt (Figure 4.2), as a response to dust radiative effect. Conversely, the precipitation weakens in the southern part of the belt, though the

reduction is not statistically significant everywhere. This makes a north-south dipole structure in response, indicating a possible northward shift of the local Hadley cell, which is confirmed hereinafter. However, over West Africa, the dipolar response pattern is not that apparent; instead, a widespread enhancement is predicted throughout the tropics. This could be attributed to the feedback from WAM circulation response, which has dominant zonal flow that covers the entire tropical lower troposphere in West Africa. This response is consistent with the EHP mechanism proposed for the monsoon intensification (*Lau et al.*, 2006, 2009), in response to dust radiative effects. By this mechanism, the warmed air in the elevated dust layer, over West Africa and the eastern Atlantic, rises and spawns a large-scale onshore flow carrying moist air from the eastern Atlantic and the Gulf of Guinea. This enhanced onshore moisture flow increases the cloudiness and rainfall during WAM season, throughout the West African tropics, which in turn makes the north-south dipolar structure of response less pronounced over West Africa. A detailed analyses of the WAM response and its sensitivity to shortwave absorption is given in the following chapter (5).

A comparison of the response among experiments (Figure 4.2) shows that the rainbelt intensity and position of the rainbelt is sensitive to dust shortwave absorption. The rainbelt intensifies and shifts further northward, as the absorption increases (DUST0.9 to DUST2.7). Moreover, as absorption increases, larger areas of the rainbelt response become statistically significant. Furthermore, the dipole pattern in the response almost vanishes as absorption reduces (DUST0.9). Over the semi-arid strip between Sahara and the tropical forest or savanna, including the Sahel region, the predicted precipitation response is about 1.5 $kg/m^2/day$ in DUST2.7 case, which is about 20% of the mean summer precipitation. The response becomes negligible and statistically insignificant as it goes to DUST0.9 case. The semi-arid region including Sahel is climatically very sensitive and ecologically vulnerable and is characterized by strong climatic variations and an erratic rainfall that ranges between 200 mm

and 600 mm annually with coefficients of variation ranging from 15 to 30% (*Fox and Rockström*, 2003). The predicted sensitivity of rainbelt response to dust shortwave absorption is thus crucial for the Sahel climate.

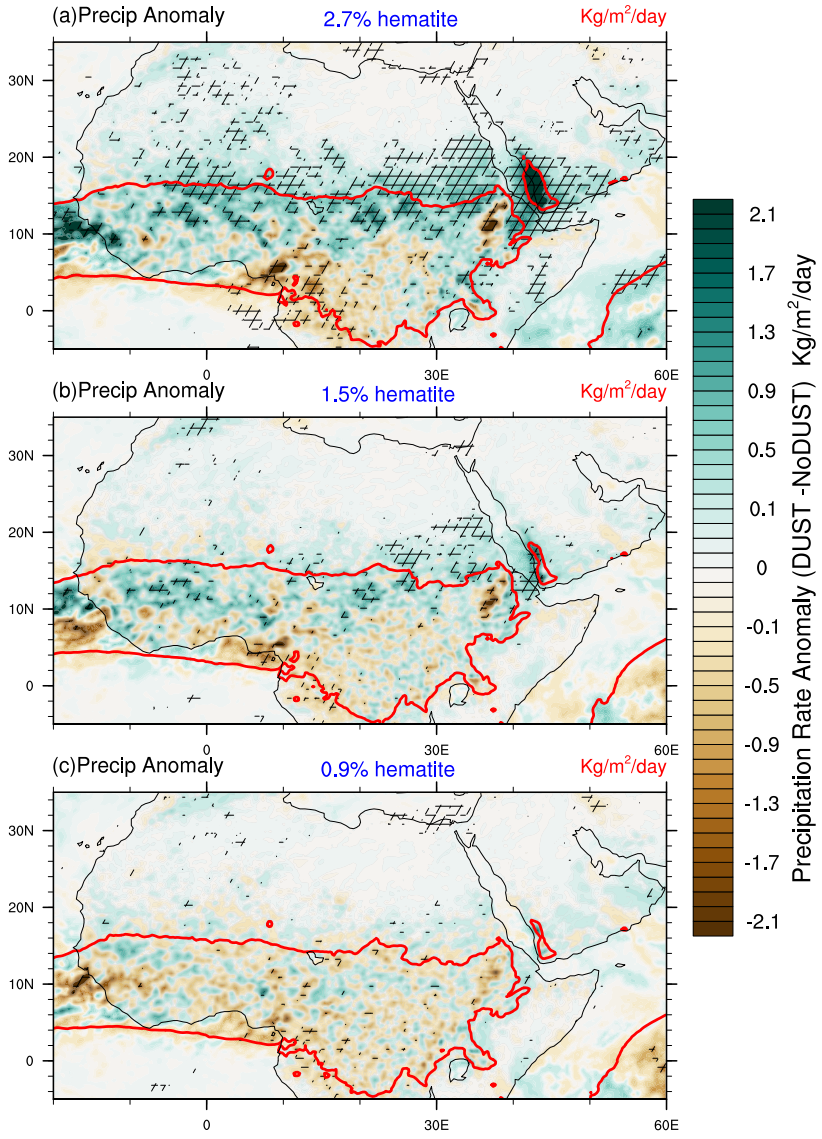

Figure 4.2: Precipitation response ($kg/m^2/day$) to dust radiative effect while dust is assumed to be a (a) very efficient (DUST2.7 case), (b) standard (DUST1.5 case) and (c) inefficient (DUST0.9 case) absorber at shortwave, during summer (JJA). The responses are estimated as the difference between simulations with dust radiative effect and without dust radiative effect. Areas where the response is statistically significant (student's t test) at 95% level, are hatched. The thick red contour overlaid on the shaded response portrays area where rainfall is above 3 $kg/m^2/day$, to depict the position of the rainbelt.

Even though the precipitation response around the rainbelt has a dipole pattern, in general, there are some "hotspots" with strikingly anomalous responses. A statistically significant intense weakening of precipitation, up to about 3 $kg/m^2/day$ (DUST2.7 case), is observed along the eastern extent of CAB (over the Ethiopian Highlands), the north-east directed convergence zone between ISM circulation and unstable air from the Congo. Another hotspot is the southwestern tip of the Arabian Peninsula, where the Tokar gap wind jet interacts with Asir escarpment mountain on the western coast of Arabia. The precipitation enhancement is about 4 $kg/m^2/day$ in DUST2.7 case, which is about 50% of the mean precipitation over this region. Another hotspot in response is over the climatological summer precipitation maxima over the Cameroon highlands and the nearby coast, where the WAM circulation interacts with the highlands. All these areas are, climatologically, very well distinguished as precipitation maxima regions during boreal summer, and the orographic precipitation is the major contributor to the mean rainfall in all of these three regions. Importantly, all these "hotspots" are sensitive to dust shortwave absorption. The response becomes negligibly small and statistically insignificant as shortwave absorption reduces (DUT0.9 case). These locally amplified precipitation responses emphasize the importance of high resolution modelling for assessing regional/local sensitivity to a certain spatially heterogeneous forcing, as in our case.

A more direct proxy for convective activities and the ascending limb of Hadley cell or rainbelt would be the cloudiness. The model performance in reproducing cloudiness in the MENA domain has been validated against ERA-Interim data (*Dee et al.*, 2011) (Figure 4.3). The model captures the mean structure, strength and spatial extent of cloudiness adequately well. Like in the case of precipitation, HiRAM better represent finer details, especially that related to orographic maxima. However, model predicts the northward extent of rainbelt much poleward. In other words, model overestimates rainfall over Sahel region.

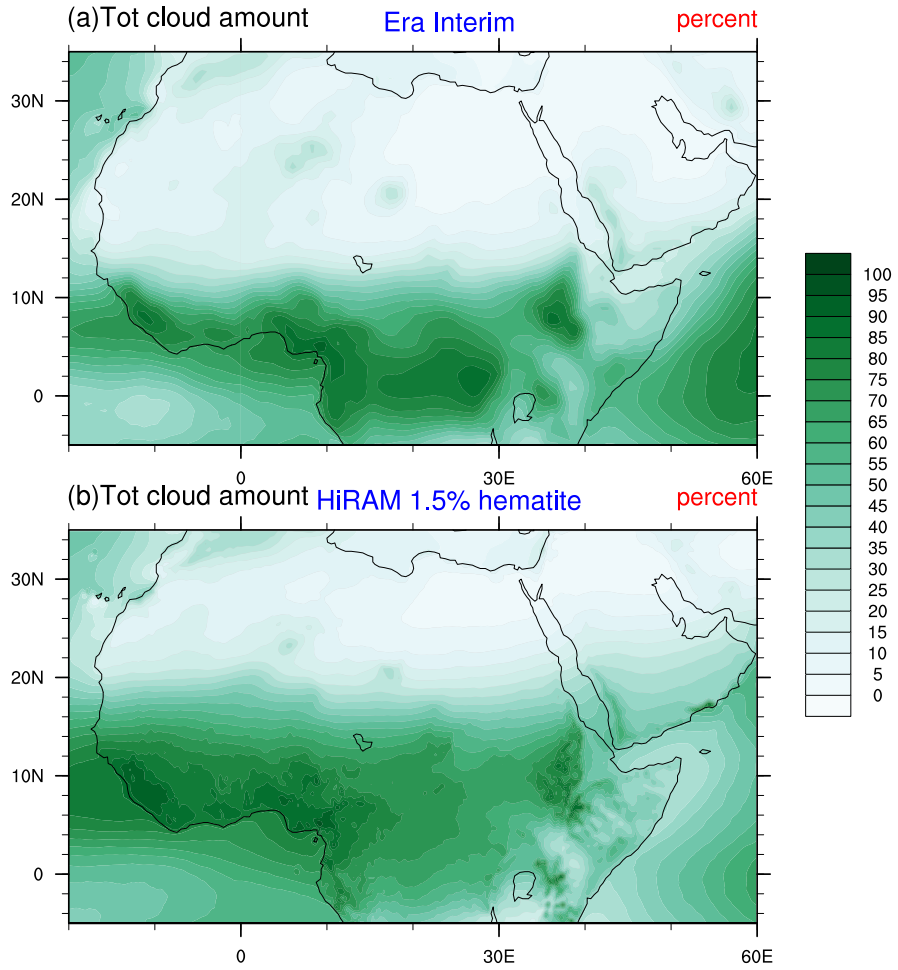

Figure 4.3: Mean Summer (JJA) total cloud amount (%) in (a) Era Interim Reanalyses and in (b) HiRAM (DUST1.5 case) simulations.

The response in cloudiness to dust forcing and its sensitivity to the uncertainty in shortwave absorption are analyzed in Figure 4.4, as a proxy for rainbelt response. Note that the dust indirect effect is not included in the simulations. Thus, the cloud response could either be from the "dust semi-direct" effect (thermodynamic effect), whereby absorption of radiation and the consequent warming of the atmosphere leads to reduction in cloud cover ("burning off clouds") by reducing the ambient relative humidity and evaporation of the clouds (*Hansen et al.*, 1997), and/or from the large-scale dynamic response to dust radiative effect. A wide-spread statistically significant enhancement in the cloudiness throughout the tropics is predicted in response to

dust radiative effect, in all three cases (Figure 4.4). The thick red contour bounds the areas with cloudiness above 70% as a proxy of the position of the rainbelt or the ascending branch of the Hadley cell. Overall, the cloud response is stronger and statistically significant in more areas, compared to the precipitation response. Unlike the precipitation response, the northward extent of cloud cover is more advanced. Cloudiness increases, especially to the north of the rainbelt, as shortwave absorption increases. In DUST0.9 experiment the response becomes almost neutral and it even shows a reversal in the sign of response. Some patches of statistically significant reduction in cloudiness over central Sahel are simulated in the DUST0.9 experiment.

A major contribution to the increased amount of cloudiness is from low clouds (not shown). However, an increase in low cloud amount in response to DDRF is a counterexample to the semi-direct effect ("burning off clouds") (*Perlwitz and Miller*, 2010). Therefore the low cloud response over Sahel could only be expected from the dominant role of global or synoptic scale dynamic response, most probably due to an anomalous northward shift of the ascending branch of Hadley cells and the overall strengthening of the local Hadley circulation. A detailed analysis of the dynamic responses to dust forcing is presented in the following sections.

In general, from the response of both cloud cover and precipitation, it is apparent that the tropical rainbelt enhances and moves farther north in response to dust induced atmospheric heating and these responses are especially sensitive to the amount of shortwave absorption. In the context of Sahelian wet/dry episodes, *Nicholson and Grist* (2001) have noted that the enhanced precipitation over the tropical semi-arid strip including the Sahel, could be either due to a change in the intensity of the tropical rainbelt and/or due to a latitudinal shift in the precipitation pattern. The dipole like responses around the tropical rainbelt in precipitation and cloudiness emphasize a possible shift in the mean meridional circulation to the north, in our case. As evident from the heating rate (Figure 3.4), dust loading acts as a hemispherically asymmetric

off-equator heating source in the lower-middle troposphere over the MENA region and possibly strengthens and moves the ascending branch of Hadley cell further north. To explicitly investigate this, a detailed analysis of the tropospheric dynamic response to dust direct radiative effect is performed in the following sections.

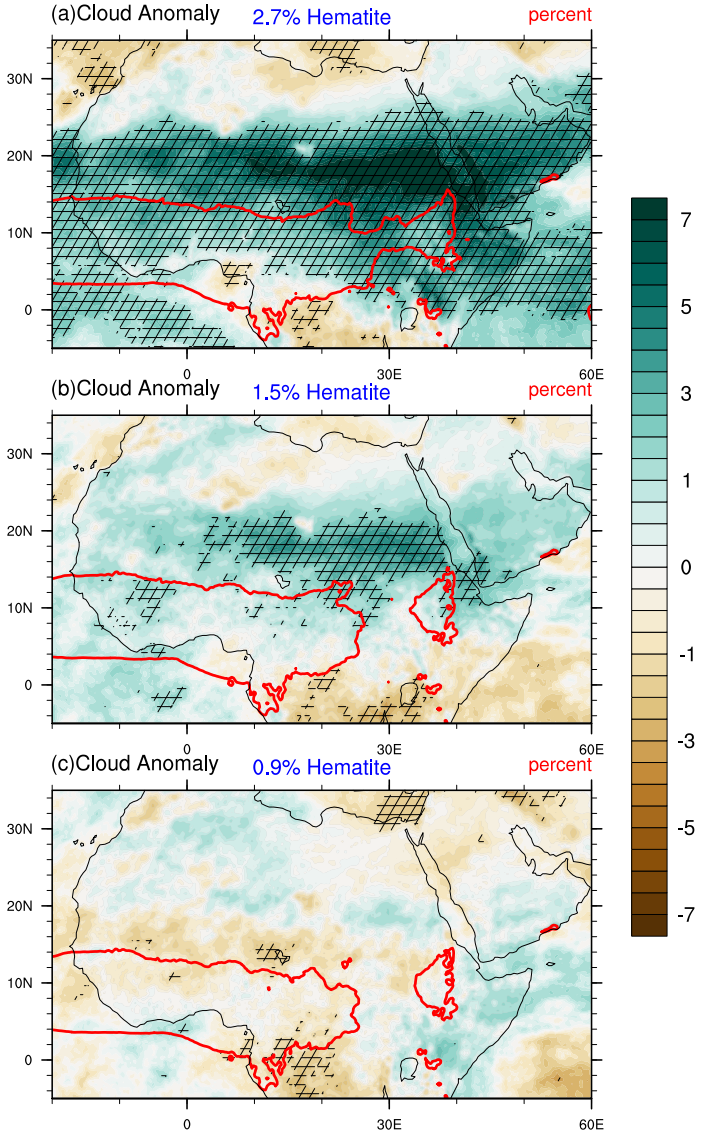

Figure 4.4: Response in total cloud amount (%), to dust radiative effect while dust is assumed to be a (a) very efficient (DUST2.7 case), (b) standard (DUST1.5 case) and (c) inefficient (DUST0.9 case) absorber at shortwave, during summer (JJA). The responses are estimated as the difference between simulations with dust radiative effect and without dust radiative effect. Areas where the response is statistically significant (student's t test) at 95% level, are hatched. The thick red contour overlaid on the shaded response portrays area where cloudiness is above 70 %, as a proxy for the position of the rainbelt.

4.2 Temperature Response over MENA

MENA is the hottest region on the globe. Therefore, even the slight variations in temperature are very crucial for the region's climate. Dust impacts the atmospheric temperature primarily and instantaneously by the absorption and scattering of radiation, and consequently through the modification of circulation and rainfall. The simulated mean summer temperature over MENA region is validated against the observed mean summer air temperature climatology from the UK Met Office Hadley Centre and the University of East Anglia Climatic Research Unit (HadCRUT) (*Brohan et al.*, 2006). In general, the model reproduces the magnitude and the pattern of spatial temperature distributions. A strong north-south gradient in the mean temperature is evident between dry Saharan desert in the north and the tropical rain forest in the south (Figure 4.5a) and it is well represented in the simulation (Figure 4.5b). Similarly, the temperature maxima associated with quasi-static heat lows such as SHL, SuHL and AHL are also well simulated. However, in general, HiRAM overestimates the temperature by a few degree, especially over the southeastern corner of Arabian Peninsula.

Figure 4.6 depicts the response in mean summer surface air temperature at 2m to the dust radiative effect, in all three cases of shortwave absorption. In general, a strong north-south gradient in the mean temperature is evident between dry Saharan desert in the north and the tropical rain forest in the south. In highly absorbing cases (DUST2.7 and DUST1.5), the temperature response 4.6 is mainly a reduction in temperature over the rainbelt, especially to the northern half of the rainbelt, where the cooling goes more than 1K. Conversely, the temperature increases (more than 1 K) to the north of the rainbelt including the Sahara region, which is characterized as the region of Hadley circulation subsiding area. However the strong dipole pattern of response between rainbelt region and Hadley subsiding region vanishes in DUST0.9 case. The response over rainbelt reverses its sign and becomes statistically

insignificant. The warming response over Sahara reduces its magnitude in this case (DUST0.9), but is statistically significant in most of the part.

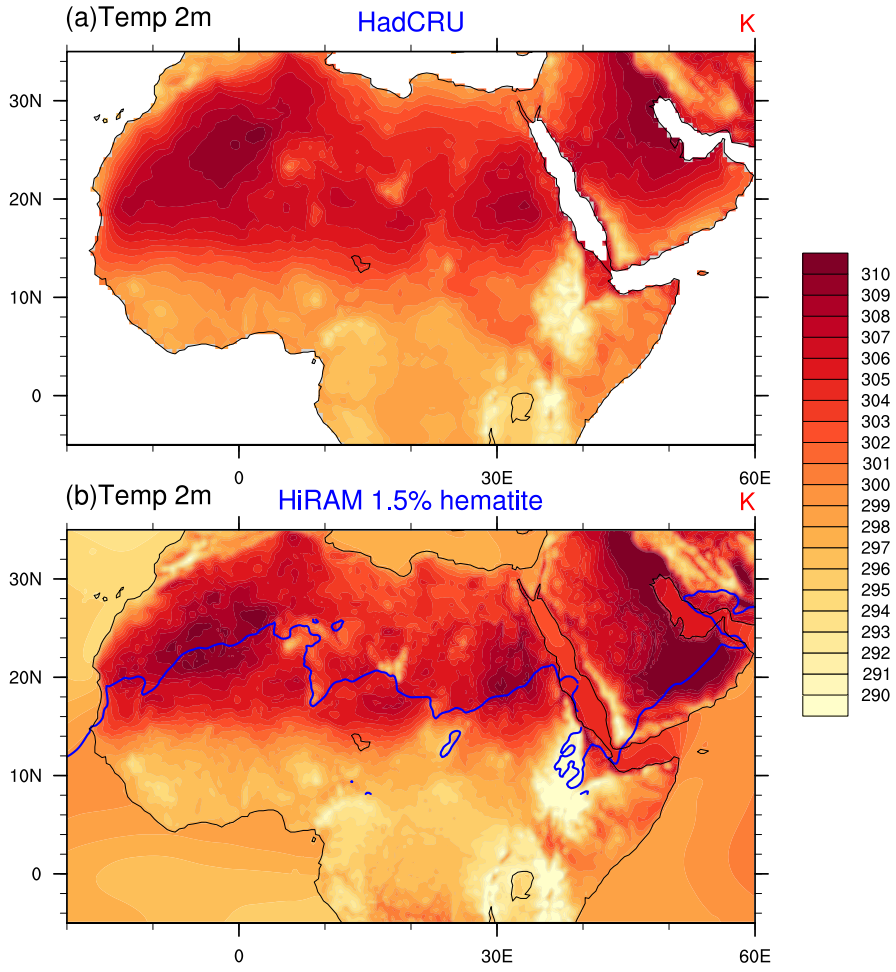

Figure 4.5: Mean Summer (JJA) air temperature at 2m (K) in (a) UK Met Office Hadley Centre and the University of East Anglia Climatic Research Unit (HadCRUT) and in (b) HiRAM (DUST1.5 case) simulations .

The positive temperature anomaly over Sahara could be due to the enhanced subsidence from a strengthened local Hadley cell, which is proved hereinafter, and the strong shortwave heating in the atmospheric boundary layer by dust (Figure 3.4). In general, temperature response is statistically more significant and has a much more consistent north-south pattern compared to the precipitation response. However, the magnitude of response is comparatively higher at the northern part of the rainbelt, where an increase in cloudiness of 8% or more is predicted. The intense cooling over

the northern half of the rainbelt, which extends to the southern Sahara, could arise from the combined influence of solar dimming due to aerosol scattering and absorption and the feedbacks from enhanced cloudiness, increased precipitation and circulation responses.

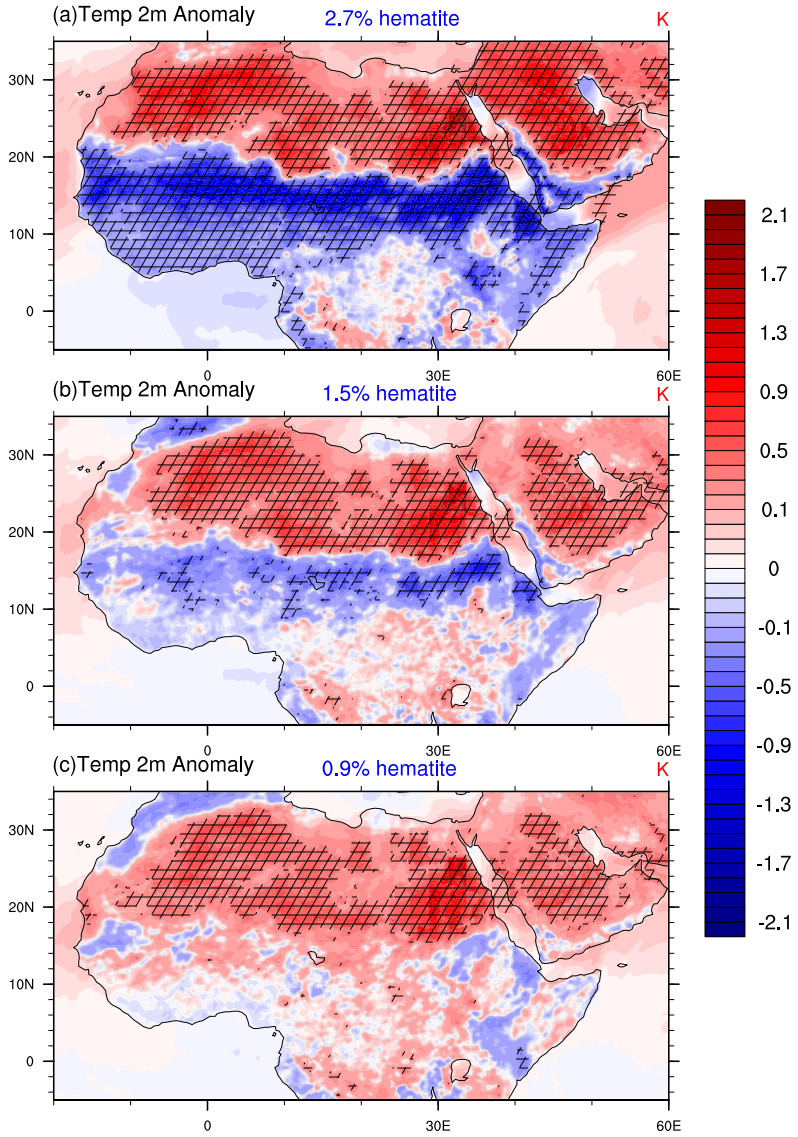

Figure 4.6: Air temperature (2m) response (K) to dust radiative effect while dust is assumed to be a (a) very efficient (DUST2.7 case), (b) standard (DUST1.5 case) and (c) inefficient (DUST0.9 case) absorber at shortwave, during summer (JJA). The responses are estimated as the difference between simulations with dust radiative effect and without dust radiative effect. Areas where the response is statistically significant (student's t test) at 95% level, are hatched.

4.3 Local Hadley and Walker Circulation Response

As a first approximation, the zonally averaged meridional picture of the dust radiative effect and the corresponding circulation response over MENA region could be summarized as an off-equatorial heating in the northern hemispheric lower-mid troposphere and the associated changes in the local Hadley circulation. However, the contribution of zonal circulation response to the predicted climate response cannot be disregarded. To explicitly demonstrate the changes in meridional and zonal overturning circulation, it is important to divide the three dimensional overturning into orthogonal two-dimensional overturning circulations. In other words, Hadley and Walker type circulations need to be separated. Conventionally, Hadley circulation is depicted by the mean meridional mass stream functions, which is calculated by vertically integrating the zonally averaged mass weighted v-wind (*Oort and Yienger*, 1996). This procedure is strictly defined for the global domain and it fails for a particular longitudinal belt as mass continuity does not hold (*Trenberth et al.*, 2000; *Webster*, 2004). Recently, *Schwendike et al.* (2014) introduced a new method for the local partitioning of the tropical overturning circulation into local Hadley and Walker circulation. In this approach, the pressure-velocity omega ($\omega = \frac{Dp}{Dt}$) can be divided into components associated with meridional (ω_ϕ) and zonal (ω_λ) overturning circulations, as

$$\omega_\phi = \frac{1}{a\cos\phi}\frac{\partial}{\partial\phi}(\psi_\phi \cos\phi) = \frac{1}{a^2\cos\phi}\frac{\partial}{\partial\phi}(\cos\phi\frac{\partial\mu}{\partial\phi}) \tag{4.1}$$

$$\omega_\lambda = \frac{1}{a\cos\phi}\frac{\partial\psi_\lambda}{\partial\lambda} = \frac{1}{a^2\cos^2\phi}\frac{\partial^2\mu}{\partial\lambda^2} \tag{4.2}$$

where potential function, μ, and vector streamfunction, Ψ, are defined in pressure coordinate as

$$\nabla_p^2 \mu = -\omega$$

and

$$\nabla_p \Psi = \omega, \tag{4.3}$$

where

$$\Psi = (\psi_\lambda, \psi_\phi) = -\nabla_p \mu \tag{4.4}$$

Hence, the vertical mass flux associated with two orthogonal circulations can be written as,

$$m_\phi = -\omega_\phi \cos\phi / g$$

and

$$m_\lambda = -\omega_\lambda \cos\phi / g \tag{4.5}$$

Vertical mass flux associated with meridional overturning (m_ϕ) and zonal overturning (m_λ) can be portrayed as the local Hadley and Walker circulations, respectively (See *Schwendike et al.* (2014) for a detailed explanation of the method of separation).

As a first step towards the analysis of the overturning circulation response, local and regional manifestation of Hadley and Walker circulations, simulated by HiRAM has been validated against ERA-Interim data. Figure 4.7 a&b compares mean summer local Hadley (m_ϕ) and Walker circulations (m_λ), depicted as the vertical mass flux ($10^{-3}\ kgm^{-2}s^{-1}$) associated with meridional and zonal overturning at 500 hPa level, respectively. Positive (negative) values indicate ascending (descending) motion. A zonally elongated band of ascending motions in the summer tropics with corresponding descent on either side of it is evident. The strength and spatial extent of ascending and descending limbs are simulated adequately well.

The local Walker circulation is depicted as the Walker component of vertical mass flux, m_λ ($kgm^{-2}s^{-1}$) (Figure 4.7 c&d). MENA in general experiences descending motion, except regions such as the Congo basin, the northwestern part of the African continent, the Ethiopian Highlands and the western coast of the Arabian peninsula, where m_λ is positive

To validate and expose the response of regional Hadley cell (m_ϕ) aloft, a vertical cross section of m_ϕ averaged between 10^0W and 60^0E is shown in Figures 4.8. The divergent circulation in the plane (U_ϕ, ω_ϕ) is overlaid as vectors to show the flow direction and cell structure. The meridional divergent wind, U_ϕ, is estimated (*Schwendike et al.*, 2014) from the definition of horizontal divergent wind in terms of velocity stream function (Ψ) as *Schwendike et al.* (2014),

$$U_\phi = -\frac{\partial \psi_\phi}{\partial p} \tag{4.6}$$

As the magnitude of ω_ϕ is significantly smaller compared to U_ϕ, the former is scaled by a factor of 100, in order to plot the wind vectors. A double cell structure of Hadley circulation with a stronger winter cell is found, over MENA . The ascending branch extends very much into the summer hemisphere and has a bell shape with tails of shallow ascent to either side of the main core. HiRAM captures the position and the strength of the ascending and descending limbs of the regional Hadley circulation, quite well.

Similarly, Figure 4.9 shows comparison of mean summer regional Walker (m_λ) cell aloft, depicted as the vertical mass flux (10^{-3} $kgm^{-2}s^{-1}$) associated with the meridionally averaged (30^0S - 30^0N) zonal overturning. The zonal divergent wind, U_λ, is estimated as,

$$U_\lambda = -\frac{\partial \psi_\lambda}{\partial p} \tag{4.7}$$

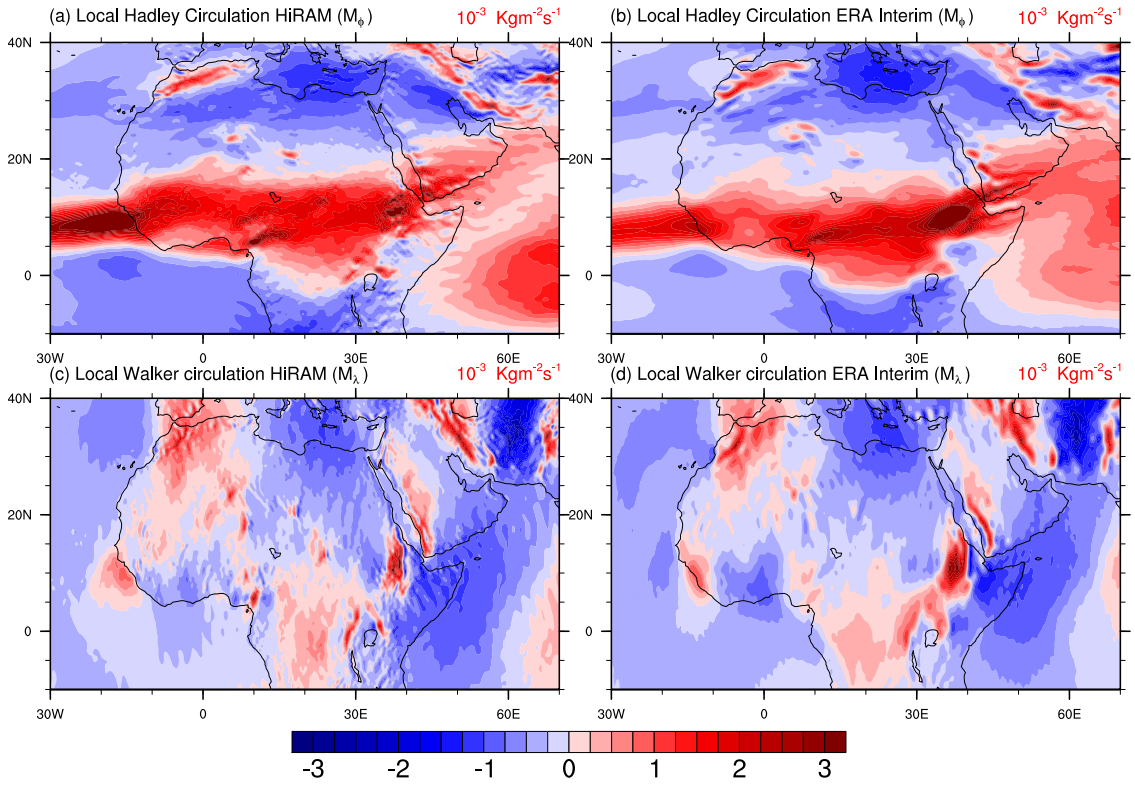

Figure 4.7: Mean Summer (JJA) local Hadley circulation over MENA in (a) HiRAM (DUST1.5 case) simulations and in (b) Era Interim Re-analyses, and local Walker circulation over MENA in (c) HiRAM (DUST1.5 case) simulations and in (d) Era Interim Re-analyses. Local Hadley circulation, m_ϕ, and local Walker circulation, m_λ are depicted as the vertical mass flux ($10^{-3}\ kgm^{-2}s^{-1}$) associated with meridional and zonal overturning at 500 hPa level, respectively. Positive values indicate ascending motion and vice versa.

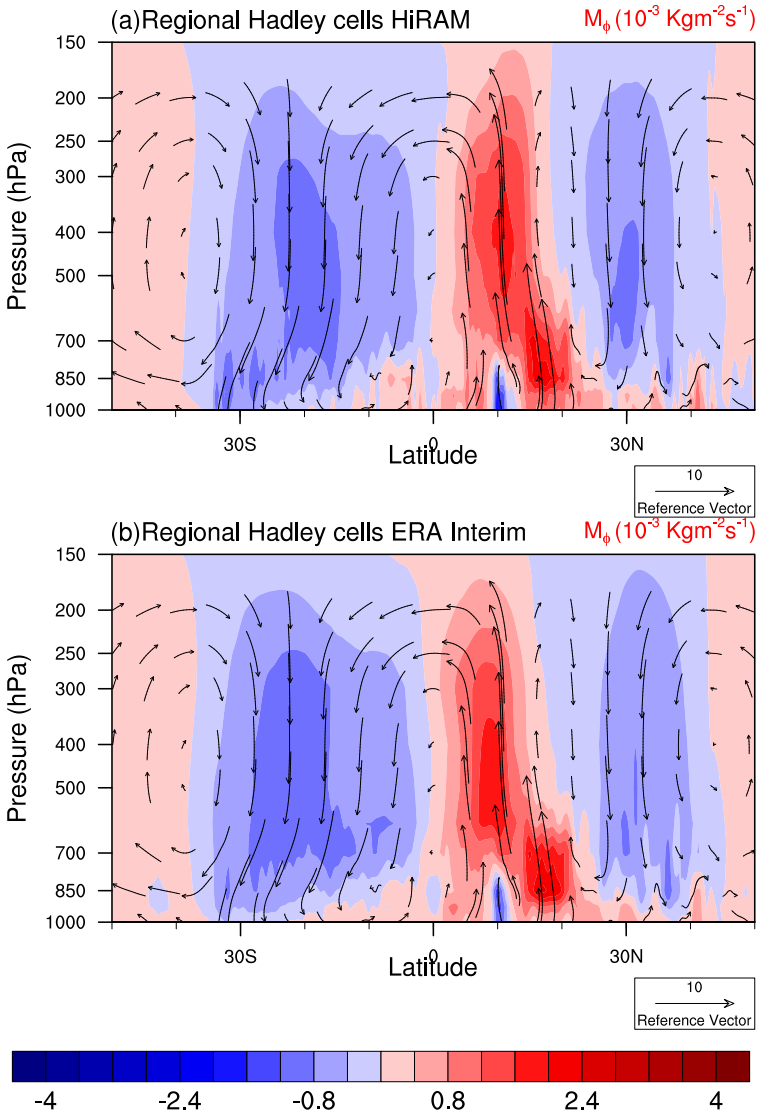

Figure 4.8: Mean Summer (JJA) Regional Hadley circulation over MENA in (a) HiRAM (DUST1.5 case) simulations and in (b) Era Interim Re-analyses. Regional Hadley circulation, m_ϕ, is depicted as the zonally averaged (20^0W - 60^0E) vertical mass flux (10^{-3} $kgm^{-2}s^{-1}$) associated with meridional overturning. Positive values indicate ascending motion and vice versa. Vectors represent the wind in the plane of cross section (U_ϕ, $\omega\phi$). The values of $\omega\phi$ are scaled by multiplying with 10^2.

In general, HiRAM simulations very well capture the mean structure, intensity and position of all the major features of the overturning circulations. The position and strength of the ascending and descending limbs of Hadley and Walker circulations, and their structure aloft are simulated quite realistically.

Figure 4.10 depicts the mean summer response in the local Hadley circulation (m_ϕ) to dust radiative effects, in various shortwave absorption cases. The response is shown as shaded contours and the mean m_ϕ in the respective experiment as contour lines, where thick contours represent ascending motion and dashed contours represent subsidence. Overall, the response is maximum at the northern edges. The general pattern of response is an intense increase in vertical mass flux at the northern half of the ascending limb of the local Hadley cell and a decrease in the southern half, although it is relatively weaker. In other words, the ascending branch strengthens in its northern border and shifts further into the summer hemisphere. Consequently, an enhanced subsidence is also evident over the southern border of the NH subsidence branch. The dipole pattern of response in m_ϕ is consistent with the pattern of the rainbelt response (Figures 4.2 4.4). In other words, it suggests that the predicted response of the rainbelt stems from the local Hadley circulation changes in response to a meridionally asymmetric heating gradient. This pattern of response and its strength are sensitive to the amount of dust shortwave absorption. As shortwave absorption weakens, the response also weakens and even reverses sign (Figure 4.10). However, regionally, consistent with the surface climate response, an east-west contrast is evident in the local Hadley circulation response, with a stronger shift (about 2^0 of latitude) over central and East Africa.

Figure 4.11 shows the mean summer response of local Walker circulation (m_λ) in all three experiments. Similar to Figure 4.10, the response is shown as shaded contours and the mean m_λ as contour lines. In general, the local Walker response is weaker compared to the local Hadley response. However, a prominent zonal circula-

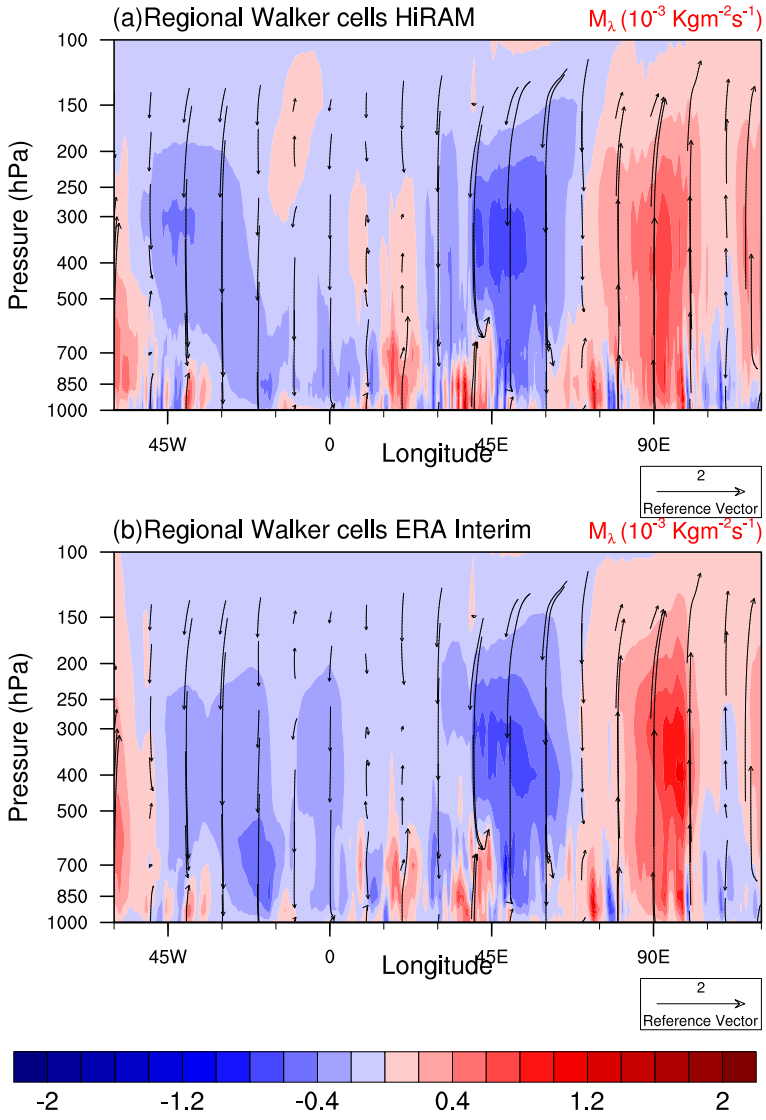

Figure 4.9: Mean Summer (JJA) Regional Walker circulation over MENA in (a) HiRAM (DUST1.5 case) simulations and in (b) Era Interim Re-analyses. Regional Walker circulation, m_λ, is depicted as the meridionally averaged (30^0S - 30^0N) vertical mass flux (10^{-3} $kgm^{-2}s^{-1}$) associated with zonal overturning. Positive values indicate ascending motion and vice versa. Vectors represent the wind in the plane of cross section (U_λ, $\omega\lambda$). The values of $\omega\lambda$ are scaled by multiplying with 10^2.

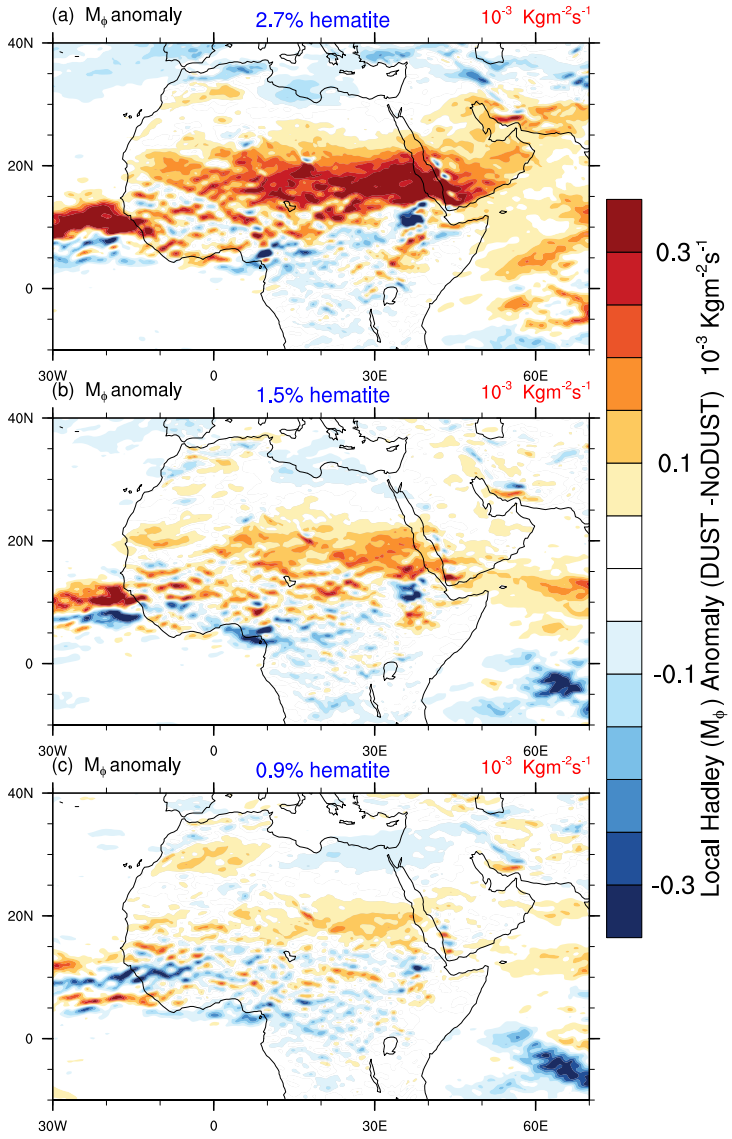

Figure 4.10: Response of local Hadley circulation over MENA, to dust radiative effect while dust is assumed to be a (a) very efficient (DUST2.7 case), (b) standard (DUST1.5 case) and (c) inefficient (DUST0.9 case) absorber at shortwave, during summer (JJA). Local Hadley circulation, m_ϕ, is depicted as the vertical mass flux (10^{-3} $kgm^{-2}s^{-1}$) associated with meridional overturning, at 500 hPa level. The responses are estimated as the difference between simulations with dust radiative effect and without dust radiative effect.

tion anomaly is predicted over the local precipitation hotspot of over the Ethiopian highlands and southern Red Sea. A strong zonally oriented dipole pattern of response is predicted here, with enhanced ascending to the east including the southern Red Sea and an enhanced subsidence to the west over the Ethiopian highlands. This region of intense convective activities is the ascending branch of global Walker circulation over East Africa during summer. The zonal dipole pattern in the response indicates the shift of this branch eastward, which might be caused by the response of the ISM to dust radiative effect (this is beyond the domain and not shown). A consistent east-west dipolar response is predicted in the precipitation too (Figures 4.2), with a weakening of precipitation over the Ethiopian Highlands and an enhancement over the southern Red Sea and southwest coast of the Arabian Peninsula.

The response in m_λ is very sensitive to the strength of dust shortwave absorption (Figure 4.11). Similar to the sensitivity of m_ϕ, the m_λ response weakens as absorption reduces. The response is strongest in the DUST2.7 case; it reduces and the dipole pattern vanishes as absorption reduces. The predicted response of the rainbelt (Figures 4.2 & 4.4) consistently exhibits similar dipole pattern and sensitivity.

The response in regional Hadley circulation (m_ϕ) over MENA, which is depicted as the change in zonally averaged (20^0W - 60^0E) vertical mass flux ($10^{-3}\ kgm^{-2}s^{-1}$) associated with meridional overturning, is shown in 4.12. The vertical mass flux enhances in the ascending limb, especially to the northern half of the limb, as a response to dust radiative effect. A northward shift in the ascending limb's position is also clearly evident. The increase in ascending motion spans the entire tropospheric column. A corresponding increase in subsidence is also predicted to the north of ascending limb, including Sahara deserts. As absorption increases the intensity of response increases (DUST0.9 to DUST27). While highly absorbing (DUST2.7) case shows a strong dipole pattern of response between ascending and descending branches of Hadley overturning cells, the pattern almost vanishes as absorption reduces (DUST0.9).

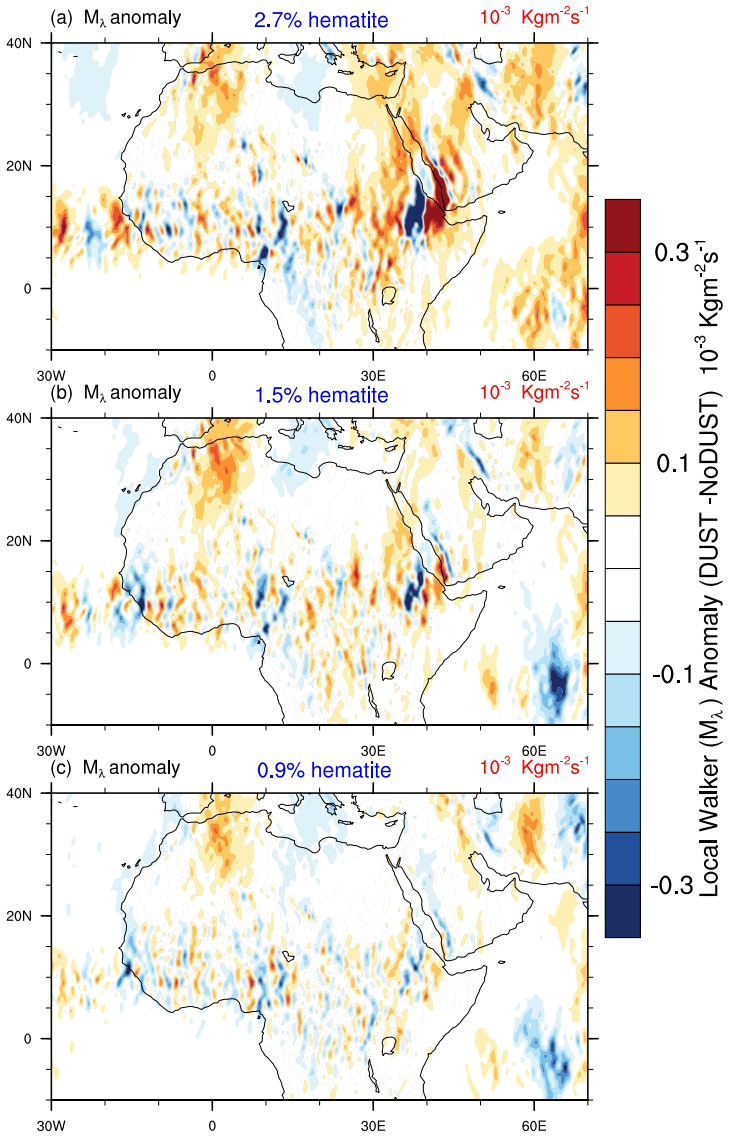

Figure 4.11: Response of local Walker circulation over MENA, to dust radiative effect while dust is assumed to be a (a) very efficient (DUST2.7 case), (b) standard (DUST1.5 case) and (c) inefficient (DUST0.9 case) absorber at shortwave, during summer (JJA). Local Walker circulation, m_λ, is depicted as the vertical mass flux (10^{-3} $kgm^{-2}s^{-1}$) associated with zonal overturning, at 500 hPa level. The responses are estimated as the difference between simulations with dust radiative effect and without dust radiative effect.

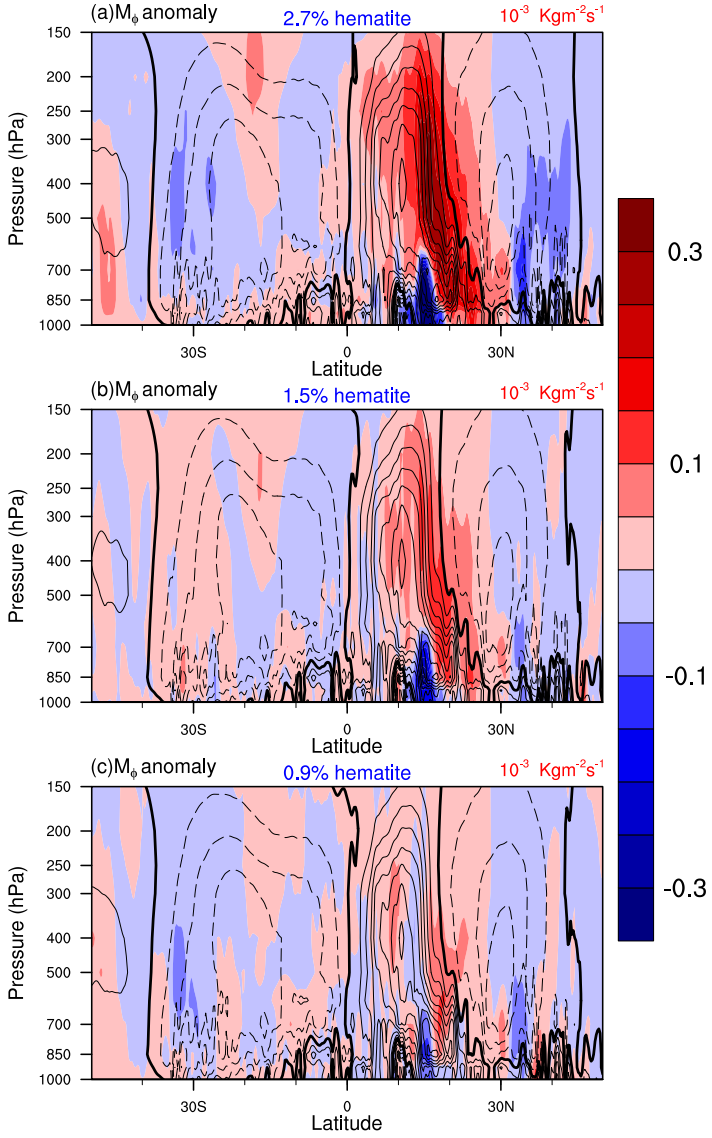

Figure 4.12: Response of regional Hadley circulation over MENA, to dust radiative effect while dust is assumed to be a (a) very efficient (DUST2.7 case), (b) standard (DUST1.5 case) and (c) inefficient (DUST0.9 case) absorber at shortwave, during summer (JJA). Regional Hadley circulation, m_ϕ, is depicted as the zonally averaged (20^0W - 60^0E) vertical mass flux (10^{-3} $kgm^{-2}s^{-1}$) associated with meridional overturning. The responses are estimated as the difference between simulations with dust radiative effect and without dust radiative effect. Black contours represent the mean overturning circulation in each experiment, where dashed contours indicate subsiding motion and solid contours indicate ascending motion. The thick contours (zero contours) are the border between ascending and descending cells.

Similarly, response in regional Walker circulation m_λ is depicted in 4.13, by portraying the changes in meridionally averaged (30^0S - 30^0N) vertical mass flux (10^{-3} $kgm^{-2}s^{-1}$) associated with zonal overturning. In general, the response is not as strong as that of regional Hadley circulation. Moreover, the responses do not span the entire troposphere. Instead, the enhancement in the ascending/descending motion is confined to the mid-troposphere. A contrasting response is predicted in the zonal overturning between East Africa and ISM region. In other words, the ascending motion associated with zonal overturning (m_λ) enhances over East Africa and weakens over ISM domain. It has been shown (e.g., *Funk et al.*, 2008; *Williams and Funk*, 2011) that the changes in convective activities over the Indian Ocean could potentially influence tropical East African rainfall patterns through anomalous Walker-type circulation. Therefore the predicted contrasting response between East Africa and ISM region could be a feedback from the weakened ISM as a response to dust radiative effect. Again, it is another instance showing the importance of high-resolution global simulation for the analyses of regional response to spatially non-homogenous aerosol forcing, as these simulations can incorporate the regional influences of a global circulation perturbation. Regarding the sensitivity of zonal overturning to shortwave absorption, like in the case of Hadley circulation, regional walker circulation response is also sensitive to the dust shortwave absorption. The magnitude of the response and the contrast between ascending and descending branches, intensifies as shortwave absorption increases (4.13).

In summary, the Walker circulation response to dust radiative effect (Figure 4.11 & 4.13) is in general weaker and shallow in vertical extent, compared to that of Hadley circulation. Therefore the separation of local Hadley and Waker cell responses indicate, as expected, that the dominant response is in the meridional direction (local Hadley circulation) as a response to meridional differential heating. However, the intense local response in zonal overturning over East Africa is important, regionally.

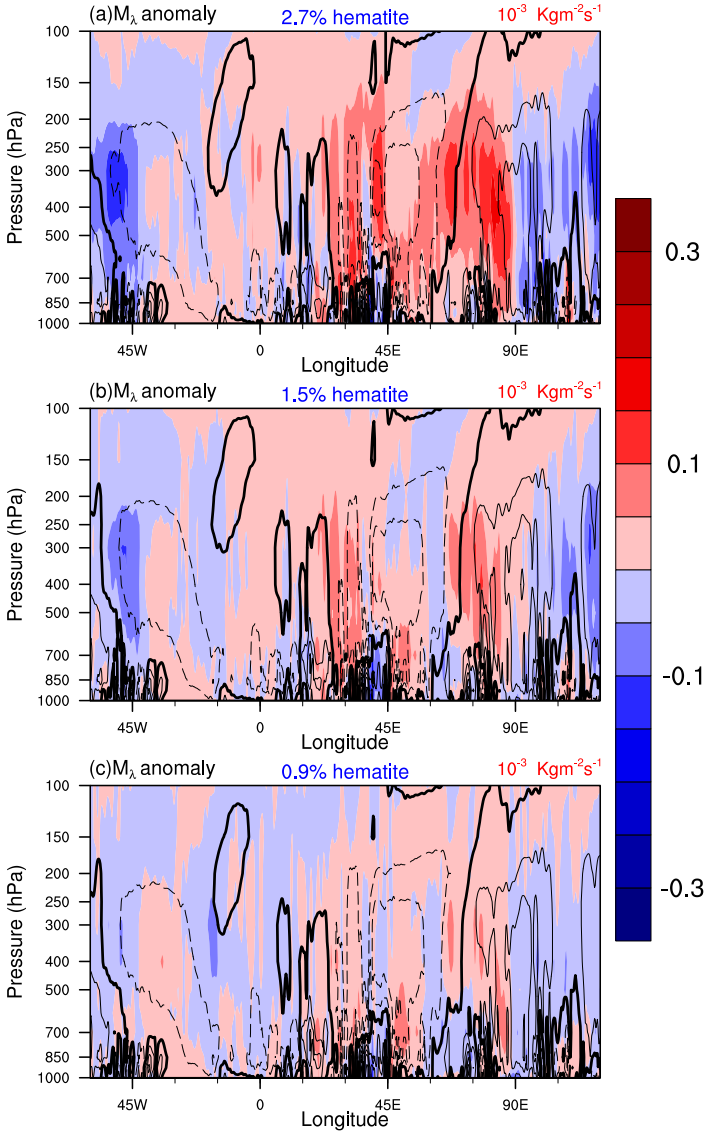

Figure 4.13: Response of regional Walker circulation across MENA, to dust radiative effect while dust is assumed to be a (a) very efficient (DUST2.7 case), (b) standard (DUST1.5 case) and (c) inefficient (DUST0.9 case) absorber at shortwave, during summer (JJA). Regional Walker circulation, m_λ, is depicted as the meridionally averaged (30^0S - 30^0N) vertical mass flux (10^{-3} $kgm^{-2}s^{-1}$) associated with zonal overturning. The responses are estimated as the difference between simulations with dust radiative effect and without dust radiative effect. Black contours represent the mean overturning circulation in each experiment, where dashed contours indicate subsiding motion and solid contours indicate ascending motion. The thick contours (zero contours) are the border between ascending and descending cells.

4.4 Discussion

The tropical rainbelt across MENA is not located just under the dust belt; rather it is located in the proximity of the dust belt, specifically in the southern border of the dust belt. Therefore the responses in the rainbelt cannot be immediately linked to the local column radiative-convective balance. The present study suggests that the responses in the rainbelt are greatly mediated by the circulation changes induced by the spatially heterogeneous distribution of dust loading and the corresponding heterogeneity in DDRF distribution. That is to say, the dust loading and the corresponding forcing is mainly confined to the NH subtropics (Figure 3.4), which could potentially influence the local meridional overturning as well as the synoptic circulations, as it perturbs the inter-hemispheric radiative heating gradient. This is consistently evident from the responses of the climate variables and circulation features in the simulations.

Analysis of the local and regional Hadley cell (Figure 4.10, 4.11, 4.12 & 4.13) reveals the substantial responses in the local Hadley circulation strength and position as a response to dust radiative effect. In general, the ascending branch of Hadley cell enhances and shifts to the summer hemisphere as a response to dust radiative effect. These responses are consistent with the previous findings on the strength and location of the Hadley cell. Using simplified models, *Held and Hou* (1980) and *Lindzen and Hou* (1988) showed that, as the heating center moves off the equator, the latitude position separating summer and winter Hadley cell moves further into the summer hemisphere. Regarding the position of Hadley cells, two major controls have been proposed; equatorial SST pattern and the cross-equatorial tropospheric temperature gradient (*Philander et al.*, 1996; *Tomas et al.*, 1999). Since we prescribe observed SST in the simulation, the response in the position of the overturning cells solely originates from the changes in the tropospheric temperature gradient that stem from the dust radiative forcing. In the present case, the dust heating confined to the NH subtropics very well functions as an off-equator additional heating source in the lower tropo-

sphere. During summer, this dust induced heating coincides with the solar insolation maxima, and thus enhances the inter-hemispheric temperature gradient primarily driven by insolation. The enhanced inter-hemispheric heating gradient strengthens and moves the ascending branch of Hadley cell into the summer hemisphere.

Several other modeling, as well as observational studies showed the sensitivity of the latitudinal position of Hadley cell and the rainbelt to the inter-hemispheric heating contrast in various contexts, in decadal to glacial-interglacial timescales (*Broccoli et al.*, 2006; *Chiang and Bitz*, 2005; *Mantsis and Clement*, 2009; *Zhang and Delworth*, 2005). In general an anomalous northward (southward) shift in the position of tropical rainbelt (mentioned as "ITCZ"in many of these studies) are observed in response to NH warming (cooling). The opposing effects of scattering and absorbing aerosols on the tropical rainbelt position has also been studied in the past (*Allen and Sherwood*, 2011; *Chung and Seinfeld*, 2005; *Roberts and Jones*, 2004; *Wang*, 2004; *Williams et al.*, 2001). While the scattering aerosols confined to the NH shift the tropical rainbelt further south due to the weakening of the inter-hemispheric temperature gradient associated with an enhanced cooling of the NH, absorbing aerosols move it further north in response to the anomalous radiative heating of the NH. *Wilcox et al.* (2010) observed a northward shift in the tropical rainbelt and circulation over the North Atlantic Ocean, in response to summertime Saharan dust outbreaks. The predicted northward shift of the local Hadley circulation and the tropical rainbelt in the current study is thus consistent with the previous results, and could be attributed to the dust induced radiative heating in the NH subtropics over MENA. Implicitly, these results also show that the variations in Saharan dust loading could potentially influence Sahel drought episodes along with other proposed mechanisms.

Analysis of the precipitation and cloudiness response to shortwave absorption (Figure 4.1 & 4.3) shows that the most sensitive part of the rainbelt to dust shortwave absorption is the northern edge. Geographically speaking, the maximum response

occurs over Sahel, the semi-arid transition zone between dry Sahara deserts to the north and humid tropical savanna (Sudanian Savanna) to the south. Precipitation response over this region varies from almost zero to 2 $kg/m^2/day$ (in DUST2.7), as shortwave absorption increases (Figure 4.2). The range of sensitivity is comparable to the mean summer precipitation over this region and is statistically significant. The response in the DUST2.7 experiment reaches up to 50% of the mean precipitation at some locations in Sahel. The economies of most of the countries in the Sahel region largely depend on rain-fed agriculture. Even a small variability in the rainy season could affect the livelihood of millions of people (International Federation of Red Cross and Red Crescent Societies; http://www.ifrc.org). Therefore, accurate representation of dust shortwave absorption is very important for the Sahel climate simulation and prediction. Unfortunately, many of the operational weather forecasting models, GCMs and even re-analyses do not include dust radiative effect, though it is proven to be extremely important for the accuracy of radiation balance in numerical weather prediction models (e.g., *Pérez et al.*, 2006; *Alpert et al.*, 1998). One reason for avoiding dust radiative effect is its large uncertainty. Hence, considering the predicted sensitivity of the rainbelt, the present study suggests serious efforts to reduce uncertainty in dust shortwave absorption for better predictability of the region's weather and climate.

It is also noteworthy that, most of the local hotspots in the climate responses, as seen from surface climate variables (Figure 4.1, 4.3 & 4.5), are over regions with complex orography. The responses in these hotspots are at least twice as large as the responses in the remaining part of the region. These locally amplified responses highlight the importance of incorporating mesoscale forcings such as orography for an accurate simulation of regional climate sensitivity. Coarser resolution GCM simulations generally lack these forcings. But the current simulations with HiRAM take into account these multi-scale forcings and effectively reproduce the locally amplified

climate features.

Chapter 5

Response of Regional Circulations

The large-scale picture of the climate response to dust radiative effect has been explained in terms of the responses in the overturning circulations, in the Chapter (4). However, there are several regional-scale circulations and wave activities embedded within the large-scale overturning, which are decisive in defining the mean structure and strength of overturning circulations to a great extent. The net climate response, therefore, depends also on the response in the regional-scale circulations and their interactions with the large-scale circulations. The real advantage of high-resolution global simulation, in this regard, is the capability to resolve such multi-scale processes and their mutual interactions in the same simulation.

One of the primary circulation system in the lower troposphere is WAM, which has significant zonal and meridional components of circulations. By functioning as the main supplier of moisture inland, especially to the dry Sahel and Sahara region, WAM acts as the key circulation feature in the region's climate. Thus, any change in WAM circulation has a direct link to the response in precipitation over MENA. Another major circulation features in the lower troposphere are the semi-permanent heat lows (thermal lows) develop in the interior deserts during peak summer season. These heat lows, including SHL, SuHL and AHL, are cyclonic circulations extending till mid-troposphere, formed by the intense heating of the surface and the consequent dry convection. These subtropical heat lows are key components of WAM and ITCZ dynamics. Therefore, the response of heat low strength and position interacts with other circulation features and hence influence the climate response over MENA.

In the middle troposphere, the atmospheric dynamics is largely dominated by AEJ and the AEWs embedded on it. Similarly, TEJ is the main circulation feature in the upper troposphere. The individual and relative positions of AEJ and TEJ, and their strength are crucial factors determining the location of the ascending limb of the regional Hadley circulation and hence the intensity and location of maximum precipitation (*Nicholson*, 2009). The strength, position and the instability of AEJ is also crucial for the development and maintenance of AEWs. AEWs are the main synoptic-scale disturbances over tropical Africa, which have a vital role in the net convective rainfall over tropical MENA, especially over Sahel.

The present chapter is dedicated to the investigation of the changes in regional scale circulations and wave activities in response to dust radiative effect, and their role in defining the net climate response over MENA. Responses in WAM, AEJ, TEJ and AEWs are discussed in separate sections. Given the socio-political and meteorological importance of the Sahel rainfall, a special emphasis is given to the mechanisms responsible for its changes. The present chapter is partly based on the contents from the two papers published as part of the current dissertation, *Bangalath and Stenchikov* (2015, 2016). The remaining part of the the chapter will constitute the main content of the two manuscripts, yet to be submitted (See Chapter 7)

5.1 West African Monsoon Response

5.1.1 Mean Circulation Response

WAM is the seasonal reversal of lower tropospheric circulation over West Africa, primarily driven by the land-sea heat contrast during the summer season. Therefore, any process that perturbs the land-sea heating contrast supposedly changes the WAM circulation. Although WAM has its origin partly outside of the MENA domain, it is considered to be one of the major drivers of climate in the region. WAM dominates the lower tropospheric dynamics and thermodynamics over West Africa. It is a crucial

component even in East Africa, as this circulation serves as the main moisture supplier from the tropical Atlantic. Therefore the dust impact on WAM circulations could effectively feedback the responses throughout MENA.

It has been shown in Figure 3.1 that dust has a differential radiative effect over continental Africa and the Atlantic Ocean. Dust has an intense warming effect over North African deserts, owing to the presence of high dust loading and the high albedo of the underlying deserts. However, the sign of DDRF reverses with intense cooling over the Atlantic Ocean, mostly because of the lower albedo of the ocean. Therefore, to a first approximation, the interaction of dust radiative effect with WAM can be seen as the enhanced land-sea heat contrast and the corresponding responses in the circulation. Apart from the land-sea contrast in radiative forcing, dust loading has a strong north-south gradient in loading with a high concentration towards North Africa. The north-south gradient in dust loading and the resulting contrast in radiative forcing could enhance the meridional component of the WAM circulation. Specifically, the enhanced atmospheric heating gradient between the Gulf of Guinea and Sahara/Sahel region essentially strengthen the meridional component of the WAM circulation. Note that the meridional component of WAM circulation constitutes the main part of the surface circulation associated with regional Hadley cell.

It should be noted that the present simulations prescribe bottom boundary condition and hence do not account for the SST changes due to reduction of solar radiation at the surface, which will further influence latent heat flux. In other words, the present study look at the atmosphere-only responses. Since WAM involves moist processes, and the moisture intake from Atlantic towards African continent is very crucial for the inland thermodyanamics, care should be taken in interpreting the present result as latent heat feedback from Atlantic ocean is not taken into account.

As the first step of analyses, the WAM circulation simulated in HiRAM is validated against ERA-Interim dataset (Figure 5.1 & 5.2). The wind at 925 hPa and 850 hPa,

which are used to analyze the response of WAM circulation, are compared with reanalyses. HiRAM effectively reproduces all the main features of the lower atmospheric circulation including WAM, West African Westerly Jet (WAWJ), ITCZ , and the Somali Low Level Jet (SLLJ) in the Arabian Sea. The wind speed and the pattern of the main circulation features are realistically simulated.

To assess the response of WAM circulation, wind responses at 925 hPa (Figure 5.3) and 850 hPa (Figure 5.4) are considered. Analyses at this two levels (850 hPa and 950 hPa) help to portray the response of WAM aloft. The wind vectors represent the mean wind in each experiment and shaded contours are the responses. In general, WAM circulation strengthens, especially just south of ITCZ location, and shifts farther north in response to dust forcing. A dipole pattern of response is evident at the convergence zone where moist WAM circulation meets the dry Harmattan wind. The wind weakens to the north of convergence (Harmattan wind) and strengthens to the south (WAM circulation), which in turn produces a north-south dipole pattern. Though the pattern of response is similar at both 925 hPa and 850 hPa level, the response is much stronger at 850 hPa. In general WAM circulation strengthens in response to dust radiative effect. The predicted enhancement is consistent with EHP hypothesis. The intense amount of dust and the associated radiative heating over the continent can effectively act as an elevated heat source, which has the potential to enhance the southwesterly onshore flow. Additionally, since the meridional component of the WAM circulation can be seen as an integral part of the surface circulation associated with the regional Hadley circulation, the inter-hemispheric heating gradient over MENA could potentially enhance the meridional component of the WAM circulation.

The response over East Africa (Figure 5.3 & 5.4) is contrastingly high and has a strong dipole structure, in all the experiments. Again, this amplified response over East Africa could be due to the significant Walker circulation response (Figure 4.11 &

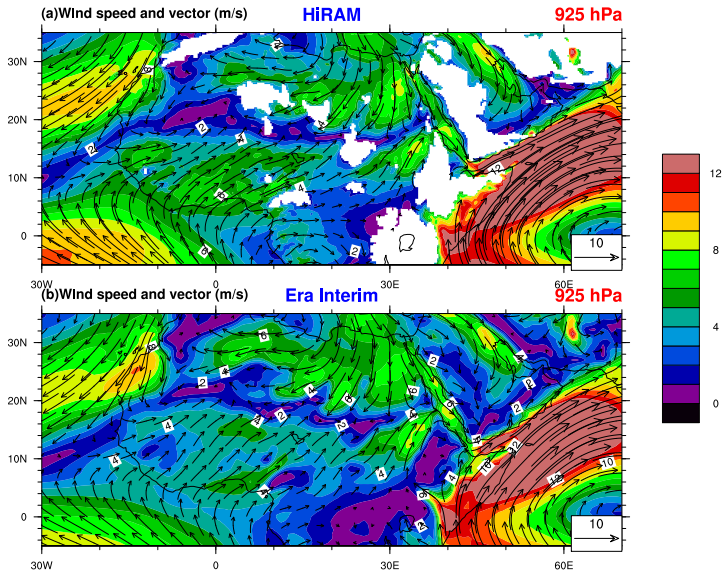

Figure 5.1: Mean Summer (JJA) wind speed and vector (m/s) in (a) HiRAM (DUST1.5 case) simulations and in (b) Era Interim Re-analyses, at 925 hPa

.

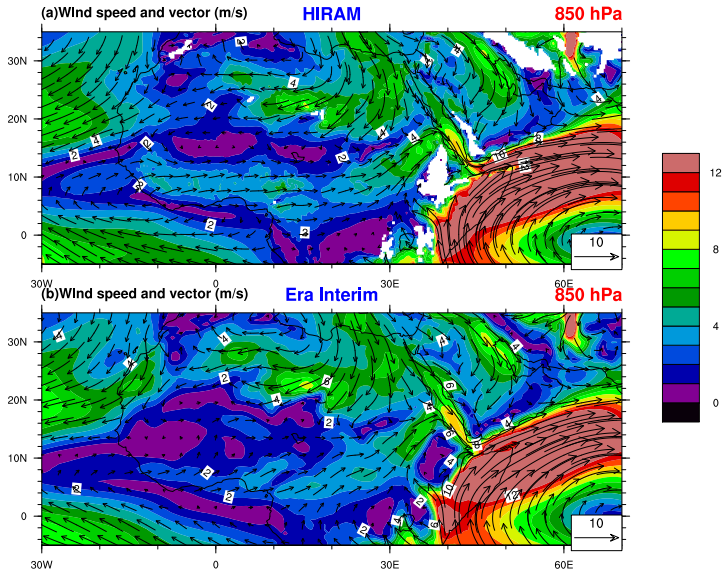

Figure 5.2: Mean Summer (JJA) wind speed and vector (m/s) in (a) HiRAM (DUST1.5 case) simulations and in (b) Era Interim Re-analyses, at 850 hPa

.

4.13) and/or due to the effect of comparatively higher DDRF over this region. Similarly, an enhanced response is predicted to the south of Arabaia Peninsula (including Gulf of Aden), where the moist SLLJ meets the elevated terrain in the west and dry and hot north-easterlies from the interior of the peninsula in the east. Although SLLJ experiences weakening as a whole in response to the dust radiative effect, locally the wind response strengthens at the northern coast of the Arabian Sea adjacent to the Arabian peninsula. This is because of the local amplification in the meridional heating gradient over this region, presumably due to enhanced AHL.

The prevailing monsoon wind has a significant meridional component at 925 hPa , whereas at 850 hPa the circulation becomes purely zonal (Figure 5.3 & 5.4). The strong zonal circulation at 850 hPa, containing WAWJ, transport moisture all the way from tropical Atlantic to East Africa, and even to the Red Sea. Any perturbation to this circulation can have huge impact in the thermodynamics of the entire tropical Africa. The enhanced circulation as a response to dust radiative effect, therefore, potentially strengthen the moisture budget inland (not shown).

A comparison of the response from all three experiments with different dust absorptivity (Figure 5.3) shows that the strength and sign of the responses are sensitive to the dust shortwave absorption. The response of wind speed weakens and the dipolar pattern of response over ITCZ diminishes, as absorption reduces. In other words, the onshore monsoon flow enhances and the equatorward Harmattan wind weakens as absorption increases. This particular response is highly favorable for the precipitation over this region, especially over Sahel, since the dry air intrusion from Sahara weakens and the moisture supply from the south enhances. At locations with maximum responses, such as the northern borders of Sahel, the wind anomaly reduces from around 2m/s (DUST2.7) to almost zero (DUST0.9). This sensitivity reaches 20% of the mean wind speed here. In DUST0.9 the wind anomaly almost vanishes in West Africa. Similarly the response over East Africa and Arabian Peninsula also

strongly depends on the dust shortwave absorption.

Although WAM is the major regional surface circulation in the domain, there are other local circulation features that are also important for the rainbelt and that respond strongly to dust forcing. WAWJ (*Grodsky et al.*, 2003), a low level jet between 8^0N - 11^0N over the eastern Atlantic and the West African coast forms during the summer season, is one such circulation. It has a pivotal role in the Sahel precipitation as it brings moisture directly from Atlantic to Sahel latitudes. The jet is in nearly geostrophic balance during most of the summer season and is super-geostrophic at its mature stage, with a maximum speed exceeding 7 m/s at 925 hPa. The model simulates the mean wind speed and position of the jet quite well (Figure 5.1 & 5.2). The jet strongly responds to the dust forcing (Figure 5.3 & 5.4), in general. However, unlike the response over land where the dipole pattern of response occurs just at the wind convergence zone, the entire jet enhances. Similar to other circulations, WAWJ response is also very sensitive to the dust shortwave absorption. Going from experiment DUST2.7 to DUST0.9, the response weakens significantly and almost neutralizes in the experiment with inefficiently absorbing dust (DUST0.9).

Since the jet is in geostrophic balance, the driving force of the jet is the meridional pressure gradient. Therefore, a significant increase of wind speed at the jet core is due to the strong response in meridional pressure gradient due to dust radiative forcing over this region. Notably, this is the only area, where the surface circulation has a significant response over the oceanic region. Even the WAM circulation, for instance over the Guinean coast, does not exhibit significant response over the ocean. Therefore, the heightened response of WAWJ and its sensitivity to shortwave absorption is particularly important, as it functions as an important moisture flux channel from the ocean towards land, especially to Sahel. In other words, the heightened response of WAWJ emphasizes the importance of high spatial resolution of models to resolve these rather local scale circulations, which are, however, crucial for the

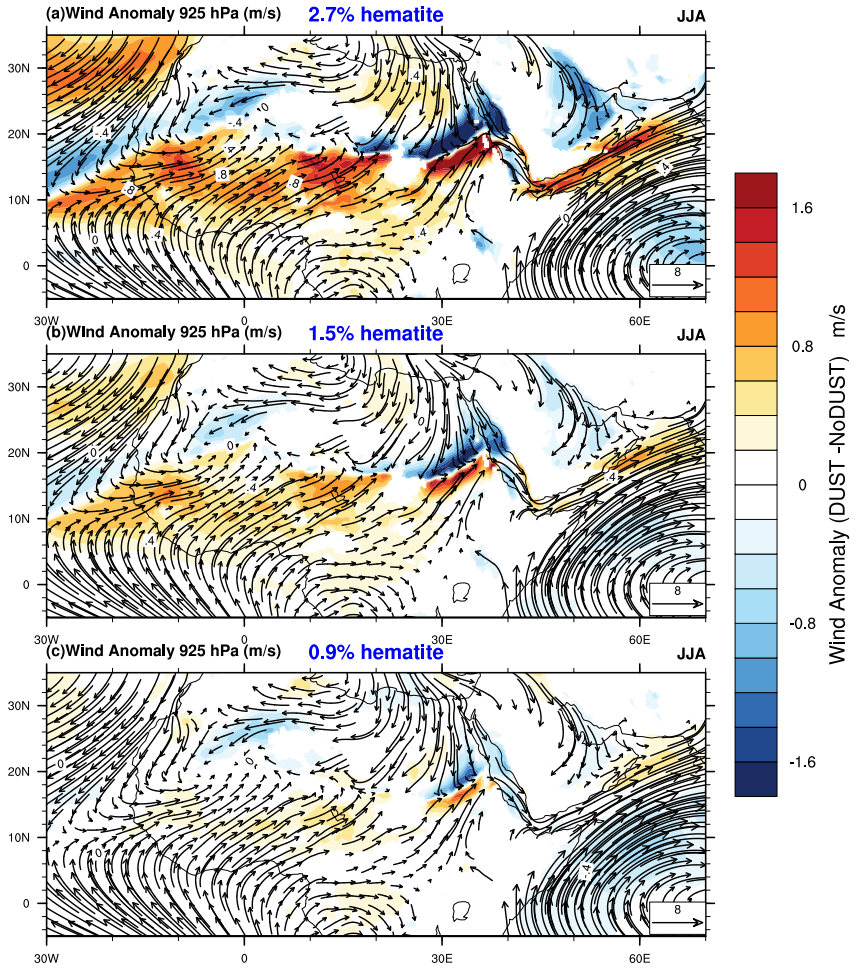

Figure 5.3: Response in 925 hPa wind speed (m/s^2)(shaded contours) to dust radiative effect while dust is assumed to be a (a) very efficient (DUST2.7 case), (b) standard (DUST1.5 case) and (c) inefficient (DUST0.9 case) absorber at shortwave, during the the the summer (JJA). Wind response at this level can effectively demonstrate the responses in WAM and WAWJ. Mean wind vectors in each experiment is overlaid.

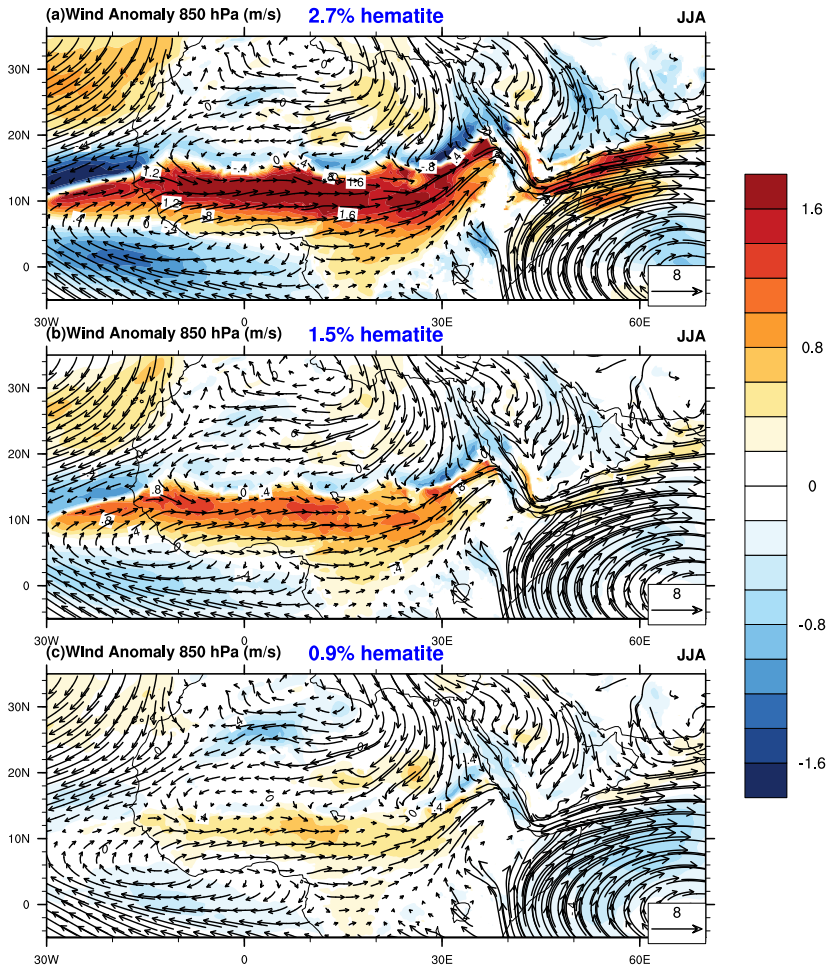

Figure 5.4: Response in 850 hPa wind speed (m/s^2)(shaded contours) to dust radiative effect while dust is assumed to be a (a) very efficient (DUST2.7 case), (b) standard (DUST1.5 case) and (c) inefficient (DUST0.9 case) absorber at shortwave, during the summer (JJA). Wind response at this level can effectively demonstrate the responses in WAM and WAWJ. Mean wind vectors in each experiment is overlaid.

regional climate.

5.1.2 Response of Monsoon "Onset" and "Jump"

The previous section mostly analyzed the response in the mean climatological characteristics of WAM. However, temporal evolution of monsoon and its variability and changes are very important for the local stakeholders, especially for the agricultural sector. The two most important temporal events in WAM evolution are the "monsoon onset" and "monsoon jump". The onset of monsoon (local onset) can be broadly defined as the time of first rains followed by uninterrupted rainy season, that could supply sufficient soil moisture for the agriculture (*Sultan and Janicot*, 2003). Meteorologically, it marks the time when monsoon and the associated climate dynamics establishes locally. Typically, WAM begins by intense rainfall over Guinean coast in the April-May Period. And the precipitation maximum stays there until late June. However, an abrupt shift in the location of rainfall maximum from 5^0N to a new quasi-stationary location around 12^0N occurs by the end of July or by the beginning of August. This abrupt shift in the favorable location of precipitation from Guinean coast to Sahel region is another important temporal event, which is called either "monsoon jump" (e.g., *Hagos and Cook*, 2007) or "regional monsoon onset" (e.g., *Sultan and Janicot*, 2003). The present study address this event characterizing the onset of intense rainfall over Sahel and the sudden suppression over Guinean coast, as "monsoon jump" from here on. This secondary spell of precipitation maximum is very important for Sahel region as it establishes unperturbed rain at the northernmost latitudes.

To investigate the influence of dust direct radiative effect on monsoon onset, more specifically the "local onset", the present study uses the definition of onset index originally defined by *Liebmann and Marengo* (2001) and later modified by *Diaconescu et al.* (2015). To calculalte this onset index, the daily accumulated rainfall anomalies

(A) at each grid point are estimated as,

$$A(day) = \sum_{n=1January}^{day} (R(n) - \mathbf{R}) \tag{5.1}$$

where $R(n)$ represents the daily rainfall. $\mathbf{R}$ is the climatological mean of rainfall at each grid point, if it is above 1 mm/day. Otherwise, $\mathbf{R}$ is fixed to 1 mm/day. This method of onset estimation effectively avoid the isolated rain events followed by dry spells and provide a more meaningful measure compared to conventional definitions of onset.

Figure 5.5 compares the mean local onset date ($A(day)$) in HiRAM simulations (DUST1.5) to GPCP and the Tropical Rainfall Measurement Mission Project (TRMM) precipitation . HiRAM simulates the local onset of WAM quite realistically, especially the pattern of the temporal evolution local onset. However, HiRAM simulates an advanced onset in lower latitudes and delayed onset in higher latitudes compared to observations, especially to that of TRMM.

The response of local onset date ($A(day)$) to dust radiative effect is shown in Figure 5.6. The hatched region represent the area where the response is statistically significant at 95 %. The statistical significance is estimated using Wilcoxon signed-rank paired test, as the onset dates are events with high interannual variability and are not normally distributed. The general pattern of local onset response reveals an east-west contrast. The onset is advanced in the central and eastern part of the continent while it is delayed over West Africa, in general. Interestingly, the east-west contrast in response, especially the statistical significance of these responses, is very sensitive to dust shortwave absorption. In highly absorbing case (DUST2.7), the onset happens about 10 days ahead of that in NoDUST case, over central and eastern part. And, this response is statistically significant. However, the delayed response over West Africa is weaker and statistically insignificant. In DUST1.5 case, the east-west dipolar response gets stronger and both the delay in West Africa and the advancement

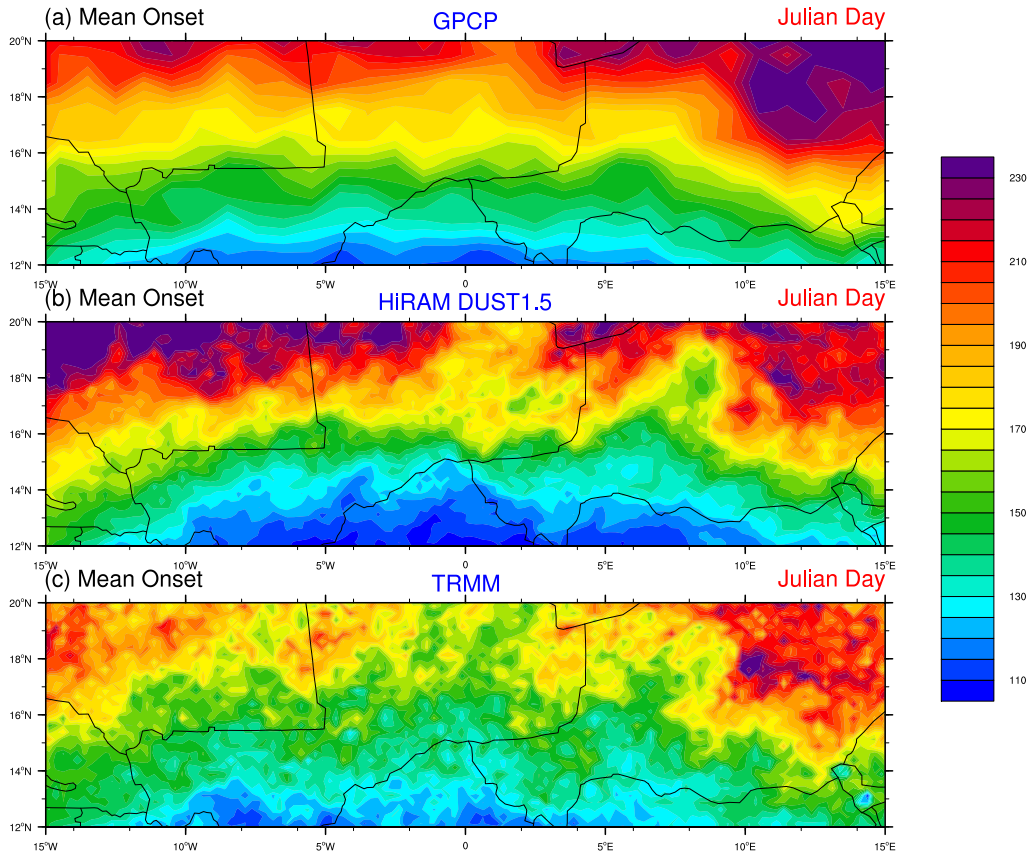

Figure 5.5: Mean (2000-2009) onset date ($A(day)$) estimated in (a) GPCP, (b) HiRAM (DUST1.5) and (c) TRMM datasets. The filled contours are the local onset date (Julian day)

.

in central to eastern part become statistically significant. Interestingly , the pattern of statistical significance reverses in DUST0.9 case. The delay in onset over West Africa becomes more pronounced and statistically significant, while the advancement over central part almost vanishes and becomes statistically insignificant.

To investigate the response in monsoon jump (regional onset), the criteria of *Sultan and Janicot* (2003) is used. The date of monsoon jump in this method is defined as the date at which 10 day smoothed, zonally averaged (10^0W - 10^0E) precipitation time series at 5^0N crosses that of at 15^0N. Therefore, the jump marks the time when

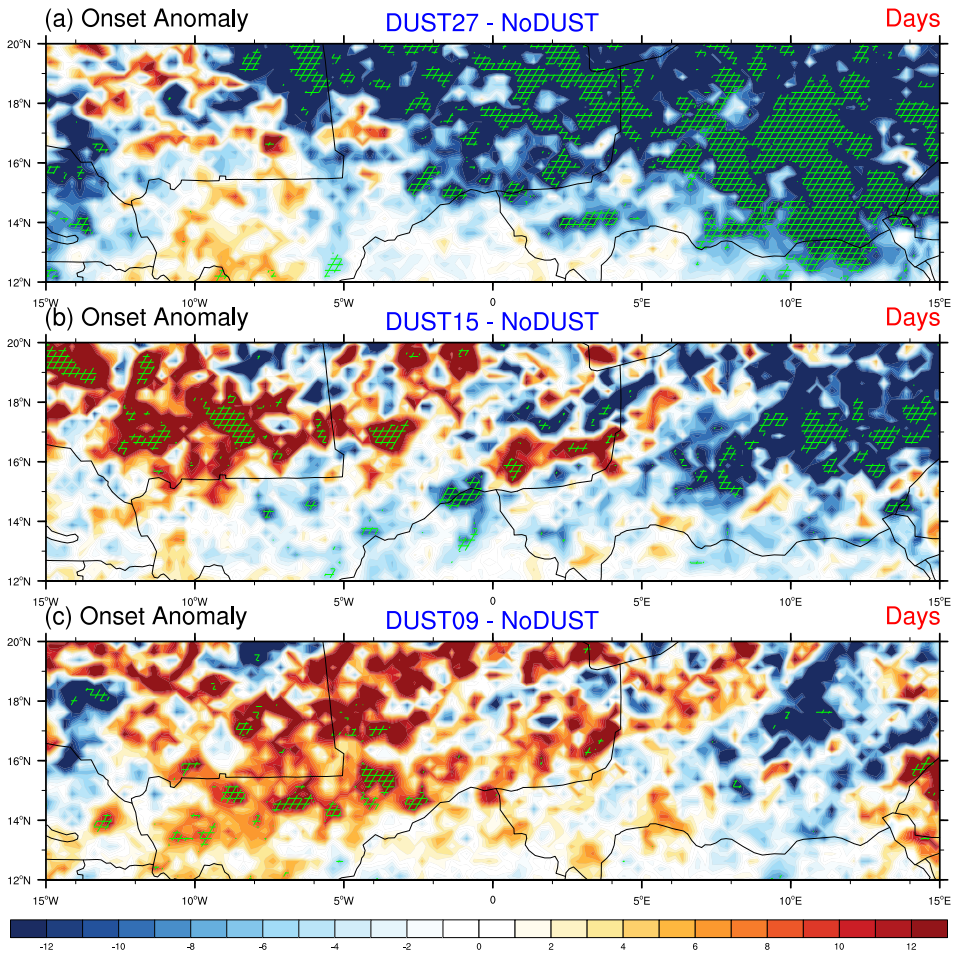

Figure 5.6: Response in the local onset date ($A(day)$) to dust radiative effect while dust is assumed to be a (a) very efficient (DUST2.7 case), (b) standard (DUST1.5 case) and (c) inefficient (DUST0.9 case) absorber at shortwave. Positive values indicate a delay (days) in onset and vice versa. The hatched regions represent the area where the response is statistically significant at 95% confidence interval. statistical significance is estimated using Wilcoxon signed-rank paired test

.

the Sahel precipitation increases with a simultaneous sudden decrease in rainfall over the Guinean coast.

The upper panel of Figure 5.7 depicts the mean picture of the monsoon jump, estimated from the mean precipitation over 33 years, in HiRAM, GPCP, and TRMM dataset. HiRAM realistically captures the date of jump compared to other two observational dataset. However, the mean precipitation at 5^0N is overestimated by HiRAM. It is associated with the precipitation overestimation over Guinean coast, which is evident in Figure 4.2. Nevertheless, the date of monsoon jump is predicted quite accurately (error not exceeding 3 days) in HiRAM.

The response in monsoon jump to dust radiative effect, estimated from 33 years composite, is depicted in the bottom panel of Figure 5.7. In all three cases, dust causes the jump to happen earlier. And, this response is sensitive to the amount of shortwave absorption. As dust shortwave absorption increases jump occurs earlier than NoDUST case. In highly absorbing case, the jump occurs about 10 days ahead compared to NoDUST case. Nevertheless, this analysis portrays the mean picture of the temporal evolution of precipitation and jump estimated using 33 years composites. Therefore, the analysis is not representative for the individual years, especially because monsoon jump has a high interannual variability. To have a more confident result on jump response, the response in the date of jump in all 33 years (3 ensemble simulation of 11-year window simulation) are shown in Figure 5.8. The mean response in the date of monsoon jump is estimated by averaging individual years jump data, instead of that from composite precipitation.The statistical significance of these responses have also been computed using Wilcoxon signed-rank paired test (see the bottom text in 5.8). Consistent with the jump response predicted from the averaged data, the response in individual years also predicts an earlier date of jump as a response to dust radiative effect. In highly absorbing (DUST 2.7) case, dust causes an earlier jump date about 10 days, which is statistically significant at 99% confidence interval.

Similarly, in moderately absorbing case (DUST1.5), dust advances the jump date by about 5 days (statistically significant at 90%.).

There are several competing explanation for the monsoon jump. A prominent theory is the interaction of monsoon circulation with SHL dynamics (e.g., *Sultan and Janicot*, 2003). It has been shown that the intensity of meridional circulation associated with SHL peaks at the beginning of the monsoon jump (*Sultan and Janicot*, 2003). It enhances the midlevel subsidence from the southern branch of the SHL transverse circulation and allows dry air intrusion from north to the ITCZ which in turn increases convective inhibition in the ITCZ region and suppress convection. However, the strengthening of cyclonic vorticity associated with the strengthening of SHL, enhance the inland moisture advection and establishes a deeper monsoon layer which ultimately increases the potential instability. At the same time, the enhanced mid-tropospheric anti-cyclonic circulation over SHL strengthens AEJ by increasing its instability character (negative meridional gradient of potential vorticity). In fact, the enhanced instability of AEJ supports the development and maintenance of AEWs. The monsoon jump occurs when the accumulated potential instability breaks the convective inhibition and releases the inertial instability of monsoon flow. In the present case, dust induced intense heating (Figure 3.4 & 4.6) in the SHL and the enhanced subsidence from intensified rainbelt, strengthen the SHL and its dynamics. The enhanced dynamics of SHL could potentially help to meet the criteria for monsoon jump much ahead of that in NoDust case, by establishing sufficient accumulated potential instability and negative meridional gradient in potential vorticity in advance. The sensitivity of monsoon to dust shortwave absorption also implicitly proves the argument, as the jump happens much earlier in high absorbing cases compared to relative less absorbing cases. However, since all these dynamic features are mutually adjusted in the simulations, it is hard to provide a clear cause-effect analysis.

Similarly, *Gu and Adler* (2004) projected the Guinean coast rainfall maximum

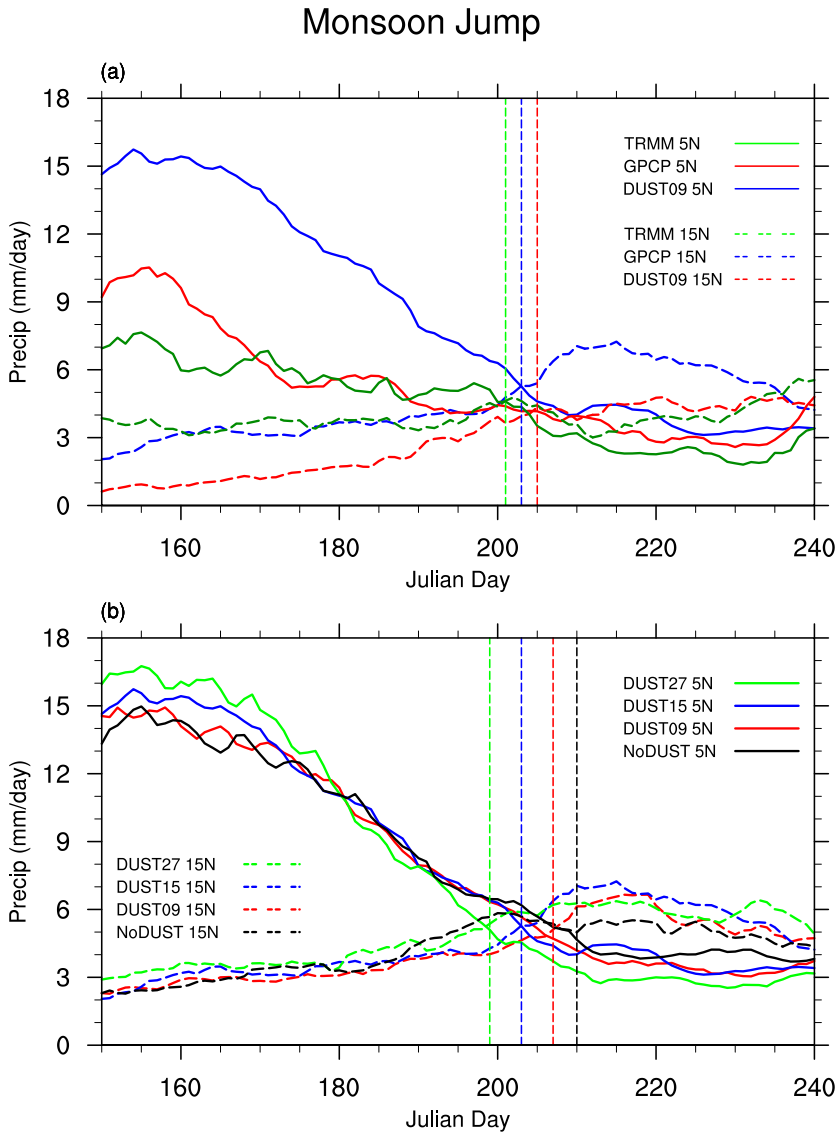

Figure 5.7: The 10-day time smoothed time series of precipitation averaged between 10^0W and 10^0E, at 15^0N and 5^0N. (a) The simulated temporal evolution precipitation in HiRAM (DUST1.5) is evaluated by comparing against two observational datasets, GPCP and TRMM. (b) The temporal evolution of precipitation in HiRAM while dust is assumed to be a very efficient (DUST2.7 case), standard (DUST1.5 case) and inefficient (DUST0.9 case) absorber at shortwave. The vertical lines mark the date of monsoon jump (Julian days), defined as the time when precipitation at 15^0N (Sahel) becomes greater than that at 5^0 (Guinean coast).

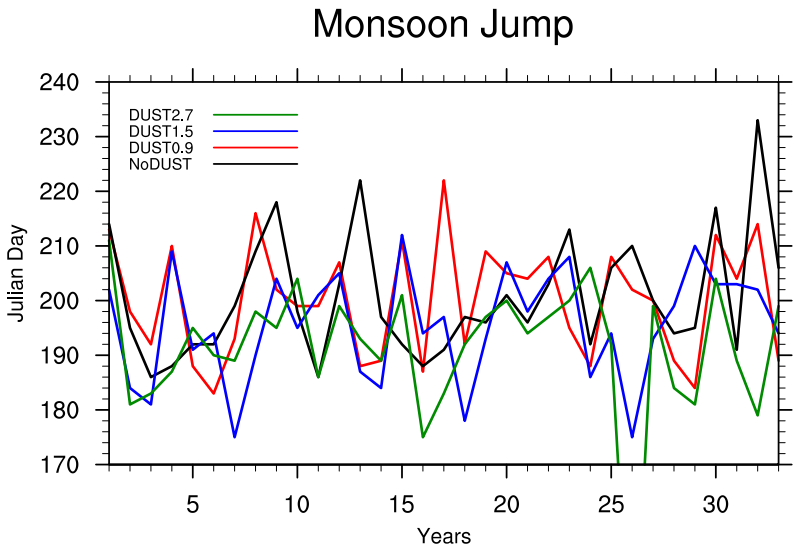

Figure 5.8: Response in monsoon jump (days) to dust radiative effect while dust is assumed to be a very efficient (DUST2.7 case), standard (DUST1.5 case) and inefficient (DUST0.9 case) absorber at shortwave, in all the 33 years (3 ensemble simulations of 11-year window simulation). The date of monsoon jump is defined as the time when precipitation at 15^0N (Sahel) becomes greater than that at 5^0 (Guinean coast). The averaged (33 years) shift in the date of monsoon jump in each case and the statistical significance of these shifts are displayed as text at the bottom of the plot. Negative values represent the an advanced monsoon jump, while positive values represent a delayed monsoon jump.

and the Sahelian rainfall maximum as two independent features, and shown that the former is controlled by the warm SST and the later is primarily driven by the northward shift AEJ and enhanced AEW activities. *Cook* (2015) made a similar conclusion on monsoon jump dynamics relating the inertial instability over Guinean coast and the shift of AEJ. It has been shown that the inertial instability develops over Guinean coast one month later compared to Atlantic marine ITCZ. The delay in instability development is due to the presence of AEJ, which establishes strong negative meridional wind gradient and hence a strong inertially stable environment. The jump in precipitation maxima happens when AEJ shifts to north. *Ramel et al.* (2006) also explain monsoon jump in connection with the abrupt shift in the location of the SHL, due to the difference in albedo between Sahel and Sahara. In summary, since the dynamics of AEJ is closely connected to SHL dynamics, the response of monsoon jump in response to the dust forcing, predicted in the present study is consistent with all the above-mentioned theories independently or in combination. The strengthening and northward shift of AEJ in response to dust forcing and its sensitivity to dust shortwave absorption are explicitly shown in the next section.

5.2 AEJ and TEJ Responses

Apart from the zonal and meridional overturning circulations, upper air jets like AEJ and TEJ could also mediate dust induced changes in the climate, especially in region's precipitation. It has already been revealed that the bulk of the precipitation over tropical Africa, especially on the western part, is linked to the AEJ and TEJ and to the wave disturbances (AEWs) associated with them (*Nicholson*, 2009). By comparing Sahelian wet and dry years' dynamics over west Africa, *Nicholson and Grist* (2001) showed that the two most striking differences were in the strength of TEJ and the strength and latitudinal position of AEJ. Similarly, using a combination of high-resolution dropsonde observations and model analyses, *Tompkins et al.* (2005) showed

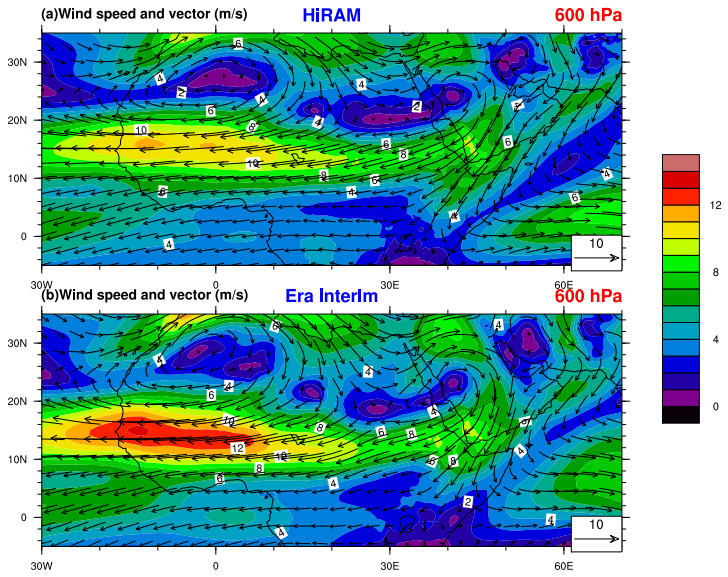

Figure 5.9: Mean Summer (JJA) wind speed and vector (m/s) in (a) HiRAM (DUST1.5 case) simulations and in (b) Era Interim Re-analyses, at 600 hPa

that the climatology of aerosol direct radiative effect in the simulations significantly improves the forecast of AEJ. The upper air vertical shear is a crucial factor in deciding occurrence of wet/dry mode in a certain year. Since the upper-air shear is greatly influenced by the relative location of the AEJ and TEJ, the latitudes of these jets are also important for the tropospheric dynamics in the region by influencing the vertical motion in general and wave activities in particular (*Nicholson et al.*, 2008). AEJ is considered to be instrumental in providing the sufficient baroclinic and barotropic instabilities for the development of AEWs (e.g., *Thorncroft and Hoskins*, 1994a,b; *Thorncroft*, 1995). AEWs are one of the most important synoptic features of the West African summer climate. Similarly, the vertical shear associated with the AEJ is important for the growth of long-lived mesoscale convective systems (MCSs) (e.g., *Houze and Betts*, 1981), which are responsible for most of the daily rainfall events in the West African region.

To analyse the response in AEJ and TEJ, wind speed at 600 hPa and 150 hPa are used, respectively. First of all, the simulated wind at 600 hPa and 150 hPa are

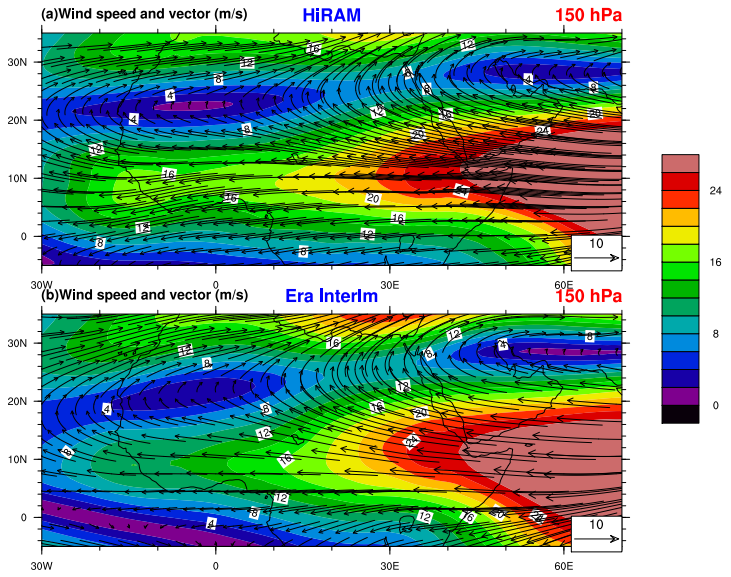

Figure 5.10: Mean Summer (JJA) wind speed and vector (m/s) in (a) HiRAM (DUST1.5 case) simulations and in (b) Era Interim Re-analyses, at 150 hPa

validated against ERA-Interim dataset (Figure 5.10 & 5.9). The HiRAM simulations very well capture the strength and position of both the jets with sufficient precision. Apart from the jets, HiRAM captures the strength and position of Asian monsoon anticyclone (Figure 5.10) and the mid-tropospheric anticyclones over SHL, SuHL and AHL (Figure 5.9).

Figure 5.11 depicts the response in AEJ as the mean summer wind response at 600 hPa. The wind speed anomaly is shown as shaded contours and the mean wind speed in each experiment is shown by contour lines in respective figures. In general, as a response to dust radiative effect, AEJ shifts northward throughout the African continent with a maximum of up to 2^0 latitudes (DUST2.7 case) over East Africa. Similar to rainbelt and local Hadley circulation responses, the AEJ response exhibits a dipole pattern: an increase (decrease) in wind speed to the north (south), which ultimately moves the jet mean position northward. Similar to precipitation and vertical velocity, an east-west contrast is also visible in the strength of the response with a heightened difference over East Africa. The strength of the response weakens

as absorption weakens (fromDUST2.7 to DUST0.9) and even the dipole pattern of response nearly disappears in DUST0.9 experiment.

It is well known that AEJ stems from the temperature structure in the troposphere that is established in association with deep moist convection in the tropical rainbelt (referred as"ITCZ " in *Thorncroft and Blackburn* (1999)) and dry convection in the lower troposphere in the Sahara; in other words, a positive meridional temperature gradient in the lower troposphere and reversal of the gradient in the mid-troposphere, between Sahara and the tropical rainbelt. The role of dust induced heating gradient in the lower-mid troposphere (Figure 3.4), hence, is to support and strengthen the positive meridional temperature gradient in the lower troposphere. It has already been known that the latitude of the jet maxima coincides with the maximum in low-level temperature gradient (*Cook*, 1999). The predicted northward shift in the jet axis is thus consistent with the heating gradient. *Mohr and Thorncroft* (2006) showed that the activity of the intense convective systems follows the seasonal migration of the AEJ and the peak in the activity occurs immediately poleward of the jet axis. Thus, the predicted northward shift of the mean AEJ axis supposedly moves the intense convective systems farther north and supports heightened activities throughout the region.

TEJ stems from the outflow of strong upper tropospheric anticyclone above the Tibetan plateau (*Koteswaram*, 1958), formed via the elevated solar heating and the latent heat release from the orographic rainfall, and the consequent geostrophic easterly current formation around 150 hPa. Although the generation mechanism is outside the domain of our interest, TEJ has a pivotal role in the MENA climate. This is a good example of the advantage of a GCM over an RCM in properly accounting for two-way interaction between global and regional responses. TEJ is thought to influence the tropical rainfall over the MENA region mainly in three ways: 1) by providing sufficient upper tropospheric shear for the development and maintenance of AEJ and

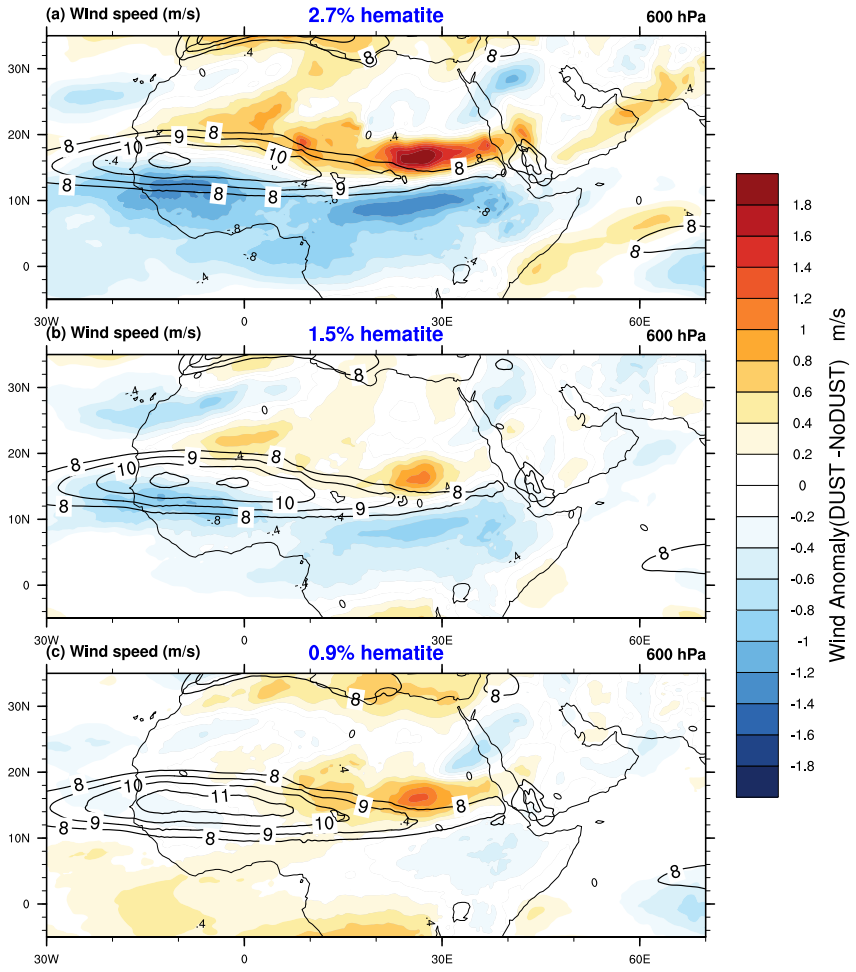

Figure 5.11: AEJ response (shaded contours) to dust radiative effect while dust is assumed to be a (a) very efficient (DUST2.7 case), (b) standard (DUST1.5 case) and (c) inefficient (DUST0.9 case) absorber at shortwave, during the summer (JJA). The response in AEJ is portrayed as the difference in 600 hPa mean wind speed (m/s^2) between simulations with dust radiative effect and without dust radiative effect. Mean wind in each experiment is overlaid as contour lines to illustrate the strength and position of AEJ.

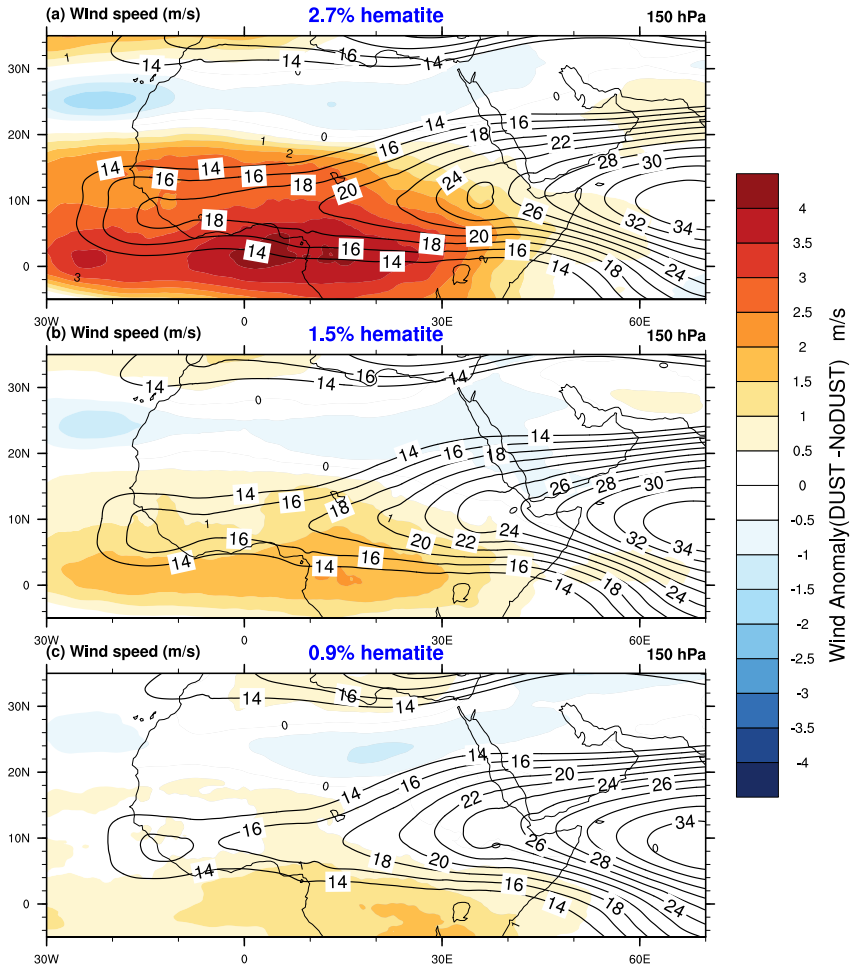

Figure 5.12: TEJ response (shaded contours) to dust radiative effect while dust is assumed to be a (a) very efficient (DUST2.7 case), (b) standard (DUST1.5 case) and (c) inefficient (DUST0.9 case) absorber at shortwave, during the summer (JJA). The response in TEJ is portrayed as the difference in 150 hPa mean wind speed (m/s^2) between simulations with dust radiative effect and without dust radiative effect. Mean wind in each experiment is overlaid as contour lines to illustrate the strength and position of TEJ.

AEW; 2) by the juxtaposition with the surface convergence (e.g, ITCZ), supporting deep convection; and 3) by providing upper air moisture supply. *Nicholson* (2001) showed that the upper troposphere shear, which is dependent on the strength of TEJ, is a key factor in the AEW development. The study also reveals that TEJ links to AEJ by providing sufficient shear near AEJ, which in turn increases the dynamic instability and allows wave development in the vertical direction. Moreover, the region of strong divergence associated with the TEJ promotes ascent in the lower and mid-troposphere. This further entrains the low-level moisture into higher levels, well into the vicinity of the AEJ (*Nicholson*, 2001). In effect, TEJ is a crucial component in the entrainment of moisture into the higher levels.

In response to DDRF, TEJ strengthens significantly throughout the jet and the axes of the jet shifts slightly farther south (Figure 5.12). However, the strengthening of the TEJ does not start from the entrance region to the domain (MENA), rather it starts to strengthen over east Africa and gradually increases towards the Atlantic. Therefore the strengthening of the TEJ could not be a direct effect of DDRF, rather a response to the anomalously heightened convective activities in the region. Conversely, the southward shift in the position of the jet continues from the ISM region. This could be related to the response of ISM to DDRF. The southward shift of the jet axis could displace the juxtaposition of the TEJ with the zone of maximum convection. Though *Hulme and Tosdevin* (1989) associate the southward shift with dry year dynamics over Sudan, it is not well known yet how it influences other regions.

5.3 African Easterly Waves

AEWs are the primary synoptic-scale disturbances and the dominant mode of variability over tropical Africa and Atlantic during the summer season. They are waves propagating westward from East Africa towards Atlantic, with a wavelength about 2000 to 4000 km with a period of 3 - 8 days, and phase speed of about 6 - 8 m/s

(e.g., *Burpee*, 1972; *Reed et al.*, 1977; *Karyampudi and Carlson*, 1988). AEWs can be seen as the cyclonic curvature maxima happens on AEJ, primarily happens in the mid-troposphere. They generally have a peak at the level of AEJ around 600 hPa to 700 hPa. The development and maintenance of AEWs were originally explained by the combined barotropic-baroclinic instability of AEJ (e.g., *Burpee*, 1972; *Charney and Stern*, 1962). However, recent studies pointed out the need of additional energy source for the development and initiation of the AEWs. (e.g., *Hsieh and Cook*, 2005, 2007, 2008; *Thorncroft and Hoskins*, 1994a,b). Diabatic heating associated with the deep convection in the rainbelt have been proposed as an essential energy source for both the initiation and maintenance of AEWs. Diabatic heating in the rainbelt produce potential vorticity and establishes a negative meridional potential vorticity gradient, which in turn invoke Charney-Stern instability (e.g., *Berry and Thorncroft*, 2012; *Hsieh and Cook*, 2005). Therefore, the deep convection within the AEWs themselves are crucial for the energetics and maintenance of AEWs. AEWs have a pivotal role in the initiation and organization of the convective rainfall over Sahel in general, and they often act as the precursor for Atlantic tropical cyclones. Therefore, a better understanding of AEW dynamics and improved predictive capabilities of the AEW season, amplitude and the location are of high societal impact.

The impact of dust radiative effect on AEWs has long been recognized (e.g., *Karyampudi and Carlson*, 1988; *Karyampudi et al.*, 1999), especially in the context of Saharan Air Layer (SAL), primarily due to their co-existence over Sahel. However, there is no consensus among these studies on the role of dust direct radiative effect in general or particularly that of SAL, on AEW development and maintenance. There are studies which predict an enhancement in AEW activities in the presence of dust (e.g., *Jones et al.*, 2004; *Ma et al.*, 2012; *Lavaysse et al.*, 2011), and those predict a suppression of the same (e.g., *Reale et al.*, 2009; *Karyampudi and Carlson*, 1988). By comparing the re-analysis and the model first guess fields, where the

former incorporate dust and the later not, *Jones et al.* (2004) concluded that the dust induced heating in the lower-troposphere and the consequent reduction of static stability enhance wave activities. Similarly, *Ma et al.* (2012) showed that the dust induced heating and the associated reduction in static stability enhance convection, which in turn favors AEW development. However, studies which predict a weakening of AEW activities, which were mostly focused on the SAL influence on AEWs, explain the weakening of AEW as a consequence of the mid-tropospheric heating in the SAL and the associated stabilization effect in the atmospheric column. However, the present study examines the role of climatological dust loading on AEWs, which takes into account the dust radiative effect over the entire region and the entire atmospheric column.

AEWs are seasonal and episodic events, with different characteristics in different time of the season. Therefore, to capture the temporal evolution of such a non-stationary time series, wavelet analysis is the right tool (*Grist*, 2002). The response in the temporal evolution of wave season, wave structure and its amplitude are thus examined in the present study using wavelet analysis. Morlet wavelet has been proven to be very efficient for AEW analysis(*Grist*, 2002; *Grist et al.*, 2002), and is chosen in the present analysis. Following *Torrence and Compo* (1998), wavelet analysis has been conducted over meridional wind at 700 hPa averaged over 10^0N - 15^0S and 10^0W - 5^0W for each of the 33 years in all the experiment set. The location of 10^0N - 15^0S ; 10^0W - 5^0W is chosen because it is considered to be the favorable location for the wave activities. The significance level of wavelet transform for each year time series has been calculated using red noise method as explained in *Torrence and Compo* (1998). The wavelet transform is very efficient in depicting the magnitude and the period of wave activities in a seasonal cycle. Therefore it is an efficient method to define the onset and the length of the wave season in each year.

Figure 5.13 depicts the modulus of wavelet transform for an individual year (2005),

to demonstrate the effectiveness of the wavelet analyses in depicting the temporal evolution of wave activities and its structure and amplitude. It also demonstrates how well HiRAM simulates the wave activities in individual years. The left y-axis represents the wavelet scale and the right y-axis represents the corresponding Fourier period in days. The x-axis originally represents the time of the year in Julian days, but it has been marked in terms of the months of the year for an easy interpretation. The overlaid dots indicate the 95% significance level of the transform. The significance is estimated against the background red-noise. The beginning of the AEW season can be interpreted as the time of the year when the transform becomes statistically significant between wavelet scale of 3 and 8. Figure 5.13 shows that HiRAM distinctly resolves AEW activities, its season and period quite realistically. The wave season in HiRAM (DUST1.5) starts in the beginning of June and ends by the end of September, in this particular year. The scale range of significant variance marks the period of wave activities as 3 - 8 days, which is very well in agreement with previous studies. Within the wave season (June-September) there are spells of active and suppressed wave activities, indicating the episodical behavior of AEWs. Although HiRAM simulations are very well in agreement with re-analyses (ERA-Interim and MERRA re-analyses) on the onset of wave season and the length of the wave season, HiRAM's wave activity has much power during the wave season compared to both re-analyses. This might be because of the lower spatial resolution of the re-analyses compared to HiRAM. Interestingly, MERRA produces more power during wave season compared to ERA-Interim re-analyses, possibly due to its slightly higher spatial resolution compared to ERA-Interim. Since there are no high spatial resolution observation or re-analyses dataset a comprehensive validation of the wave activities in HiRAM is not possible. However, given the accurate prediction of the temporal evolution of wave season consistent with previous studies, it could be reasonably assumed that the relatively higher power in HiRAM seemed to be realistic owing to higher spatial resolution.

Although, wavelet analyses of each year provide a very detailed information of the time evolution of wave season in each year, it is not practically viable to draw conclusions from the wavelet transforms of all 33 individual years in four various HiRAM experiments. Therefore, we made averages of wavelet transforms for all the 33 years in each experiment. It should be noted that, by averaging multi-year wavelet spectrum, the detailed information in local time will be partially lost. Nevertheless, it provides the average distribution of power in time. Since AEWs are strictly seasonal (June-September), and since the present study is interested in the average response in AEW activities rather than individual cases, it's useful to analyze the multi-year averaged wavelet spectrum in each experiment. Figure 5.14 depicts the average modulus of wavelet transform in all four HiRAM cases and two re-analyses. The power is concentrated between June - September over a scale of 3-8 days (Fourier period) and it represents AEWs. The obvious pattern of seasonality and amplitude evident even after averaging multi-year wavelet analyses, implicitly proves that HiRAM realistically simulates AEW season. Most importantly, HiRAM predicts the two peaks in wave amplitude (*Burpee*, 1972), one in the middle of June and another in August-September, and the break in between the two peaks, quite realistically even in the averaged picture. Comparison between simulations with and without dust shows that dust radiative effect influences AEW activity. Presence of dust enhances the mean amplitude of the wave activities and broadens the wave season (It is shown explicitly, later). A comparison across different cases of HiRAM experiment depicts the fact that AEW activities are quite sensitive to dust shortwave absorption. As shortwave absorption increases the length of the season broadens and amplitude increases.

To explicitly demonstrate the response in the power and seasonality of AEWs in each case, the scale-averaged (3-8) mean wavelet power is depicted in Figure 5.15. The scale-averaged wavelet power in certain scale band can be seen as the variance at that particular band (*Torrence and Compo*, 1998). Therefore, it is very useful in

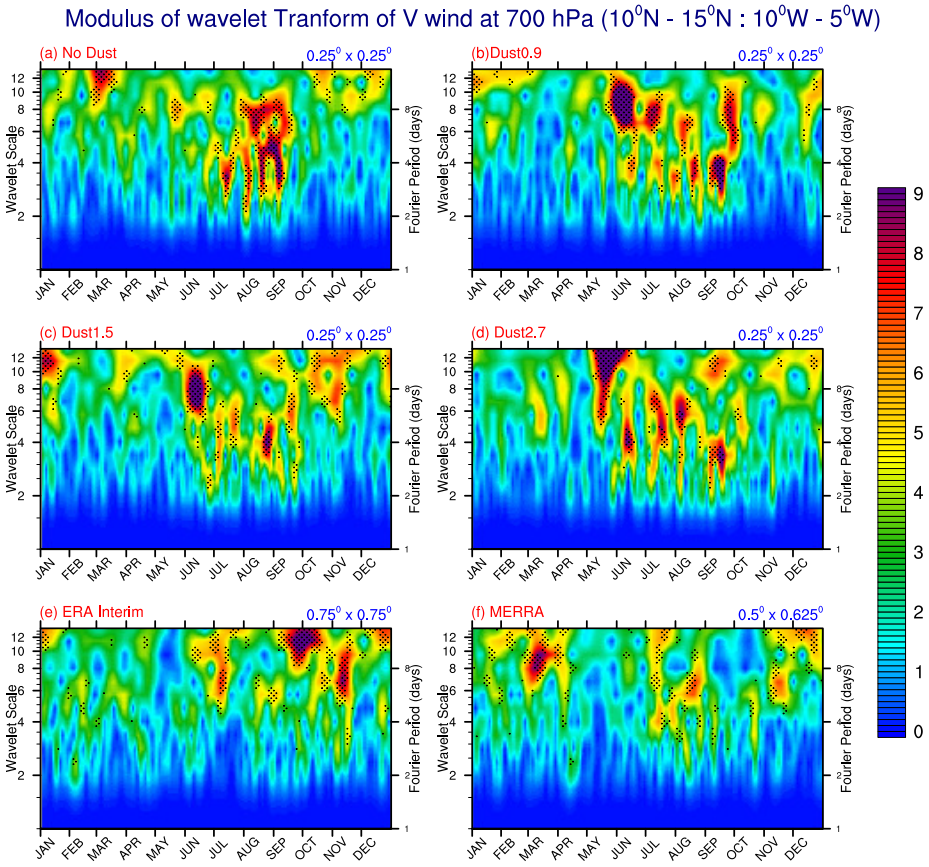

Figure 5.13: Modulus of the wavelet transform of the 700mb daily meridional wind at (10^0N - 15^0S ; 10^0W - 5^0W), for four HiRAM cases and two re-analyses (ERA-Interim and MERRA), for the year 2005. The dots indicate 95% confidence level.

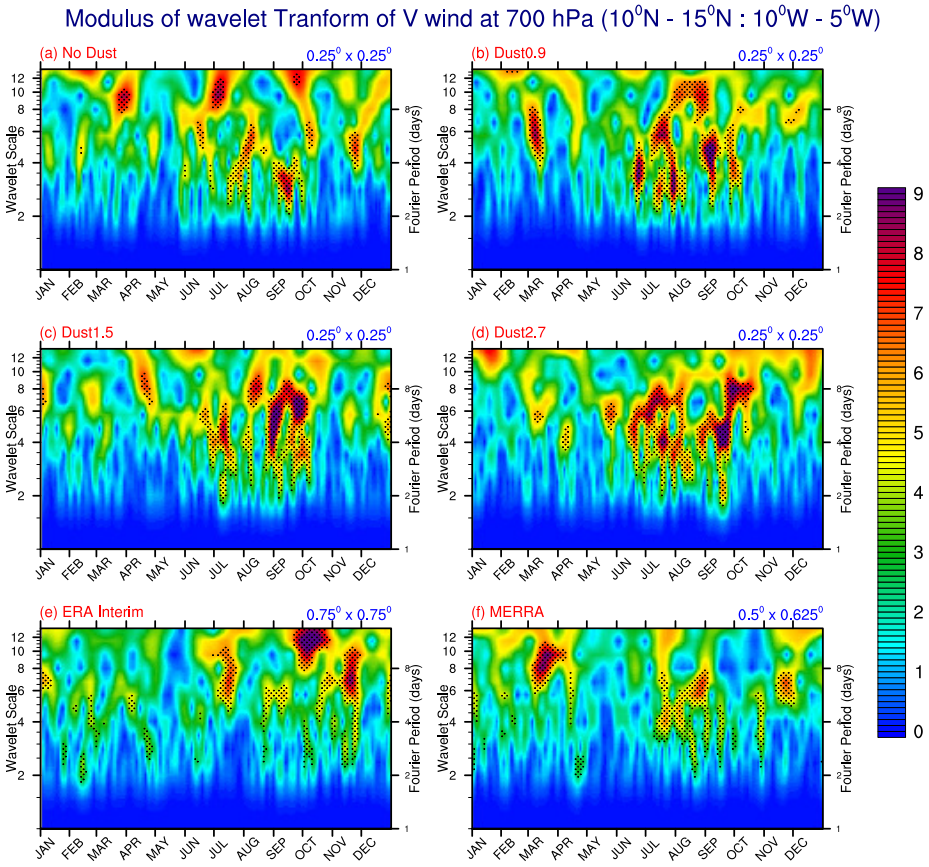

Figure 5.14: Mean modulus (2000 - 2009) of the wavelet transform of the 700mb daily meridional wind at (10^0N - 15^0S ; 10^0W - 5^0W), for four HiRAM cases and two re-analyses (ERA-Interim and MERRA). The dots indicate 95% confidence level.

analyzing the difference between two different time series. The upper panel shows comparison of AEW activities in HiRAM (DUST1.5) against two re-analyses, ERA-Interim and MERRA. HiRAM simulates the onset of the wave season, its break in July and the second peak in September adequately well. HiRAM also captures the enhanced amplitude of the second peak (August-September) compared to the first one (June-July), realistically. The bottom panel of Figure 5.15 represents the seasonal evolution of AEW activities, in all four cases of HiRAM experiments. The figure explicitly portrays the impact of dust on the amplitude, onset and the length of AEW season. In general, dust enhances the wave amplitude and broadens the wave season. A comparison among various cases reveals the strong sensitivity of the amplitude, onset date and the duration of the wave season, to dust shortwave absorption. The amplitude and the length of the wave season increase as shortwave absorption increases. Moreover, the length of each spells broaden as shortwave absorption increases. Similarly, The wave season starts earlier and ends late in the DUST2.7 case compared to other less absorbing cases.

The predicted response in AEW season and amplitude in response to dust and the sensitivity of response to dust shortwave absorption are in good agreement with the previous studies (e.g., *Jones et al.*, 2004; *Ma et al.*, 2012; *Lavaysse et al.*, 2011). Note that the present study is not particularly investigating the response of AEW to SAL and associated radiative forcing; rather, the study attempts to estimate the response and sensitivity of AEWs to a seasonally varying mean dust field. The results are consistent with the explanation by *Jones et al.* (2004), as the dust induced lower tropospheric heating is evident from the maps of radiative heating rate (Figure 3.4) and the air temperature response (Figure 4.6). The results are also consistent with the diabatic heating argument by *Berry and Thorncroft* (2012) and *Hsieh and Cook* (2005). The intensification of the rainbelt as evident from Figure 4.2 and the associated diabatic heating release, could potentially invoke Charney-Stern instability by

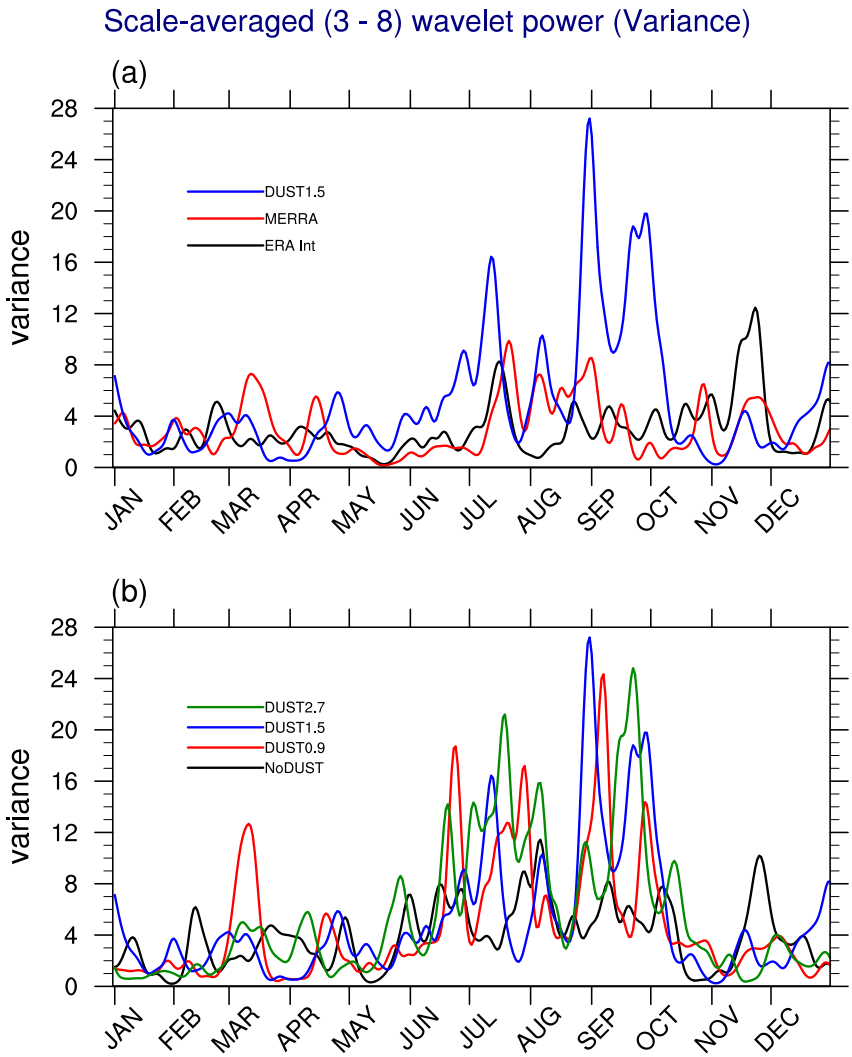

Figure 5.15: Mean scale-averaged wavelet power (variance) of the wavelet transform between 3-8 day period, of the 700mb daily meridional wind at (10^0N - 15^0S ; 10^0W - 5^0W). (a) The temporal evolution of scale-averaged wavelet power in HiRAM (DUST1.5) is evaluated by comparing against two re-analyses datasets, ERA-Interim and MERRA. (b) The temporal evolution of scale-averaged wavelet power in HiRAM while dust is assumed to be a very efficient (DUST2.7 case), standard (DUST1.5 case) and inefficient (DUST0.9 case) absorber at shortwave.

enhancing the meridional potential vorticity gradient. This will definitely leads to enhancement of the AEW activities.

Chapter 6

Conclusion

6.1 Concluding Remarks

Dust-climate interaction over MENA has long been studied, as it is the "dustiest" region around the globe. However, the quantitative and qualitative understanding of the role of dust direct radiative effect on MENA climate is still rudimentary; partly because of the complexity of various physical and chemical processes involved and the uncertainties associated, and partly because of the lack of right modeling and computational capabilities. The present dissertation investigates dust direct radiative effect on MENA climate with a special emphasis on the sensitivity of climate response to dust shortwave absorption, which is one of the most uncertain components of dust direct radiative effect. Simulations are conducted with and without dust radiative effect, to differentiate the effect of dust on climate. To elucidate the sensitivity of climate response to dust shortwave absorption, simulations with dust assume three different cases of dust shortwave absorption, representing dust as a very efficient, standard and inefficient shortwave absorber. Dust is not uniformly distributed in space and time. Therefore, radiative effect of dust invokes circulations at various scales ranging from global overturning circulations to regional scale jets. Since climate at the regional scale is determined by all these multi-scale circulations, perturbations in all such circulations have to be taken into account for an accurate prediction of regional climate response to dust radiative effect. To incorporate multi-scale circulation responses, the present study takes advantage of the high spatial resolution capabilities

of an AGCM, HiRAM. AMIP-style global high-resolution simulations are conducted at a spatial resolution of 25 km. Such global high-resolution simulations also help to overcome the two-way interaction issue arising from the forced boundary conditions in RCMs.

Comparison of simulations with and without dust radiative effect illustrates significant impact of dust radiative effect on MENA climate. The most striking result is the intense response in the strength and the latitudinal extent of the tropical rainbelt. Dust-induced radiative perturbations increase the precipitation and widen the rainbelt northward, resulting in a dipole-like structure in response throughout the region. It has been shown that dust-induced changes in the regional Hadley circulation and other major regional circulations favor the strengthening and the northward shift of rainbelt. Another important response is in the temperature field. The temperature significantly reduces under the rainbelt and increases over subtropical deserts. Temperature response is consistent with the enhanced precipitation and cloudiness in the rainbelt and the consequent anomalous subsidence over subtropics.

The study specifically investigates the role of global and regional circulations in mediating the climate response over the region. One of the most significant circulation response is in the local Hadley circulation. In response to meridionally asymmetric radiative forcing, the ascending branch of the local Hadley circulation enhances and shifts farther north into the summer hemisphere. It clearly indicates that the dust-induced radiative heating confined in the NH subtropics effectively functions as a hemispherically asymmetric off-equator heating source and alters the meridional heating gradient. Associated with the shifts in the zonally averaged mean meridional circulation, AEJ, which also depends on the meridional heating gradient, moves further north by a few degrees. These responses in the circulation features are in phase with the predicted response of the rainbelt. WAM is another important circulation feature significantly responsive to dust radiative effects. As a major component of

the lower atmospheric zonal circulation, the enhanced WAM circulation extends the moisture supply inland, which is a crucial factor for the tropical rainbelt. Another important response is in the AEWs. The intensity and the duration of the wave season increase as a response to dust radiative effect. Overall, the dust-induced changes in the tropospheric dynamics support the predicted response in precipitation and temperature.

In conclusion, the northward shift of the ascending branch of Hadley cell, AEJ and ITCZ along with strengthening of WAM circulation, support an enhancement and shift of the tropical rainbelt. The changes in circulations as the response to dust radiative effect are similar to those occurring during wet years, in many ways. Comparison with the studies that explored the differential atmospheric dynamics in wet and dry years (e.g., *Hulme*, 1996; *Lamb*, 1978; *Janicot*, 1992a) reveals that the DDRF impact on the circulation has similarities to wet year dynamics. In response to DDRF, a northward shift in the AEJ axes and the ITCZ and the strengthening of TEJ is predicted, which are characteristic features of the wet year dynamics. Many of the previous studies have already indicated the possible role of dust in the prolonged desiccation over Sahel (e.g., *Brooks and Legrand*, 2000; *Prospero and Lamb*, 2003; *Yoshioka et al.*, 2007). Our results strongly suggest that changes in the dust loading could potentially influence the precipitation over semi-arid equatorial Africa and hence it is essential to include dust radiative effect in the simulations and future projections of this region's climate.

The dissertation examined the sensitivity of the all the above-mentioned climate responses by comparing results from three different shortwave absorption cases. The rainbelt and the temperature responses are sensitive to shortwave absorption. The rainbelt strengthens and moves northward as shortwave absorption increases. Similarly the temperature response also enhances as shortwave absorption increases. It has been shown that the response in rainbelt and temperature are greatly medi-

ated by the responses in the regional Hadley circulation as well as the embedded regional circulations, which depends on the dust-induced meridional heating gradient. Therefore, sensitivity in the inter-hemispheric heating gradient could potentially make those circulations sensitive to shortwave absorption. Local and regional Hadley circulation response is strongly sensitive to shortwave absorption; as absorption and associated heating increases, the Hadley circulation further enhances and moves farther poleward. Regional circulation features such as WAM, AEJ and WAWJ respond similarly since they also strongly depend on the meridional heating/temperature gradient. These regional circulations intensify and move farther poleward as shortwave absorption increases. Similarly, the response in AEW is also sensitive to shortwave absorption. The amplitude and the duration of the wave season increase in response to increasing shortwave absorption. It all indicates that the sensitivity of the rainbelt stems from the sensitivity of these multi-scale circulations to meridionally asymmetric shortwave heating induced by dust. To sum up, the present study demonstrates the sensitivity of the MENA climate and the driving circulations, to a plausible range of dust shortwave absorption. The results also demonstrate how the sensitivity in driving circulations decide the sensitivity of rainbelt to dust shortwave absorption.In other words, the sensitivity of circulations to shortwave absorption is further evidence for the mechanism proposed for the dust-rainbelt interaction

The variability in the hematite content or SSA of dust is carefully chosen in the current study to bracket the spectrum of possible ranges of dust shortwave absorption, which helps to demonstrate the corresponding sensitivity of climate responses. The dust optical properties for these three cases are derived by assuming dust has a hematite content of 2.7%, 1.5% and 0.9%, respectively (*Balkanski et al.*, 2007). However, the shortwave absorption also depends on many other factors such as the albedo of the underlying surface, dust size distribution and the vertical structure of the dust loading. Therefore, the sign and magnitude of radiative forcing and climate

response could vary under different environmental conditions, even for the same dust optical properties. In the present study, even in the least absorbing case (DUST0.9), TOA forcing is slightly positive over bright Saharan and Arabian deserts. Nevertheless, a number of other factors could potentially change the sign of TOA forcing and corresponding climate responses. For instance, dust size distribution with a larger fraction of small particles or a darker surface albedo could change the sign of TOA forcing from positive to negative over those deserts, for the same set of dust refractive indices. This is why some studies estimated negative DDRF at TOA over these deserts (e.g., *Yoshioka et al.*, 2007). Therefore, a final verdict on the possible range of the uncertainty related to dust shortwave absorption cannot be made by overlooking the uncertainty in the other factors on which dust shortwave absorption depends. However, the present study clearly demonstrates the sensitivity of the MENA dust belt, and the multi-scale circulations associated with it, to a realistic range of dust shortwave absorptivity, by only changing the hematite content and keeping all other factors constant. Nevertheless, these results can be interpreted for changes in shortwave absorption due to any other reason.

It is noteworthy that the response in the rainbelt and the associated circulation responses, such as local Hadley and Walker circulations, AEJ and surface circulation, have a significant east-west contrast. In general, the effects of shortwave absorption are stronger over East Africa, the southern Red Sea and the southwest tip of the Arabian Peninsula. This is an important feature and needs to be better understood. First of all, the forcing itself has an east-west contrast in the present simulations with higher values in East Africa, which could make heightened response there. Apart from this, analyses of Walker circulation demonstrate that East Africa (specifically the Ethiopian Highlands and the southern Red Sea) experience significant response, unlike any other region. This differential response in the Walker circulation could also contribute to the predicted east-west contrast in the precipitation belt. In addition,

from the surface circulation point of view, West Africa has more zonal component of wind associated with WAM and WAWJ, while over East Africa the surface circulation is more meridional. Therefore, it is expected to predict a differential meridional circulation response over East Africa, provided that the large scale forcing is primarily meridionally oriented. Furthermore, East Africa has many "hot spots" in the climatological mean summer precipitation associated with orographic features such as the Ethiopian High Lands and Asir escarpment mountains in the southwest tip of the Arabian Peninsula, and areas with high local surface winds such as Tokar gap jet. These hot spots in the climatological mean precipitation and surface wind are well captured in our simulations, and they could influence the heightened response predicted over East Africa.

A main scientific question posed in the dissertation is whether dust direct radiative effect green Sahel or not? The analysis of precipitation clearly shows that the Sahel gets increased rainfall as a response to dust. In fact, the maximum response and sensitivity are predicted at the northern edges of the rainbelt, which is geographically over Sahel. The precipitation response can even go to 50% of the total precipitation in some location in Sahel. Considering the social and ecological vulnerability of the Sahel region, the predicted sensitivity of rainbelt suggests the importance of accurate representation of dust shortwave absorption in the numerical models, for an accurate simulation of the region's climate and weather.

It is well known that the Atlantic SST in general, and specifically the near equatorial SST gradient, plays an important role in the rainbelt over MENA region (e.g., *Folland et al.*, 1986; *Nicholson*, 2013; *Davey et al.*, 2002; *Cook*, 2008). However, the present study investigates the atmosphere-only sensitivity to dust shortwave absorption, using AMIP-type simulations with observed SST as bottom boundary conditions. This approach provides an ideal ocean forcing and helps to avoid the cold SST bias in equatorial ocean common to most of the coupled GCMs, and hence helps to

improve the representation of the strength and position of the climatological mean rainbelt. However, any changes in SST due to dust radiative forcing could potentially alter the latent heat flux feedback and hence the sign and magnitude of the predicted response. Since SST being kept constant in AMIP-type simulations, the present study does not take the SST into account. Simulations with fully coupled or mixed layer ocean simulations are necessary to incorporate this effect, which is beyond the scope of the present dissertation.

Finally, There are some shortcomings and limitations in this study. First of all, the current study does not include indirect radiative forcing, which is proven to be a significant contributor by modifying cloud properties. Furthermore, the study assumes constant optical properties spatially and temporally when in reality they change and have strong dependency on source regions (e.g., *Perlwitz et al.*, 2015). It should also be noted that the simulations do not take into account the feedback of the rainbelt response on dust generation (e.g., *Yoshioka et al.*, 2007; *Marsham et al.*, 2011) since the dust loading is prescribed from offline estimation. All these issues should be addressed separately or together in future studies to better estimate the sensitivity.

6.2 Summary

- The tropical rainbelt across MENA strengthens and move farther northward into deserts, in response to dust direct radiative forcing.
- In response to dust direct radiative effect, the atmospheric temperature under the rainbelt cools and that over subtropical deserts warms.
- The response in precipitation (rainbelt) and temperature over MENA are greatly mediated by the response in multi-scale circulations to dust radiative effect.
- The regional Hadley circulation gets strengthened and shifts farther northward as a response to dust direct radiative effect.

- Regional circulations such as WAM, AEJ and WAWJ strengthens in response to dust.
- Dust radiative effect leads to intense AEWs and longer wave season.
- All the responses in climate and circulations are significantly sensitive to dust shortwave absorption, especially those depends on the meridional temperature gradient over MENA.
- Sahel greens in response to dust shortwave absorption, and the greening is very sensitive to shortwave absorption. More absorbing dust makes Sahel greener.

6.3 Future Research Work

The research done as part of the current dissertation can be extended in the following directions.

- Repeat the experiments in the present dissertation with a coupled fully dynamic ocean model or mixed layer model to quantify the role of SST feedback in dust climate interaction.
- Conduct experiments with fully interactive dust module to better quantify the dust direct radiative effect, by incorporating feedbacks on dust generation.
- Expand the work by incorporating dust indirect radiative effect.

REFERENCES

Ackerman, S. A., and H. Chung (1992), Radiative effects of airborne dust on regional energy budgets at the top of the atmosphere, *Journal of Applied Meteorology*, *31*(2), 223–233, doi:10.1175/1520-0450(1992)031.

Adler, R. F., G. J. Huffman, A. Chang, R. Ferraro, P.-P. Xie, J. Janowiak, B. Rudolf, U. Schneider, S. Curtis, D. Bolvin, et al. (2003), The version-2 global precipitation climatology project (GPCP) monthly precipitation analysis (1979-present), *Journal of hydrometeorology*, *4*(6), 1147–1167, doi:10.1175/1525-7541(2003)004.

Ahn, H.-J., S.-U. Park, and L.-S. Chang (2007), Effect of direct radiative forcing of Asian dust on the meteorological fields in East Asia during an Asian dust event period, *Journal of Applied Meteorology and Climatology*, *46*(10), 1655–1681, doi: 10.1175/JAM2551.1.

Allen, R. J., and S. C. Sherwood (2011), The impact of natural versus anthropogenic aerosols on atmospheric circulation in the Community Atmosphere Model, *Climate dynamics*, *36*(9-10), 1959–1978, doi:10.1007/s00382-010-0898-8.

Alpert, P., Y. Kaufman, Y. Shay-El, D. Tanre, A. Da Silva, S. Schubert, and J. Joseph (1998), Quantification of dust-forced heating of the lower troposphere, *Nature*, *395*(6700), 367–370, doi:10.1038/26456.

Anderson, J. L., V. Balaji, A. J. Broccoli, W. F. Cooke, et al. (2004), The new GFDL global atmosphere and land model AM2-LM2: Evaluation with prescribed SST simulations, *Journal of Climate*, *17*(24), 4641.

Balkanski, Y., M. Schulz, T. Claquin, and S. Guibert (2007), Reevaluation of Mineral aerosol radiative forcings suggests a better agreement with satellite and AERONET data, *Atmospheric Chemistry and Physics*, *7*(1), 81–95, doi:10.5194/acp-7-81-2007.

Bangalath, H. K., and G. Stenchikov (2015), Role of dust direct radiative effect on the tropical rainbelt over Middle East and North Africa: A high resolution AGCM study, *Journal of Geophysical Research: Atmospheres*, *120*, 4564–4584, doi:10.1002/2015JD023122.

Bangalath, H. K., and G. Stenchikov (2016), Sensitivity of the Middle East–North African Tropical Rainbelt to Dust Shortwave Absorption: A High-Resolution AGCM Experiment, *Journal of Climate*, *29*(19), 7103–7126, doi:http://dx.doi.org/10.1175/JCLI-D-15-0827.1.

Berry, G. J., and C. D. Thorncroft (2012), African easterly wave dynamics in a mesoscale numerical model: The upscale role of convection, *Journal of the Atmospheric Sciences*, *69*(4), 1267–1283.

Biasutti, M., and A. Giannini (2006), Robust Sahel drying in response to late 20th century forcings, *Geophysical Research Letters*, *33*(11), doi:10.1029/2006GL026067.

Boyle, J., and S. A. Klein (2010), Impact of horizontal resolution on climate model forecasts of tropical precipitation and diabatic heating for the TWP-ICE period, *Journal of Geophysical Research: Atmospheres (1984–2012)*, *115*(D23), doi:10.1029/2010JD014262.

Bretherton, C. S., J. R. McCaa, and H. Grenier (2004), A new parameterization for shallow cumulus convection and its application to marine subtropical cloud-topped boundary layers. Part I: Description and 1D results, *Monthly weather review*, *132*(4), 864–882, doi:10.1175/1520-0493(2004)132⟨0864:ANPFSC⟩2.0.CO;2.

Broccoli, A. J., K. A. Dahl, and R. J. Stouffer (2006), Response of the ITCZ to Northern Hemisphere cooling, *Geophysical Research Letters*, *33*(1), doi:10.1029/2005GL024546.

Brohan, P., J. J. Kennedy, I. Harris, S. F. Tett, and P. D. Jones (2006), Uncertainty estimates in regional and global observed temperature changes: A new data set from 1850, *Journal of Geophysical Research: Atmospheres (1984–2012)*, *111*(D12), doi:10.1029/2005JD006548.

Brooks, N., and M. Legrand (2000), Dust variability over northern Africa and rainfall in the Sahel, in *Linking climate change to land surface change*, pp. 1–25, Springer, doi:10.1007/0-306-48086-7-1.

Burpee, R. W. (1972), The origin and structure of easterly waves in the lower troposphere of North Africa, *Journal of the Atmospheric Sciences*, *29*(1), 77–90, doi:10.1175/1520-0469(1972)029⟨0077:TOASOE⟩2.0.CO;2.

Carlson, T. N., and S. G. Benjamin (1980), Radiative heating rates for Saharan dust, *Journal of the Atmospheric Sciences*, *37*(1), 193–213, doi:10.1175/1520-0469(1980)037%3C0193:RHRFSD%3E2.0.CO;2.

Cess, R., G. Potter, S. Ghan, and W. Gates (1985), The climatic effects of large injections of atmospheric smoke and dust-a study of climate feedback mechanisms with one-dimensional and 3-dimensional climate models, *Journal of Geophysical Reasearch:Atmospheres*, *90*(D 7), 2937–2950, doi:10.1029/JD090iD07p12937.

Charlson, R. J., S. Schwartz, et al. (1992), Climate forcing by anthropogenic aerosols, *Science*, *255*(5043), 423.

Charney, J. G., and M. Stern (1962), On the stability of internal baroclinic jets in a rotating atmosphere, *Journal of the Atmospheric Sciences*, *19*(2), 159–172.

Chiang, J. C., and C. M. Bitz (2005), Influence of high latitude ice cover on the marine Intertropical Convergence Zone, *Climate Dynamics*, *25*(5), 477–496, doi:10.1007/s00382-005-0040-5.

Chiapello, I., and C. Moulin (2002), TOMS and METEOSAT satellite records of the variability of Saharan dust transport over the Atlantic during the last two decades (1979–1997), *Geophysical Research Letters*, *29*(8), 17–1.

Chin, M. (2009), *Atmospheric aerosol properties and climate impacts*, DIANE Publishing.

Christopher, S. A., and J. Zhang (2002), Shortwave aerosol radiative forcing from MODIS and CERES observations over the oceans, *Geophysical Research Letters*, *29*(18).

Chung, S. H., and J. H. Seinfeld (2005), Climate response of direct radiative forcing of anthropogenic black carbon, *Journal of Geophysical Research: Atmospheres (1984–2012)*, *110*(D11), doi:10.1029/2004JD005441.

Chỳlek, P., and J. A. Coakley (1974), Aerosols and climate, *Science*, *183*(4120), 75–77, doi:10.1126/science.183.4120.75.

Claquin, T., M. Schulz, Y. Balkanski, and O. Boucher (1998), Uncertainties in assessing radiative forcing by mineral dust, *Tellus B*, *50*(5).

Colarco, P. R., E. P. Nowottnick, C. A. Randles, B. Yi, P. Yang, K.-M. Kim, J. A. Smith, and C. G. Bardeen (2014), Impact of radiatively interactive dust aerosols in the NASA GEOS-5 climate model: Sensitivity to dust particle shape and refractive index, *Journal of Geophysical Research: Atmospheres*, *119*(2), 753–786, doi:10.1002/2013JD020046.

Cook, K. H. (1999), Generation of the African easterly jet and its role in determining West African precipitation, *Journal of climate*, *12*(5), 1165–1184, doi:10.1175/1520-0442(1999)012.

Cook, K. H. (2008), Climate science: the mysteries of Sahel droughts, *Nature Geoscience*, *1*(10), 647–648, doi:10.1038/ngeo320.

Cook, K. H. (2015), Role of inertial instability in the West African monsoon jump, *Journal of Geophysical Research: Atmospheres*, *120*(8), 3085–3102.

Dai, A., P. J. Lamb, K. E. Trenberth, M. Hulme, P. D. Jones, and P. Xie (2004), The recent Sahel drought is real, *International Journal of Climatology*, *24*(11), 1323–1331, doi:10.1002/joc.1083.

d'Almeida, G. A. (1989), Desert aerosol: characteristics and effects on climate, in *Paleoclimatology and paleometeorology: Modern and past patterns of global atmospheric transport*, pp. 311–338, Springer.

Darwin, C. (1846), An account of the Fine Dust which often falls on Vessels in the Atlantic Ocean., *Quarterly Journal of the Geological Society*, *2*(1-2), 26–30.

Davey, M., M. Huddleston, K. Sperber, P. Braconnot, F. Bryan, D. Chen, R. Colman, C. Cooper, U. Cubasch, P. Delecluse, et al. (2002), STOIC: a study of coupled model climatology and variability in tropical ocean regions, *Climate Dynamics*, *18*(5), 403–420, doi:10.1007/s00382-001-0188-6.

Dee, D., S. Uppala, A. Simmons, P. Berrisford, P. Poli, S. Kobayashi, U. Andrae, M. Balmaseda, G. Balsamo, P. Bauer, et al. (2011), The ERA-Interim reanalysis: Configuration and performance of the data assimilation system, *Quarterly Journal of the royal meteorological society*, *137*(656), 553–597.

Diaconescu, E. P., P. Gachon, J. Scinocca, and R. Laprise (2015), Evaluation of daily precipitation statistics and monsoon onset/retreat over western Sahel in multiple data sets, *Climate Dynamics*, *45*(5-6), 1325–1354.

Dubovik, O., B. Holben, T. F. Eck, A. Smirnov, Y. J. Kaufman, M. D. King, D. Tanré, and I. Slutsker (2002), Variability of absorption and optical properties of key aerosol types observed in worldwide locations, *Journal of the atmospheric sciences*, *59*(3), 590–608, doi:10.1175/1520-0469(2002)059⟨0590:VOAAOP⟩2.0.CO;2.

Folland, C., T. Palmer, and D. Parker (1986), Sahel rainfall and worldwide sea temperatures, 1901–85, *Nature*, *320*(6063), 602–607.

Forster, P., V. Ramaswamy, P. Artaxo, T. Berntsen, R. Betts, D. W. Fahey, J. Haywood, J. Lean, D. C. Lowe, G. Myhre, et al. (2007), Changes in atmospheric constituents and in radiative forcing. Chapter 2, in *Climate Change 2007. The Physical Science Basis*, Cambridge University Press, Cambridge, United Kingdom and New York, NY, USA.

Fox, P., and J. Rockström (2003), Supplemental irrigation for dry-spell mitigation of rainfed agriculture in the Sahel, *Agricultural water management*, *61*(1), 29–50, doi:10.1016/S0378-3774(03)00008-8.

Freidenreich, S., and V. Ramaswamy (1999), A new multiple-band solar radiative parameterization for general circulation models, *Journal of Geophysical Research: Atmospheres (1984–2012)*, *104*(D24), 31,389–31,409, doi:10.1029/1999JD900456.

Funk, C., M. D. Dettinger, J. C. Michaelsen, J. P. Verdin, M. E. Brown, M. Barlow, and A. Hoell (2008), Warming of the Indian Ocean threatens eastern and southern African food security but could be mitigated by agricultural development, *Proceedings of the National Academy of Sciences*, *105*(32), 11,081–11,086, doi:10.1073/pnas.0708196105.

Ginoux, P., M. Chin, I. Tegen, J. M. Prospero, B. Holben, O. Dubovik, and S.-J. Lin (2001), Sources and distributions of dust aerosols simulated with the GOCART model, *Journal of Geophysical Research: Atmospheres (1984–2012)*, *106*(D17), 20,255–20,273, doi:10.1029/2000JD000053.

Ginoux, P., L. W. Horowitz, V. Ramaswamy, I. V. Geogdzhayev, B. N. Holben, G. Stenchikov, and X. Tie (2006), Evaluation of aerosol distribution and optical depth in the Geophysical Fluid Dynamics Laboratory coupled model CM2. 1 for present climate, *Journal of Geophysical Research: Atmospheres (1984–2012)*, *111*(D22), doi:10.1029/2005JD006707.

Giorgi, F., and L. O. Mearns (1991), Approaches to the simulation of regional climate change: a review, *Reviews of Geophysics*, *29*(2), 191–216, doi:10.1029/90RG02636.

Goudie, A. S., and N. J. Middleton (1992), The changing frequency of dust storms through time, *Climatic change*, *20*(3), 197–225.

Grist, J. P. (2002), Easterly waves over Africa. Part I: The seasonal cycle and contrasts between wet and dry years, *Monthly Weather Review*, *130*(2), 197–211.

Grist, J. P., S. E. Nicholson, and A. I. Barcilon (2002), Easterly waves over Africa. Part II: observed and modeled contrasts between wet and dry years, *Monthly Weather Review*, *130*(2), 212–225.

Grodsky, S. A., J. A. Carton, and S. Nigam (2003), Near surface westerly wind jet in the Atlantic ITCZ, *Geophysical Research Letters*, *30*(19), doi:10.1029/2003GL017867.

Gu, G., and R. F. Adler (2004), Seasonal evolution and variability associated with the West African monsoon system, *Journal of climate*, *17*(17), 3364–3377.

Gunn, R., and B. Phillips (1957), An experimental investigation of the effect of air pollution on the initiation of rain, *Journal of Meteorology*, *14*(3), 272–280.

Hack, J. J., J. M. Caron, G. Danabasoglu, K. W. Oleson, C. Bitz, and J. E. Truesdale (2006), CCSM-CAM3 climate simulation sensitivity to changes in horizontal resolution, *Journal of climate*, *19*(11), 2267–2289, doi:10.1175/JCLI3764.1.

Hagos, S. M., and K. H. Cook (2007), Dynamics of the West African monsoon jump, *Journal of Climate*, *20*(21), 5264–5284, doi:10.1175/2007JCLI1533.1.

Hansen, J., M. Sato, and R. Ruedy (1997), Radiative forcing and climate response, *Journal of Geophysical Research: Atmospheres (1984–2012)*, *102*(D6), 6831–6864, doi:10.1029/96JD03436.

Hansen, J., M. Sato, R. Ruedy, L. Nazarenko, A. Lacis, G. Schmidt, G. Russell, I. Aleinov, M. Bauer, S. Bauer, et al. (2005), Efficacy of climate forcings, *Journal of Geophysical Research: Atmospheres (1984–2012)*, *110*(D18), doi:10.1029/2005JD005776.

Haywood, J., and O. Boucher (2000), Estimates of the direct and indirect radiative forcing due to tropospheric aerosols: A review, *Reviews of geophysics*, *38*(4), 513–543.

Haywood, J., and V. Ramaswamy (1998), Global sensitivity studies of the direct radiative forcing due to anthropogenic sulfate and black carbon aerosols, *Journal of Geophysical Research: Atmospheres (1984–2012)*, *103*(D6), 6043–6058, doi:10.1029/97JD03426.

Haywood, J., P. Francis, S. Osborne, M. Glew, N. Loeb, E. Highwood, D. Tanré, G. Myhre, P. Formenti, and E. Hirst (2003), Radiative properties and direct radiative effect of Saharan dust measured by the C-130 aircraft during SHADE: 1. Solar spectrum, *Journal of Geophysical Research: Atmospheres (1984–2012)*, *108*(D18), doi:10.1029/2002JD002687.

Haywood, J. M., P. N. Francis, M. D. Glew, and J. P. Taylor (2001), Optical properties and direct radiative effect of Saharan dust: A case study of two Saharan dust outbreaks using aircraft data, *Journal of Geophysical Research: Atmospheres (1984–2012)*, *106*(D16), 18,417–18,430, doi:10.1029/2000JD900319.

Held, I., T. Delworth, J. Lu, K. u. Findell, and T. Knutson (2005), Simulation of Sahel drought in the 20th and 21st centuries, *Proceedings of the National Academy of Sciences of the United States of America*, *102*(50), 17,891–17,896, doi:10.1073/pnas.0509057102.

Held, I. M., and A. Y. Hou (1980), Nonlinear axially symmetric circulations in a nearly inviscid atmosphere, *Journal of the Atmospheric Sciences*, *37*(3), 515–533, doi:10.1175/1520-0469(1980)037.

Horowitz, L. W., S. Walters, D. L. Mauzerall, L. K. Emmons, P. J. Rasch, C. Granier, X. Tie, J.-F. Lamarque, M. G. Schultz, G. S. Tyndall, et al. (2003), A global simulation of tropospheric ozone and related tracers: Description and evaluation of MOZART, version 2, *Journal of Geophysical Research: Atmospheres (1984–2012)*, *108*(D24), doi:10.1029/2002JD002853.

Houghton, J. T., Y. Ding, D. J. Griggs, M. Noguer, P. J. van der Linden, X. Dai, K. Maskell, and C. Johnson (2001), Climate change 2001: the scientific basis.

Houze, R. A., and A. K. Betts (1981), Convection in GATE, *Reviews of Geophysics*, *19*(4), 541–576, doi:10.1029/RG019i004p00541.

Hsieh, J.-S., and K. H. Cook (2005), Generation of African easterly wave disturbances: Relationship to the African easterly jet, *Monthly weather review*, *133*(5), 1311–1327.

Hsieh, J.-S., and K. H. Cook (2007), A study of the energetics of African easterly waves using a regional climate model, *Journal of the Atmospheric Sciences*, *64*(2), 421–440.

Hsieh, J.-S., and K. H. Cook (2008), On the instability of the African easterly jet and the generation of African waves: Reversals of the potential vorticity gradient, *Journal of the Atmospheric Sciences*, *65*(7), 2130–2151.

Hulme, M. (1996), Recent climatic change in the world's drylands, *Geophysical Research Letters*, *23*(1), 61–64, doi:10.1029/95GL03586.

Hulme, M., and N. Tosdevin (1989), The tropical easterly jet and Sudan rainfall: a review, *Theoretical and applied climatology*, *39*(4), 179–187, doi:10.1007/BF00867945.

Jacobson, M. Z., and D. G. Streets (2009), Influence of future anthropogenic emissions on climate, natural emissions, and air quality, *Journal of Geophysical Research (Atmospheres)*, *114*, 8118.

Janicot, S. (1992a), Spatiotemporal variability of West African rainfall. Part I: Regionalizations and typings, *Journal of Climate*, *5*(5), 489–497, doi:10.1175/1520-0442(1992)005.

Janicot, S. (1992b), Spatiotemporal variability of West African rainfall. Part II: Associated surface and airmass characteristics, *Journal of Climate*, *5*(5), 499–511, doi:10.1175/1520-0442(1992)005.

Jickells, T., and L. Spokes (2001), The Biogeochemistry of Iron in Seawater, edited by: Turner, DR and Hunter, K.

Jish Prakash, P., G. Stenchikov, S. Kalenderski, S. Osipov, and H. Bangalath (2014), The impact of dust storms on the Arabian Peninsula and the Red Sea, *Atmospheric Chemistry and Physics Discussions*, *14*(13), 19,181–19,245, doi:10.5194/acp-15-199-2015.

Jones, C., N. Mahowald, and C. Luo (2004), Observational evidence of African desert dust intensification of easterly waves, *Geophysical research letters*, *31*(17).

Jung, T., M. Miller, T. Palmer, P. Towers, N. Wedi, D. Achuthavarier, J. Adams, E. Altshuler, B. Cash, J. Kinter Iii, et al. (2012), High-resolution global climate simulations with the ECMWF model in Project Athena: Experimental design,

model climate, and seasonal forecast skill, *Journal of Climate*, *25*(9), 3155–3172, doi:10.1175/JCLI-D-11-00265.1.

Karyampudi, V. M., and T. N. Carlson (1988), Analysis and numerical simulations of the Saharan air layer and its effect on easterly wave disturbances, *Journal of the Atmospheric Sciences*, *45*(21), 3102–3136.

Karyampudi, V. M., S. P. Palm, J. A. Reagen, H. Fang, et al. (1999), Validation of the Saharan dust plume conceptual model using lidar, Meteosat, and ECMWF data, *Bulletin of the American Meteorological Society*, *80*(6), 1045.

Kaufman, Y., D. Tanré, O. Dubovik, A. Karnieli, and L. Remer (2001), Absorption of sunlight by dust as inferred from satellite and ground-based remote sensing, *Geophysical Research Letters*, *28*(8), 1479–1482, doi:10.1029/2000GL012647.

Kaufman, Y. J. (1987), Satellite sensing of aerosol absorption, *Journal of Geophysical Research: Atmospheres (1984–2012)*, *92*(D4), 4307–4317, doi:10.1029/JD092iD04p04307.

Kaufman, Y. J., D. Tanré, and O. Boucher (2002), A satellite view of aerosols in the climate system, *Nature*, *419*(6903), 215–223.

Konare, A., A. Zakey, F. Solmon, F. Giorgi, S. Rauscher, S. Ibrah, and X. Bi (2008), A regional climate modeling study of the effect of desert dust on the West African monsoon, *Journal of Geophysical Research: Atmospheres (1984–2012)*, *113*(D12), doi:10.1029/2007JD009322.

Koteswaram, P. (1958), The easterly jet stream in the tropics, *Tellus*, *10*(1), 43–57, doi:10.1111/j.2153-3490.1958.tb01984.x.

Lamb, P. J. (1978), Case studies of tropical Atlantic surface circulation patterns during recent sub-Saharan weather anomalies: 1967 and 1968, *Monthly Weather Review*, *106*(4), 482–491, doi:10.1175/1520-0493(1978)106.

Lamb, P. J., and R. A. Peppler (1992), Further case studies of tropical Atlantic surface atmospheric and oceanic patterns associated with sub-Saharan drought, *Journal of climate*, *5*(5), 476–488, doi:10.1175/1520-0442(1992)005.

Lau, K., M. Kim, and K. Kim (2006), Asian summer monsoon anomalies induced by aerosol direct forcing: the role of the Tibetan Plateau, *Climate Dynamics*, *26*(7-8), 855–864, doi:10.1007/s00382-006-0114-z.

Lau, K., K. Kim, Y. Sud, and G. Walker (2009), A GCM study of the response of the atmospheric water cycle of West Africa and the Atlantic to Saharan dust radiative forcing, in *Annales Geophysicae*, vol. 27, pp. 4023–4037, Copernicus GmbH, doi: 10.5194/angeo-27-4023-2009.

Lau, N.-C., and J. J. Ploshay (2009), Simulation of synoptic-and subsynoptic-scale phenomena associated with the East Asian summer monsoon using a high-resolution GCM, *Monthly Weather Review*, *137*(1), 137–160, doi:10.1175/2008MWR2511.1.

Lavaysse, C., J.-P. Chaboureau, and C. Flamant (2011), Dust impact on the West African heat low in summertime, *Quarterly Journal of the Royal Meteorological Society*, *137*(658), 1227–1240.

Levin, Z., E. Ganor, and V. Gladstein (1996), The effects of desert particles coated with sulfate on rain formation in the eastern Mediterranean, *Journal of Applied Meteorology*, *35*(9), 1511–1523, doi:10.1175/1520-0450(1996)035.

Li, X., H. Maring, D. Savoie, K. Voss, J. Prospero, et al. (1996), Dominance of mineral dust in aerosol light-scattering in the North Atlantic trade winds, *Nature*, *380*(6573), 416–419.

Liao, H., and J. Seinfeld (1998), Radiative forcing by mineral dust aerosols: sensitivity to key variables, *Journal of Geophysical Research: Atmospheres (1984–2012)*, *103*(D24), 31,637–31,645, doi:10.1029/1998JD200036.

Liao, H., Y. Zhang, W.-T. Chen, F. Raes, and J. H. Seinfeld (2009), Effect of chemistry-aerosol-climate coupling on predictions of future climate and future levels of tropospheric ozone and aerosols, *Journal of Geophysical Research: Atmospheres*, *114*(D10).

Liebmann, B., and J. Marengo (2001), Interannual variability of the rainy season and rainfall in the Brazilian Amazon Basin, *Journal of Climate*, *14*(22), 4308–4318.

Lin, S.-J. (2004), A "vertically Lagrangian" finite-volume dynamical core for global models, *Monthly Weather Review*, *132*(10), 2293–2307, doi:10.1175/1520-0493(2004)132.

Lindzen, R. S., and A. V. Hou (1988), Hadley circulations for zonally averaged heating centered off the equator, *Journal of the Atmospheric Sciences*, *45*(17), 2416–2427, doi:10.1175/1520-0469(1988)045.

Liou, K.-N., and S.-C. Ou (1989), The role of cloud microphysical processes in climate: An assessment from a one-dimensional perspective, *Journal of Geophysical Research: Atmospheres*, *94*(D6), 8599–8607.

Ma, P.-L., K. Zhang, J. J. Shi, T. Matsui, and A. Arking (2012), Direct radiative effect of mineral dust on the development of African Easterly waves in late summer, 2003–07, *Journal of Applied Meteorology and Climatology*, *51*(12), 2090–2104.

Mahowald, N., K. Kohfeld, M. Hansson, Y. Balkanski, S. P. Harrison, I. C. Prentice, M. Schulz, and H. Rodhe (1999), Dust sources and deposition during the last glacial maximum and current climate: A comparison of model results with paleodata from ice cores and marine sediments, *Journal of Geophysical Research: Atmospheres*, *104*(D13), 15,895–15,916.

Mahowald, N. M., and C. Luo (2003), A less dusty future?, *Geophysical Research Letters*, *30*(17).

Mahowald, N. M., A. R. Baker, G. Bergametti, N. Brooks, R. A. Duce, T. D. Jickells, N. Kubilay, J. M. Prospero, and I. Tegen (2005), Atmospheric global dust cycle and iron inputs to the ocean, *Global biogeochemical cycles*, *19*(4).

Mahowald, N. M., M. Yoshioka, W. D. Collins, A. J. Conley, D. W. Fillmore, and D. B. Coleman (2006), Climate response and radiative forcing from mineral aerosols during the last glacial maximum, pre-industrial, current and doubled-carbon dioxide climates, *Geophysical Research Letters*, *33*(20).

Mahowald, N. M., S. Engelstaedter, C. Luo, A. Sealy, P. Artaxo, C. Benitez-Nelson, S. Bonnet, Y. Chen, P. Y. Chuang, D. D. Cohen, et al. (2009), Atmospheric Iron Deposition: Global Distribution, Variability, and Human Perturbations*, *Annual Review of Marine Science*, *1*, 245–278.

Manabe, S., and R. T. Wetherald (1967), Thermal equilibrium of the atmosphere with a given distribution of relative humidity.

Mantsis, D. F., and A. C. Clement (2009), Simulated variability in the mean atmospheric meridional circulation over the 20th century, *Geophysical Research Letters*, *36*(6), doi:10.1029/2008GL036741.

Marsham, J. H., P. Knippertz, N. S. Dixon, D. J. Parker, and G. Lister (2011), The importance of the representation of deep convection for modeled dust-generating

winds over West Africa during summer, *Geophysical Research Letters*, *38*(16), doi: 10.1029/2011GL048368.

Middleton, N. (1985), Effect of drought on dust production in the Sahel.

Miller, R. (2012), Adjustment to radiative forcing in a simple coupled ocean-atmosphere model, *Journal of Climate*, *25*(22), 7802–7821, doi:10.1175/JCLI-D-11-00119.1.

Miller, R., and I. Tegen (1998), Climate response to soil dust aerosols., *Journal of climate*, *11*(12), doi:10.1175/1520-0442(1998)011.

Miller, R., and I. Tegen (1999), Radiative forcing of a tropical direct circulation by soil dust aerosols, *Journal of the atmospheric sciences*, *56*(14), 2403–2433, doi: 10.1175/1520-0469(1999)056.

Miller, R., I. Tegen, and J. Perlwitz (2004a), Surface radiative forcing by soil dust aerosols and the hydrologic cycle, *Journal of Geophysical Research: Atmospheres (1984–2012)*, *109*(D4), doi:10.1029/2003JD004085.

Miller, R., J. Perlwitz, and I. Tegen (2004b), Feedback upon dust emission by dust radiative forcing through the planetary boundary layer, *Journal of Geophysical Research: Atmospheres (1984–2012)*, *109*(D24), doi:10.1029/2004JD004912.

Milton, S., G. Greed, M. Brooks, J. Haywood, B. Johnson, R. Allan, A. Slingo, and W. Grey (2008), Modeled and observed atmospheric radiation balance during the West African dry season: Role of mineral dust, biomass burning aerosol, and surface albedo, *Journal of Geophysical Research: Atmospheres (1984–2012)*, *113*(D23), doi:10.1029/2007JD009741.

Mitchell, J., R. Davis, W. a. Ingram, and C. Senior (1995), On surface temperature, greenhouse gases, and aerosols: Models and observations, *Journal of Climate*, *8*(10), 2364–2386, doi:10.1175/1520-0442(1995)008.

Mohr, K. I., and C. D. Thorncroft (2006), Intense convective systems in West Africa and their relationship to the African easterly jet, *Quarterly Journal of the Royal Meteorological Society*, *132*(614), 163–176, doi:10.1256/qj.05.55.

Moulin, C., C. E. Lambert, F. Dulac, and U. Dayan (1997), Control of atmospheric export of dust from North Africa by the North Atlantic Oscillation, *NATURE*, *387*, 691.

Moulin, C., H. R. Gordon, V. F. Banzon, and R. H. Evans (2001), Assessment of Saharan dust absorption in the visible from SeaWiFS imagery, *Journal of Geophysical Research: Atmospheres (1984–2012)*, *106*(D16), 18,239–18,249, doi: 10.1029/2000JD900812.

Myhre, G., F. Stordal, M. Johnsrud, A. Ignatov, M. I. Mishchenko, I. V. Geogdzhayev, D. Tanré, J.-L. Deuzé, P. Goloub, T. Nakajima, et al. (2004), Intercomparison of satellite retrieved aerosol optical depth over the ocean, *Journal of the atmospheric sciences*, *61*(5), 499–513.

Myhre, G., F. Stordal, M. Johnsrud, D. J. Diner, I. V. Geogdzhayev, J. M. Haywood, B. Holben, T. Holzer-Popp, A. Ignatov, R. Kahn, et al. (2005), Intercomparison of satellite retrieved aerosol optical depth over ocean during the period September 1997 to December 2000, *Atmospheric Chemistry and Physics*, *5*(6), 1697–1719.

Nicholson, S. (2000), Land surface processes and Sahel climate, *Reviews of Geophysics*, *38*(1), 117–139, doi:10.1029/1999RG900014.

Nicholson, S., A. Barcilon, and M. Challa (2008), An analysis of West African dynamics using a linearized GCM*, *Journal of the Atmospheric Sciences*, *65*(4), 1182–1203, doi:10.1175/2007JAS2194.1.

Nicholson, S. E. (1980), The nature of rainfall fluctuations in subtropical West Africa, *Monthly Weather Review*, *108*(4), 473–487, doi:10.1175/1520-0493(1980)108⟨0473:TNORFI⟩2.0.CO;2.

Nicholson, S. E. (2001), Climatic and environmental change in Africa during the last two centuries, *Climate Research*, *17*(2), 123–144, doi:10.3354/cr017123.

Nicholson, S. E. (2009), A revised picture of the structure of the "monsoon" and land ITCZ over West Africa, *Climate Dynamics*, *32*(7-8), 1155–1171, doi:10.1007/s00382-008-0514-3.

Nicholson, S. E. (2013), The West African Sahel: A review of recent studies on the rainfall regime and its interannual variability, *ISRN Meteorology*, *2013*, doi: 10.1155/2013/453521.

Nicholson, S. E. (2014a), A detailed look at the recent drought situation in the Greater Horn of Africa, *Journal of Arid Environments*, *103*, 71–79, doi:10.1016/j.jaridenv.2013.12.003.

Nicholson, S. E. (2014b), The predictability of rainfall over the Greater Horn of Africa. Part I. Prediction of seasonal rainfall., *Journal of Hydrometeorology*, *15*(2014), 1011–1027, doi:10.1175/JHM-D-13-062.1.

Nicholson, S. E., and A. K. Dezfuli (2013), The relationship of rainfall variability in western equatorial Africa to the tropical oceans and atmospheric circulation. Part I: The boreal spring, *Journal of Climate*, *26*(1), 45–65, doi:10.1175/JCLI-D-11-00653.1.

Nicholson, S. E., and J. Grist (2001), A conceptual model for understanding rainfall variability in the West African Sahel on interannual and interdecadal timescales, *International Journal of Climatology*, *21*(14), 1733–1757, doi:10.1002/joc.648.

Oort, A. H., and J. J. Yienger (1996), Observed interannual variability in the Hadley circulation and its connection to ENSO, *Journal of Climate*, *9*(11), 2751–2767, doi:10.1175/1520-0442(1996)009.

Osborne, S., B. Johnson, J. Haywood, A. Baran, M. Harrison, and C. McConnell (2008), Physical and optical properties of mineral dust aerosol during the Dust and Biomass-burning Experiment, *Journal of Geophysical Research: Atmospheres (1984–2012)*, *113*(D23), doi:10.1029/2007JD009551.

Ott, L., B. Duncan, S. Pawson, P. Colarco, M. Chin, C. Randles, T. Diehl, and E. Nielsen (2010), Influence of the 2006 Indonesian biomass burning aerosols on tropical dynamics studied with the GEOS-5 AGCM, *Journal of Geophysical Research*, *115*(D14), D14,121, doi:10.1029/2009jd013181.

Otto, S., E. Bierwirth, B. Weinzierl, K. Kandler, M. Esselborn, M. Tesche, A. Schladitz, M. Wendisch, and T. Trautmann (2009), Solar radiative effects of a Saharan dust plume observed during SAMUM assuming spheroidal model particles, *Tellus B*, *61*(1), 270–296, doi:10.1111/j.1600-0889.2008.00389.x.

Patterson, E., D. Gillette, and B. Stockton (1977), Complex index of refraction between 300 and 700 nm for Saharan aerosols, *Journal of Geophysical Research*, *82*(21), 3153–3160.

Penner, J., R. Charlson, S. Schwartz, J. Hales, N. Laulainen, L. Travis, R. Leifer, T. Novakov, J. Ogren, and L. Radke (1994), Quantifying and minimizing uncertainty of climate forcing by anthropogenic aerosols, *Bulletin of the American Meteorological Society*, *75*(3), 375–400.

Penner, J. E., M. Andreae, H. Annegarn, L. Barrie, J. Feichter, D. Hegg, A. Jayaraman, R. Leaitch, D. Murphy, J. Nganga, et al. (2001), Aerosols, their direct and indirect effects, in *Climate Change 2001: The Scientific Basis. Contribution of Working Group I to the Third Assessment Report of the Intergovernmental Panel on Climate Change*, pp. 289–348, Cambridge University Press.

Pérez, C., S. Nickovic, G. Pejanovic, J. M. Baldasano, and E. Özsoy (2006), Interactive dust-radiation modeling: A step to improve weather forecasts, *Journal of Geophysical Research: Atmospheres (1984–2012)*, *111*(D16), doi:10.1029/2005JD006717.

Perlwitz, J., and R. L. Miller (2010), Cloud cover increase with increasing aerosol absorptivity: A counterexample to the conventional semidirect aerosol effect, *Journal of Geophysical Research: Atmospheres (1984–2012)*, *115*(D8), doi:10.1029/2009JD012637.

Perlwitz, J., I. Tegen, and R. L. Miller (2001), Interactive soil dust aerosol model in the GISS GCM: 1. Sensitivity of the soil dust cycle to radiative properties of soil dust aerosols, *Journal of Geophysical Research: Atmospheres (1984–2012)*, *106*(D16), 18,167–18,192, doi:10.1029/2000JD900668.

Perlwitz, J., C. Pérez García-Pando, and R. Miller (2015), Predicting the mineral composition of dust aerosols–Part 1: Representing key processes, *Atmospheric Chemistry and Physics Discussions*, *15*(3), 3493–3575, doi:10.5194/acp-15-11593-2015.

Philander, S., D. Gu, G. Lambert, T. Li, D. Halpern, N. Lau, and R. Pacanowski (1996), Why the ITCZ is mostly north of the equator, *Journal of Climate*, *9*(12), 2958–2972, doi:10.1175/1520-0442(1996)009.

Prospero, J. (1998), Air-borne dust fluxes to a deep water sediment trap, *Global Biogeochemical Cycles*, *12*(2), 311–320.

Prospero, J. M., and P. J. Lamb (2003), African droughts and dust transport to the Caribbean: Climate change implications, *Science*, *302*(5647), 1024–1027, doi:10.1126/science.1089915.

Prospero, J. M., and R. T. Nees (1986), Impact of the North African drought and El Nino on mineral dust in the Barbados trade winds.

Prospero, J. M., P. Ginoux, O. Torres, S. E. Nicholson, and T. E. Gill (2002), Environmental characterization of global sources of atmospheric soil dust identified with the Nimbus 7 Total Ozone Mapping Spectrometer (TOMS) absorbing aerosol product, *Reviews of geophysics*, *40*(1), 2–1, doi:10.1029/2000RG000095.

Putman, W. M., and S.-J. Lin (2007), Finite-volume transport on various cubed-sphere grids, *Journal of Computational Physics*, *227*(1), 55–78, doi:10.1016/j.jcp.2007.07.022.

Putman, W. M., S.-J. Lin, and B.-W. Shen (2005), Cross-platform performance of a portable communication module and the NASA finite volume general circulation model, *International Journal of High Performance Computing Applications*, *19*(3), 213–223, doi:10.1177/1094342005056101.

Ramanathan, V., and J. Coakley (1978), Climate modeling through radiative-convective models, *Reviews of Geophysics and Space Physics*, *16*(4), 465–489.

Ramanathan, V., P. Crutzen, J. Kiehl, and D. Rosenfeld (2001), Aerosols, climate, and the hydrological cycle, *science*, *294*(5549), 2119–2124, doi:10.1126/science.1064034.

Ramaswamy, V., and J. Kiehl (1985), Sensitivities of the radiative forcing due to large loadings of smoke and dust aerosols, *Journal of Geophysical Research: Atmospheres (1984–2012)*, *90*(D3), 5597–5613, doi:10.1029/JD090iD03p05597.

Ramaswamy, V., O. Boucher, J. Haigh, D. Hauglustaine, J. Haywood, G. Myhre, T. Nakajima, G. Shi, S. Solomon, R. E. Betts, et al. (2001), *Climate Change 2001: The Scientifi c Basis. Contribution of Working Group I to the Third Assessment Report of the Intergovernmental Panel on Climate Change*, chap. Radiative forcing of climate change, pp. 349–416, Cambridge University Press.

Ramel, R., H. Gallée, and C. Messager (2006), On the northward shift of the West African monsoon, *Climate Dynamics*, *26*(4), 429–440.

Randles, C., P. Colarco, and A. da Silva (2013), Direct and semi-direct aerosol effects in the NASA GEOS-5 AGCM: aerosol-climate interactions due to prognostic versus prescribed aerosols, *J. Geophys. Res. Atmos.*, *118*(1), 149–169, doi:10.1029/2012jd018388.

Raut, J.-C., and P. Chazette (2008), Radiative budget in the presence of multi-layered aerosol structures in the framework of AMMA SOP-0, *Atmospheric Chemistry and Physics*, *8*(22), 6839–6864, doi:10.5194/acpd-8-12461-2008.

Rayner, N., D. E. Parker, E. Horton, C. Folland, L. Alexander, D. Rowell, E. Kent, and A. Kaplan (2003), Global analyses of sea surface temperature, sea ice, and night marine air temperature since the late nineteenth century, *Journal of Geophysical Research: Atmospheres (1984–2012)*, *108*(D14), doi:10.1029/2002JD002670.

Reale, O., W. K. Lau, K.-M. Kim, and E. Brin (2009), Atlantic tropical cyclogenetic processes during SOP-3 NAMMA in the GEOS-5 global data assimilation and forecast system, *Journal of the Atmospheric Sciences*, *66*(12), 3563–3578.

Reed, R. J., D. C. Norquist, and E. E. Recker (1977), The structure and properties of African wave disturbances as observed during Phase III of GATE, *Monthly Weather Review*, *105*(3), 317–333.

Remer, L., et al. (2009), *Executive summary, atmospheric aerosol properties and climate impacts. A report by the US climate change science program and the subcommittee on global change research*, National Aeronautics and Space Administration, Washington, DC, USA.

Roberts, D. L., and A. Jones (2004), Climate sensitivity to black carbon aerosol from fossil fuel combustion, *Journal of Geophysical Research: Atmospheres (1984–2012)*, *109*(D16), doi:10.1029/2004JD004676.

Rodwell, M. J., and B. J. Hoskins (1996), Monsoons and the dynamics of deserts, *Quarterly Journal of the Royal Meteorological Society*, *122*(534), 1385–1404, doi:10.1002/qj.49712253408.

Rotstayn, L. D., and U. Lohmann (2002), Tropical rainfall trends and the indirect aerosol effect, *Journal of Climate*, *15*(15), 2103–2116, doi:10.1175/1520-0442(2002)015.

Ryder, C., E. Highwood, P. Rosenberg, J. Trembath, J. Brooke, M. Bart, A. Dean, J. Crosier, J. Dorsey, H. Brindley, et al. (2013), Optical properties of Saharan dust aerosol and contribution from the coarse mode as measured during the Fennec 2011 aircraft campaign, *Atmospheric Chemistry and Physics*, *13*(1), 303–325, doi:10.5194/acp-13-303-2013.

Schulz, M., C. Textor, S. Kinne, Y. Balkanski, S. Bauer, T. Berntsen, T. Berglen, O. Boucher, F. Dentener, S. Guibert, et al. (2006), Radiative forcing by aerosols as derived from the AeroCom present-day and pre-industrial simulations, *Atmospheric Chemistry and Physics*, *6*(12), 5225–5246, doi:10.5194/acp-6-5225-2006.

Schwarzkopf, M. D., and V. Ramaswamy (1999), Radiative effects of CH4, N2O, halocarbons and the foreign-broadened H2O continuum: A GCM experiment, *Journal of Geophysical Research: Atmospheres (1984–2012)*, *104*(D8), 9467–9488, doi:10.1029/1999JD900003.

Schwendike, J., P. Govekar, M. J. Reeder, R. Wardle, G. J. Berry, and C. Jakob (2014), Local partitioning of the overturning circulation in the tropics and the connection to the Hadley and Walker circulations, *Journal of Geophysical Research: Atmospheres*, *119*(3), 1322–1339, doi:10.1002/2013JD020742.

Shaffrey, L. C., I. Stevens, W. Norton, M. Roberts, P. L. Vidale, J. Harle, A. Jrrar, D. Stevens, M. J. Woodage, M.-E. Demory, et al. (2009), UK HiGEM: The new UK high-resolution global environment model-model description and basic evaluation, *Journal of Climate*, *22*(8), 1861–1896, doi:10.1175/2008JCLI2508.1.

Shindell, D., and G. Faluvegi (2009), Climate response to regional radiative forcing during the twentieth century, *Nature Geoscience*, *2*(4), 294–300, doi:10.1038/ngeo473.

Shindell, D., M. Schulz, Y. Ming, T. Takemura, G. Faluvegi, and V. Ramaswamy (2010), Spatial scales of climate response to inhomogeneous radiative forcing, *Journal of Geophysical Research: Atmospheres (1984–2012)*, *115*(D19), doi:10.1029/2010JD014108.

Slingo, A., T. P. Ackerman, R. Allan, E. I. Kassianov, S. A. McFarlane, G. Robinson, J. C. Barnard, M. Miller, J. Harries, J. Russell, et al. (2006), Observations of the impact of a major Saharan dust storm on the atmospheric radiation balance, *Geophysical Research Letters*, *33*(24), doi:10.1029/2006GL027869.

Sokolik, I. N., and O. B. Toon (1996), Direct radiative forcing by anthropogenic airborne mineral aerosols, *Nature*, *381*(6584), 681–683, doi:10.1038/381681a0.

Sokolik, I. N., and O. B. Toon (1999), Incorporation of mineralogical composition into models of the radiative properties of mineral aerosol from UV to IR wavelengths,

Journal of Geophysical Research: Atmospheres (1984–2012), *104*(D8), 9423–9444, doi:10.1029/1998JD200048.

Solmon, F., M. Mallet, N. Elguindi, F. Giorgi, A. Zakey, and A. Konaré (2008), Dust aerosol impact on regional precipitation over western Africa, mechanisms and sensitivity to absorption properties, *Geophysical Research Letters*, *35*(24), doi: 10.1029/2008GL035900.

Solmon, F., N. Elguindi, and M. Mallet (2012), Radiative and climatic effects of dust over West Africa, as simulated by a regional climate model, *Climate Research*, *52*, 97–113.

Solomon, S. (2007), *Climate change 2007-the physical science basis: Working group I contribution to the fourth assessment report of the IPCC*, vol. 4, Cambridge University Press.

Stier, P., J. H. Seinfeld, S. Kinne, and O. Boucher (2007), Aerosol absorption and radiative forcing, *Atmospheric Chemistry and Physics*, *7*(19), 5237–5261, doi:10.5194/acp-7-5237-2007.

Sud, Y. C., E. Wilcox, W.-M. Lau, G. K. Walker, X.-H. Liu, A. Nenes, D. Lee, K.-M. Kim, Y. Zhou, and P. Bhattacharjee (2009), Sensitivity of boreal-summer circulation and precipitation to atmospheric aerosols in selected regions-Part 1: Africa and India, in *Annales Geophysicae*, vol. 27, pp. 3989–4007, doi:10.5194/angeo-27-3989-2009.

Sultan, B., and S. Janicot (2000), Abrupt shift of the ITCZ over West Africa and intra-seasonal variability, *Geophysical Research Letters*, *27*(20), 3353–3356, doi: 10.1029/1999GL011285.

Sultan, B., and S. Janicot (2003), The West African monsoon dynamics. Part II: The "preonset" and "onset" of the summer monsoon, *Journal of climate*, *16*(21), 3407–3427.

Suzuki, T. (2011), Seasonal variation of the ITCZ and its characteristics over central Africa, *Theoretical and Applied Climatology*, *103*(1-2), 39–60, doi:10.1007/s00704-010-0276-9.

Tanré, D., Y. Kaufman, B. e. a. Holben, B. Chatenet, A. Karineli, F. Lavenu, L. Blarel, O. Dubovik, and L. Remer (2001), Climatology of dust aerosol size

distribution and optical properties derived from remotely sensed data in the solar spectrum, *Journal of Geophysical Research*, *106*(18), 205–18, doi:10.1029/2000JD900663.

Tegen, I., A. A. Lacis, and I. Fung (1996), The influence on climate forcing of mineral aerosols from disturbed soils, *Nature*, *380*(6573), 419–422, doi:10.1038/380419a0.

Tegen, I., P. Hollrig, M. Chin, I. Fung, D. Jacob, and J. Penner (1997), Contribution of different aerosol species to the global aerosol extinction optical thickness: Estimates from model results, *Journal of Geophysical Research: Atmospheres*, *102*(D20), 23,895–23,915.

Tegen, I., M. Werner, S. Harrison, and K. Kohfeld (2004), Relative importance of climate and land use in determining present and future global soil dust emission, *Geophysical Research Letters*, *31*(5).

Thorncroft, C. (1995), An idealized study of African easterly waves. III: More realistic basic states, *Quarterly Journal of the Royal Meteorological Society*, *121*(527), 1589–1614, doi:10.1002/qj.49712152706.

Thorncroft, C., and M. Blackburn (1999), Maintenance of the African easterly jet, *Quarterly Journal of the Royal Meteorological Society*, *125*(555), 763–786, doi:10.1002/qj.49712555502.

Thorncroft, C., and B. Hoskins (1994a), An idealized study of African easterly waves. I: A linear view, *Quarterly Journal of the Royal Meteorological Society*, *120*(518), 953–982, doi:10.1002/qj.49712051809.

Thorncroft, C., and B. Hoskins (1994b), An idealized study of African easterly waves. II: A nonlinear view, *Quarterly Journal of the Royal Meteorological Society*, *120*(518), 983–1015, doi:10.1002/qj.49712051810.

Tomas, R. A., J. R. Holton, and P. J. Webster (1999), The influence of cross-equatorial pressure gradients on the location of near-equatorial convection, *Quarterly Journal of the Royal Meteorological Society*, *125*(556), 1107–1127, doi:10.1002/qj.1999.49712555603.

Tompkins, A., C. Cardinali, J.-J. Morcrette, and M. Rodwell (2005), Influence of aerosol climatology on forecasts of the African Easterly Jet, *Geophysical research letters*, *32*(10), doi:10.1029/2004GL022189.

Torrence, C., and G. P. Compo (1998), A practical guide to wavelet analysis, *Bulletin of the American Meteorological society*, *79*(1), 61–78.

Trenberth, K. E., and A. Solomon (1994), The global heat balance: Heat transports in the atmosphere and ocean, *Climate Dynamics*, *10*(3), 107–134, doi:10.1007/BF00210625.

Trenberth, K. E., D. P. Stepaniak, and J. M. Caron (2000), The global monsoon as seen through the divergent atmospheric circulation, *Journal of Climate*, *13*(22), 3969–3993, doi:10.1175/1520-0442(2000)013.

Volz, F. E. (1973), Infrared optical constants of ammonium sulfate, Sahara dust, volcanic pumice, and flyash, *Applied Optics*, *12*(3), 564–568, doi:10.1364/AO.12.000564.

Žagar, N., G. Skok, and J. Tribbia (2011), Climatology of the ITCZ derived from ERA Interim reanalyses, *Journal of Geophysical Research: Atmospheres (1984–2012)*, *116*(D15), doi:10.1029/2011JD015695.

Wang, C. (2004), A modeling study on the climate impacts of black carbon aerosols, *Journal of Geophysical Research: Atmospheres (1984–2012)*, *109*(D3), doi:10.1029/2003JD004084.

Webster, P. J. (2004), The elementary Hadley circulation, in *The Hadley Circulation: Present, Past and Future*, pp. 9–60, Springer, doi:10.1007/978-1-4020-2944-8.

Wilcox, E. M., K. Lau, and K.-M. Kim (2010), A northward shift of the North Atlantic Ocean Intertropical Convergence Zone in response to summertime Saharan dust outbreaks, *Geophysical Research Letters*, *37*(4), doi:10.1029/2009GL041774.

Williams, A. P., and C. Funk (2011), A westward extension of the warm pool leads to a westward extension of the Walker circulation, drying eastern Africa, *Climate Dynamics*, *37*(11-12), 2417–2435, doi:10.1007/s00382-010-0984-y.

Williams, K., A. Jones, D. Roberts, C. Senior, and M. Woodage (2001), The response of the climate system to the indirect effects of anthropogenic sulfate aerosol, *Climate Dynamics*, *17*(11), 845–856, doi:10.1007/s003820100150.

Woodward, S., D. Roberts, and R. Betts (2005), A simulation of the effect of climate change–induced desertification on mineral dust aerosol, *Geophysical Research Letters*, *32*(18).

Yoshioka, M., N. M. Mahowald, A. J. Conley, W. D. Collins, D. W. Fillmore, C. S. Zender, and D. B. Coleman (2007), Impact of desert dust radiative forcing on Sahel precipitation: Relative importance of dust compared to sea surface temperature variations, vegetation changes, and greenhouse gas warming, *Journal of Climate*, *20*(8), 1445–1467, doi:10.1175/JCLI4056.1.

Yu, J.-Y., and J. D. Neelin (1997), Analytic approximations for moist convectively adjusted regions, *Journal of the atmospheric sciences*, *54*(8), 1054–1063, doi:10.1175/1520-0469(1997)054.

Yue, X., H. Wang, H. Liao, and K. Fan (2010), Direct climatic effect of dust aerosol in the NCAR Community Atmosphere Model Version 3 (CAM3), *Advances in Atmospheric Sciences*, *27*, 230–242, doi:10.1007/s00376-009-8170-z.

Yue, X., H. Wang, H. Liao, and D. Jiang (2011a), Simulation of the direct radiative effect of mineral dust aerosol on the climate at the Last Glacial Maximum, *Journal of Climate*, *24*(3), 843–858, doi:10.1175/2010JCLI3827.1.

Yue, X., H. Liao, H. Wang, S. Li, and J. Tang (2011b), Role of sea surface temperature responses in simulation of the climatic effect of mineral dust aerosol, *Atmospheric Chemistry and Physics*, *11*(12), 6049–6062, doi:10.5194/acp-11-6049-2011.

Zender, C. S., R. Miller, and I. Tegen (2004), Quantifying mineral dust mass budgets: Terminology, constraints, and current estimates, *Eos, Transactions American Geophysical Union*, *85*(48).

Zhang, D., A. Zakey, X. Gao, F. Giorgi, and F. Solmon (2009), Simulation of dust aerosol and its regional feedbacks over East Asia using a regional climate model, *Atmospheric Chemistry and Physics*, *9*(4), 1095–1110, doi:10.5194/acp-9-1095-2009.

Zhang, R., and T. L. Delworth (2005), Simulated tropical response to a substantial weakening of the Atlantic thermohaline circulation, *Journal of Climate*, *18*(12), 1853–1860, doi:10.1175/JCLI3460.1.

Zhao, M., I. M. Held, S.-J. Lin, and G. A. Vecchi (2009), Simulations of global hurricane climatology, interannual variability, and response to global warming using a 50-km resolution GCM, *Journal of Climate*, *22*(24), 6653–6678, doi:10.1175/2009JCLI3049.1.

APPENDICES

7 Papers Submitted and Under Preparation

7.1 Papers Published

• Bangalath, H. K., and G. Stenchikov (2015), Role of dust direct radiative effect on the tropical rainbelt over Middle East and North Africa: A high resolution AGCM study, Journal of Geophysical Research: Atmospheres, 120, 4564–4584, doi:10.1002/2015JD023122.

• Bangalath, H. K., and G. Stenchikov (2016), Sensitivity of the Middle East–North African tropical rainbelt to dust shortwave absorption: A high-resolution AGCM experiment, Journal of Climate, 29 (19), 7103–7126, doi:http://dx.doi.org/10.1175/JCLI-D-15-0827.1.

7.2 Papers To Be Submitted

• Hamza Kunhu Bangalath, Jerry Raj, and Georgiy Stenchikov, "Dust Direct Radiative Effect on West African Monsoon "Onset" and "Jump"", *To be submitted (Geophysical Research Letters).*

• Hamza Kunhu Bangalath, Jerry Raj, and Georgiy Stenchikov, "Dust Direct Radiative Effect on African Easterly Waves and Their Sensitivity to Shortwave Absorption", *To be submitted (Climate Dynamics).*